INTERNATIONAL ATOMIC ENERGY AGENCY
UNITED NATIONS EDUCATIONAL, SCIENTIFIC AND CULTURAL ORGANIZATION

INTERNATIONAL CENTRE FOR THEORETICAL PHYSICS
34100 TRIESTE (ITALY) - P.O.B. 586 - MIRAMARE - STRADA COSTIERA 11 - TELEPHONE: 2240-1
CABLE: CENTRATOM - TELEX 460392-1

IC/87/SMR/204 - 13

WINTER COLLEGE ON

ATOMIC AND MOLECULAR PHYSICS

(9 March - 3 April 1987)

(ANALYTICAL LASER SPECTROSCOPY 1)

Fluorescence: Basic Principles

Instrumentation and Methodology

N. OMENETTO

Joint Research Centre
Ispra (Va), Italy

ICTP WINTER COLLEGE ON ATOMIC AND MOLECULAR PHYSICS

TRIESTE , March 1987

"ANALYTICAL LASER SPECTROSCOPY 1"

Lecturer : N. OMENETTO

Joint Research Centre

Ispra (Va) , Italy

II.

☆ Fluorescence: Basic Principles

☆ Instrumentation and Methodology

Chapter from
Analytical Laser Spectroscopy
Edited by Dr. Nicolo Omenetto

CHAPTER

4

ATOMIC FLUORESCENCE SPECTROSCOPY WITH LASER EXCITATION

N. OMENETTO
Istituto di Chimica Generale
Università di Pavia
Pavia, Italy
and
J. D. WINEFORDNER
Department of Chemistry
University of Florida
Gainesville, Florida

4.1 INTRODUCTION

Atomic fluorescence emitted by several atomic species has been largely studied by physicists in the early twentieth century (1). However, its *analytical* birth, foreseen by Alkemade in 1962 (2), dates back to 1964, when Winefordner and Vickers (3) described their first experiments carried out with a conventional atomic absorption atomizer—a flame burning at atmospheric pressure. Since the fluorescence radiance is linearly proportional to the source radiance over the absorption linewidth of the atoms, it soon became apparent that atomic fluorescence, like all types of luminescence, was a source intensity-starved method. Indeed, except in a few favorable cases, the excitation provided by the available atomic absorption line sources, such as hollow-cathode discharge lamps, has proved to be completely inadequate for obtaining good signals and signal-to-noise ratios.

Therefore, the major field of technologic research in atomic fluorescence spectroscopy has been the investigation of a great variety of light sources possessing, among other desirable features such as stability, long life, low cost, and high versatility, the most critical of all, namely, high intensity. Several types of sources gave satisfactory results (4). These include high-intensity hollow-cathode lamps provided with a boosting auxiliary discharge, demountable hollow-cathode lamps, and spectral vapor discharge lamps. A common feature of these sources is their lack of versatility, since a rather limited number of elements can be successfully excited. Continuum sources such as high-pressure xenon arcs should overcome this problem, despite their lack of intensity in the ultraviolet region. The most promising source has been the microwave-excited electrodeless discharge lamp because of its greater spectral output over the absorption bandwidth compared to the other sources. A great deal of research has been devoted to optimize the output performances of such lamps and to eliminate operating inconveniences as well as a somewhat poor reliability. Both disadvantages seem to be overcome by careful thermostating of the lamp (5).

In addition to the problem of source intensity, it is generally recognized that atomizer noise is of primary importance for flames and electrothermal atomizers in the spectral region above 300 nm. Of all noises present in a fluorescence setup, assuming negligible scattering, the total photodetector shot noise is probably the dominating noise in the system. If this is the case, best results would be achieved by pulsing the excitation source with a low duty cycle (therefore achieving high peak intensities) and gating the detector so that the noise is measured only during the short "on" time of the detector.

When all these considerations are put together, one can easily understand why the pulsed, tunable dye laser (6–8) seemed to be the problem-solving tool for atomic fluorescence analysis. In fact, the dye laser has the following unique features: (i) it is continuously tunable over the visible region and, with frequency doubling, down to 250 nm; (ii) it provides extremely high peak powers, of several tens of kilowatts; (iii) it has a great degree of coherence both spatial as well as temporal, thereby leading to very high power densities (small spot size) and narrow linewidths (monochromaticity); and (iv) it is pulsed with a very low duty cycle so that the maximum benefit of signal-to-noise ratio should be obtained for background noise-limited systems by gated operation. As a consequence of laser excitation, the expected results are therefore better detection sensitivities (because of the source intensity) and better information power and selectivity (because of the source resolution and bandwidth).

This chapter deals essentially with the theory and analytical results obtained when pulsed dye lasers are used in combination with conventional flames and electrothermal atomizers in atomic fluorescence spectroscopy. Other fluorescence results obtained by excitation via a cw laser are reported elsewhere in this book (Chapter 8). The features of the laser-excited fluorescence technique are discussed in terms of excitation and deexcitation processes (Sects. 4.2 and 4.3), saturation effects for two- and three-level systems (Sect. 4.4), the influence of source irradiance upon the shape of the calibration curves (Sect. 4.5), and the possibility of local sensing of physical parameters such as temperature, quantum efficiency, and concentrations (Sect. 4.6). The general instrumental setups used by different workers are discussed in Sect. 4.7, and the analytical results, mostly given in terms of detection limits referred to aqueous solutions, are reported in Sect. 4.8. The reader is also referred to two review articles (7,8) concerned with the general applicability of tunable dye lasers to analytical spectroscopy, thereby including the fluorescence technique.

4.2 TYPES OF FLUORESCENCE TRANSITIONS

During the rapid development of atomic fluorescence, several authors have described the fluorescence process under study by different names so that some confusion and ambiguity has resulted as far as terminology is concerned. With the advent of tunable dye lasers, this possibility of confusion increased since many new fluorescence transitions were observed. Because of this, an effort was made by the authors of this chapter (9) to propose a consistent nomenclature with an attempt to utilize,

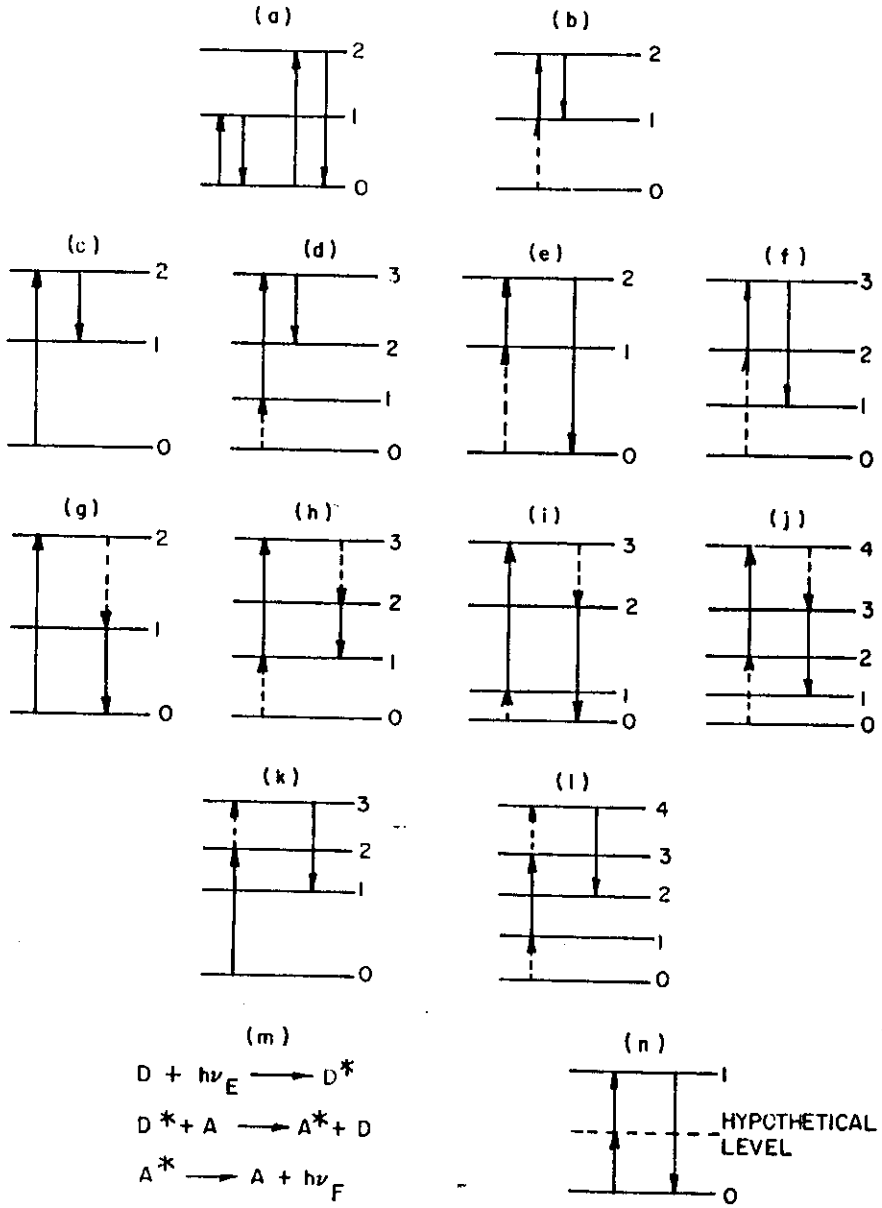

Fig. 4.1. Types of atomic fluorescence transitions (the spacings between atomic levels is not indicative of any specific atom): (*a*) resonance fluorescence (either process); (*b*) excited-state resonance fluorescence; (*c*) Stokes direct-line fluorescence; (*d*) excited-state Stokes direct-line fluorescence; (*e*) anti-Stokes direct-line fluorescence; (*f*) excited-state anti-Stokes direct-line fluorescence; (*g*) Stokes stepwise-line fluorescence; (*h*) excited-state Stokes stepwise-line fluorescence; (*i*) anti-Stokes stepwise-line fluorescence; (*j*) excited-state anti-Stokes stepwise-line fluorescence; (*k*) thermally assisted Stokes or anti-Stokes stepwise-line fluorescence (depending upon whether the absorbed radiation has shorter or longer wavelengths than the fluorescent radiation); (*l*) excited-state thermally assisted Stokes or anti-Stokes stepwise-line fluorescence (depending upon whether the absorbed radiation has shorter or longer wavelengths) than the fluorescence radiation); (*m*) senstized fluorescence (D = donor; D* = excited donor; A = acceptor; A* = excited acceptor; $h\nu_E$ = exciting radiation; $h\nu_F$ = fluorescence radiation); (*n*) two-photon excitation fluorescence (multiphoton processes involving more than two photons are even less probable than the two-photon process). From N. Omenetto and J. D. Winefordner, *Appl. Spectrosc.* **26**, 555 (1972). Reproduced by permission.

whenever possible, the terminology previously reported by the different authors in the field.

Basically, there are five types of atomic fluorescence transitions, which are reported, together with possible variations, in Fig. 4.1. *Resonance fluorescence*[1] results when the same lower and upper levels are involved in the excitation–deexcitation processes. Because of the usually high value of the fundamental constants characterizing the resonance fluorescence transitions, their radiance is significantly greater than for other transitions; and as a result most analytical measurements have involved these lines. *Direct-line fluorescence* results when the *same* upper level is involved in the radiational excitation and deexcitation processes. If *different* upper levels are involved in the radiational excitation and deexcitation processes, then *stepwise-line fluorescence* results. *Sensitized fluorescence* results when one species, called the donor, is excited and transfers excitation energy to an atom of the same or another species, called the acceptor, either of which deexcites radiationally. Finally, *multiphoton fluorescence*[2] results when two or more photons excite an atomic species which then radiationally deexcites. It should be pointed out that these two last processes are likely to be unimportant for analytical studies in flames and other common atomizers.

If the excitation energy is *greater* than the fluorescence energy, this type of fluorescence is termed *Stokes*; if the fluorescence energy is greater than the excitation energy, the process is called *anti-Stokes*. If the radiational excitation *and* fluorescence processes involve only excited states, the fluorescence process is said to be *excited*. If the excitation

[1] Strictly speaking, resonance fluorescence implies that the lower level of the transition is the ground state. Although this process is the most common in atomic fluorescence, the definition given above is more general than this and includes transitions not involving the ground state as the lower state in the transition.

[2] Excitation can be via two photons of same frequency with virtual level involved or via two photons of different frequency involving real levels.

process involves a collisional excitation *following* the radiational excitation, the process is called *thermally assisted.*

The identification of the excitation and deexcitation processes involved in a fluorescence transition is important for several reasons. First of all, it helps elucidating the relative contributions of the different exciting lines as well as those of thermal collisions in populating the fluorescent level, thereby permitting the correct nomenclature to be used for the process. For example, there are several cases (Ga, In, etc.) in which the "resonance fluorescence" signal observed is due to a mixture of "resonance fluorescence" and "anti-Stokes direct-line fluorescence" ((*a*) and (*e*) in Fig. 4.1) *unless* one of the transitions is filtered from the source. Secondly, the evaluation of the quantum efficiency requires a clear knowledge of the overall process. Finally, one can take advantage of the difference existing between the excitation and fluorescence wavelengths to eliminate scattered light, which is known to interfere to variable extents (depending upon the atomizer and instrumental setup) in all resonance fluorescence measurements.[3] To accomplish this task with conventional sources is rarely easy, occasionally feasible, and most of the time impossible because of the stringent requirements on filters to isolate the line(s) of interest and the consequent decrease of the source intensity to unacceptably low levels. Moreover, the intensity of the different potentially exciting lines emitted by the source is governed and fixed by the discharge parameters. From this point of view it is clear that the laser represents an ideal source because of its tunability, with similar output intensities, over any of the lines of interest and because no filters are required to isolate the transitions. Also, the excited level population is greatly enhanced, thereby favoring efficient mixing between adjacent levels resulting in strong fluorescence emission.

Several fluorescence processes, depicted in Fig. 4.1, have been observed with laser excitation of some transition elements in a nitrous oxide–acetylene flame (10). As examples, the partial Grotrian diagrams for the elements vanadium and scandium are given in Figs. 4.2 and 4.3; the corresponding (partial) fluorescence spectra are reported in Figs. 4.4 and 4.5. Table 4.1 explains the different excitation and deexcitation processes for scandium according to the nomenclature described. Figure 4.6 shows the very minute signals obtained in an air–hydrogen flame and attributed to a two-photon excitation process for the elements zinc and cadmium (11).

To our best knowledge, no other example of multiphoton excitation in flames at atmospheric pressure has been reported so far. Steinfeld (8)

[3] When a continuum excitation source with no disperser is used, scatter occurs at *all* fluorescence wavelengths, that is, at resonance and nonresonance lines.

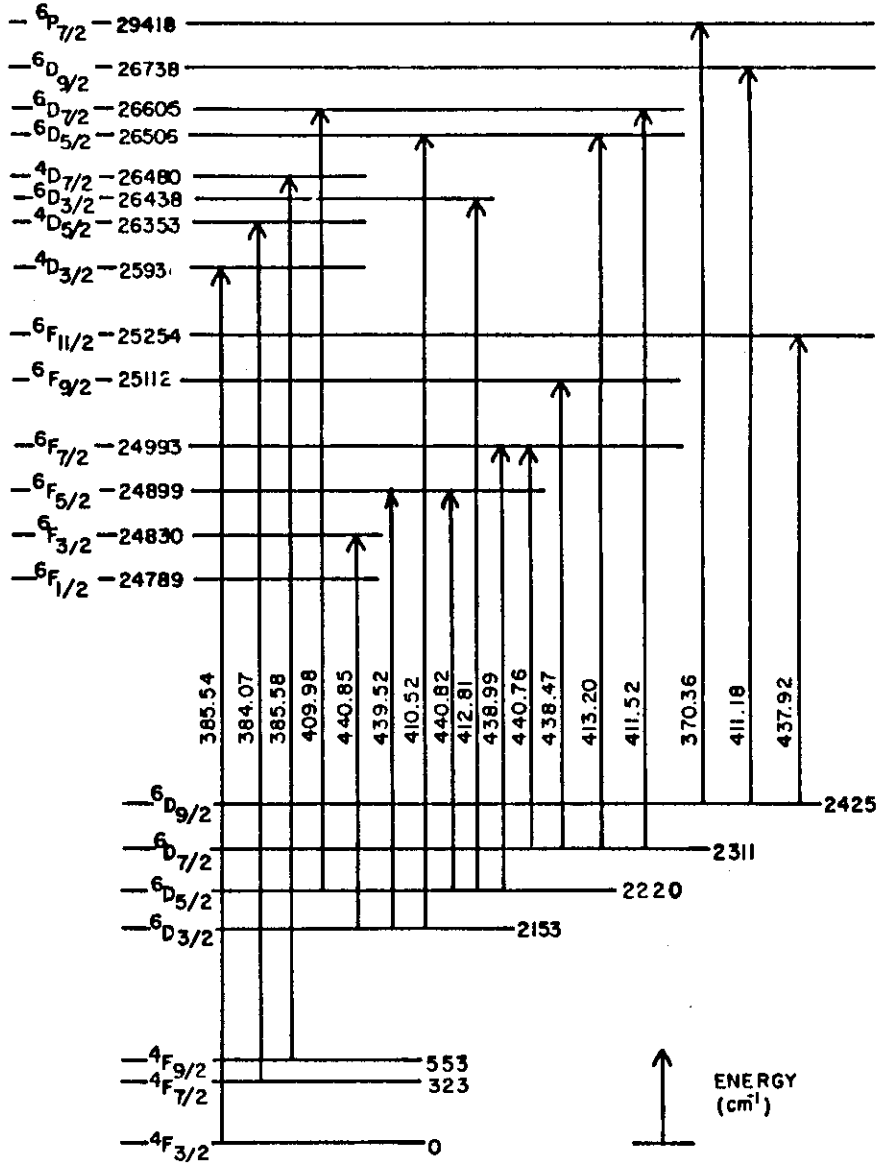

Fig. 4.2. Partial atomic energy level diagram for vanadium: From N. Omenetto, N. N. Hatch, L. M. Fraser, and J. D. Winefordner, *Spectrochim. Acta*, **28B**, 65 (1973). Reproduced by permission.

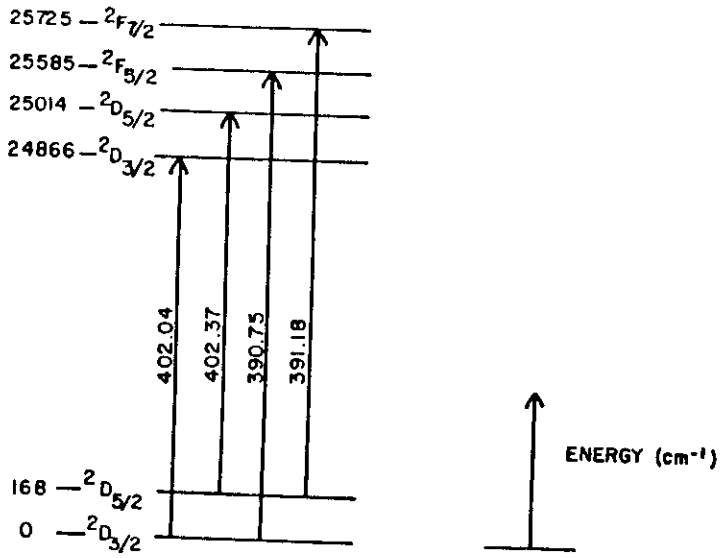

Fig. 4.3. Partial atomic energy level diagram for scandium. From N. Omenetto, N. N. Hatch, L. M. Fraser, and J. D. Winefordner, *Spectrochim. Acta*, **28B**, 65(1973). Reproduced by permission.

indicates that the energy levels involved in the so-called two-photon atomic fluorescence observed for both Cd (228.8 nm) and Zn (213.9 nm) are difficult to understand because the same upper and lower levels cannot be connected by both two-photon and one-photon transitions (parity forbidden). However, due to the poor detection limits obtained (~10 ppm) for Zn and Cd (11), no further work was performed in this area, and the results still remain a mystery.

4.3 KINETIC CONSIDERATIONS

In all resonance fluorescence measurements the signal has been stated to be linearly dependent upon the value of the quantum efficiency Y_{21} of the transition involving a lower state 1 and an upper state 2. By definition, Y_{21} is generally given by the ratio between the number of quanta per unit time emitted as fluorescence and the number of quanta per unit time absorbed by the atoms in the lower level of the transition. This ratio results in the so-called *Stern-Volmer relationship* and represents the ratio of the transition probability per unit time for spontaneous emission to the total probability of deexcitation per unit time (12,13). Clearly, in the atomizer, there are several processes other than the

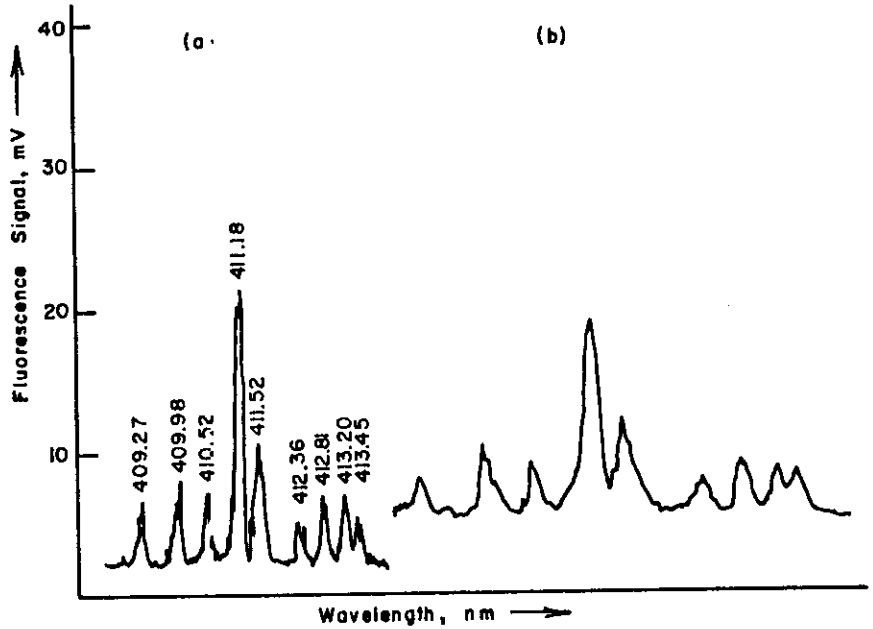

Fig. 4.4. Partial atomic fluorescence spectrum of vanadium-wavelength scanning; 50 μm slit (0.1 nm spectral bandwidth); 1000 ppm vanadium. (*a*) Laser excitation set at 411.18 nm; (*b*) laser excitation set at 370.35 nm, full-scale sensitivity increased 2.5 times as compared to (*a*), scan speed decreased to half as compared to (*a*). All these fluorescence transitions are due to excited Stokes stepwise-line fluorescence. From N. Omenetto, N. N. Hatch, L. M. Fraser, and J. D. Winefordner, *Spectrochim. Acta*, **28B**, 65 (1973). Reproduced by permission.

radiative ones, such as inelastic collisions and chemical reactions, concurring to the formation and/or destruction of an excited state. If a metal atom M in a gas of molecules Z is considered, the following inelastic process can be written

$$M_1 + Z \rightleftharpoons M_2 + Z \tag{1}$$

proceeding in both directions because of the principle of microscopic reversibility (assuming the system is in thermodynamic equilibrium). The *overall rate* or velocity of the forward process is indicated as

$$v_{12} = k'_{12}[M_1][Z] \tag{2a}$$

where $[M_1]$ and $[Z]$ are the numbers of atoms and molecules per unit volume. A similar relation holds for the rate of the reverse process (quenching). The coefficient k'_{12} is the bimolecular *rate constant* for the reaction. Usually, the concentration $[Z]$ is included in the rate constant by

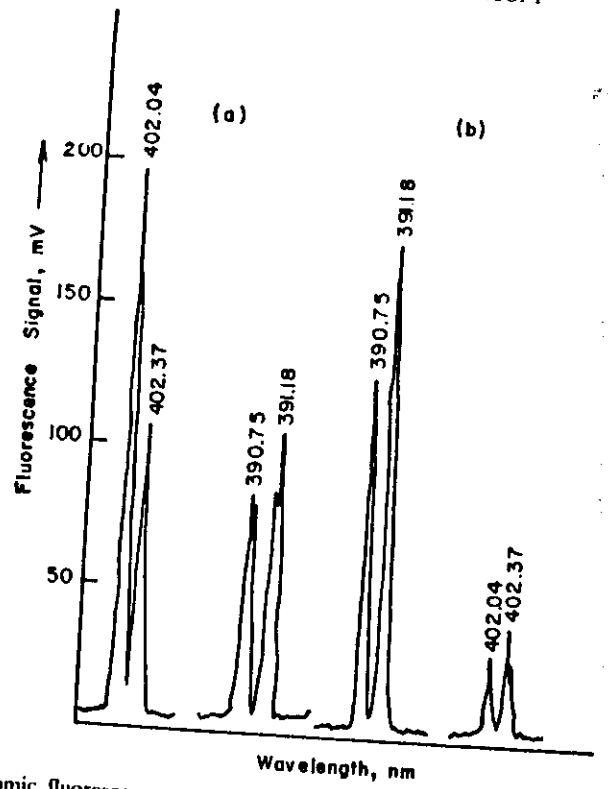

Fig. 4.5. Atomic fluorescence transitions of scandium-wavelength scanning: 50 μm slit (0.1 nm spectral bandwidth); 1000 ppm scandium. (*a*) Laser excitation set at 402.14 nm; (*b*) laser excitation set at 391.0 nm. From N. Omenetto, N. N. Hatch, L. M. Fraser, and J. D. Winefordner, *Spectrochim. Acta*, **28B**, 65 (1973). Reproduced by permission.

defining a unimolecular rate constant $k_{12} \equiv k'_{12}[Z]$ (pseudo-first-order kinetics). The *overall rate* of the reverse process shown in Eq. (1) is

$$v_{21} = k'_{21}[M_2][Z] \tag{2b}$$

The definition of quantum efficiency is given by

$$Y_{21} = \frac{A_{21}}{A_{21} + k_{21}} \tag{3}$$

where A_{21} is the Einstein transition probability, in s^{-1}, for spontaneous emission. In terms of *lifetimes*,

$$Y_{21} = \tau/\tau_{sp} \tag{4}$$

where $\tau\,[\equiv(A_{21} + k_{21})^{-1}]$ represents the mean lifetime of level 2 and $\tau_{sp}\,[\equiv(A_{21})^{-1}]$ gives the radiative lifetime.

TABLE 4.1
Observed Fluorescence Transitions for Atomic Scandium[a]

Laser excitation, nm	Fluorescence wavelength, nm	Type of fluorescence transitions
	402.04	resonance fluorescence and anti-Stokes stepwise-line fluorescence
402.04	402.37	excited resonance fluorescence and thermally assisted Stokes stepwise-line fluorescence
402.37	390.75	thermally assisted anti-Stokes stepwise-line fluorescence (2 transitions)
	391.18	thermally assisted anti-Stokes stepwise-line fluorescence and excited thermally assisted anti-Stokes stepwise-line fluorescence
	390.75	resonance fluorescence and anti-Stokes stepwise-line fluorescence
390.75	391.18	thermally assisted Stokes stepwise-line fluorescence and excited resonance fluorescence
391.18	402.04	Stokes stepwise-line fluorescence (2 transitions)
	402.37	Stokes stepwise-line fluorescence and excited Stokes stepwise-line fluorescence

[a] From N. Omenetto, N. N. Hatch, L. M. Fraser, and J. D. Winefordner, *Spectrochim. Acta*, **28B**, 65 (1973). Reproduced by permission.

If we take a system characterized only by a ground level 1 and an excited level 2, then by definition

$$Y_{21} = \frac{(n_2 - n_2^{th})A_{21}}{B_{12}\rho_{\nu_{12}} n_1} \tag{i}$$

where n_i are the actual populations of the levels, n_i^{th} are the thermal population of the levels, A_{21} is the spontaneous transition probability, B_{12} is the Einstein coefficient for induced absorption, and $\rho_{\nu_{12}}$ is the spectral radiation density of a continuum-exciting source. Neglecting stimulated emission, the balance equations (see also Sect. 4.4) are

$$n_1(B_{12}\rho_{\nu_{12}} + k_{12}) = n_2(A_{21} + k_{21}) \tag{ii}$$

$$n_1^{th} k_{12} = n_2^{th}(A_{21} + k_{21}) \tag{iii}$$

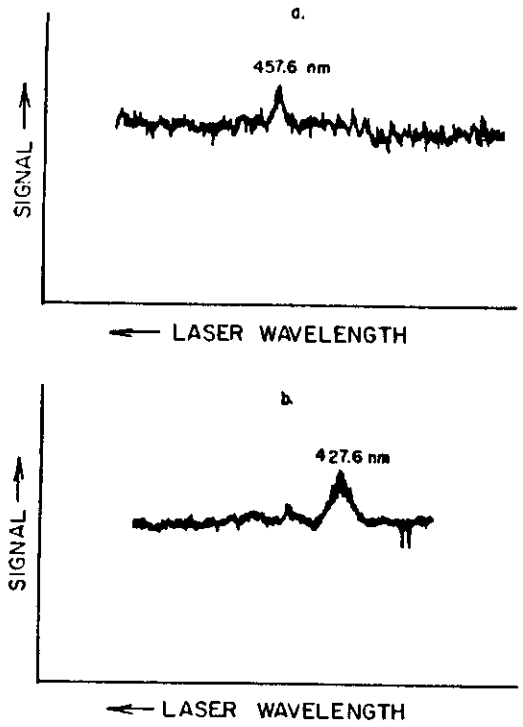

Fig. 4.6. Two-photon atomic fluorescence of cadmium and zinc. (*a*) Cadmium-monochromator at 228.8 nm, excitation scanned over 457.6 nm; (*b*) zinc-monochromator at 213.8 nm, excitation scanned over 427.6 nm. Reprinted with permission from L. M. Fraser and J. D. Winefordner, *Anal. Chem.*, **44**, 1444 (1972). Copyright by the American Chemical Society.

Subtracting (ii) from (iii) and remembering that $(n_1 - n_1^{(h)}) = -(n_2 - n_2^{(h)})$, then after rearranging

$$B_{12}\rho_{\nu_{12}} n_1 = (n_2 - n_2^{(h)})(A_{21} + k_{21} + k_{12}) \qquad \text{(iv)}$$

and making use of (i),

$$Y_{21} = A_{21}/\{(A_{21} + k_{21})[1 + k_{12}/(k_{21} + A_{21})]\} \qquad \text{(v)}$$

It can be easily seen from Eq. (iii) that the ratio between the square brackets in Eq. (v) is in most cases negligible compared to unity because of the Boltzmann factor. This derivation demonstrates that the formula given by Eq. (3) can be safely applied in most cases. See also reference 14.

In an atomizer where thermodynamic equilibrium prevails, the rate at which each particular process proceeds exactly equals the rate of the reverse process because of the *principle of detailed balance.* Therefore, $(v_1)_e = (v_2)_e$, and

$$(k_{12})_e/(k_{21})_e = [M_2]_e/[M_1]_e = (g_2/g_1)\exp(-E/kT) \qquad (5)$$

where the Boltzmann distribution has been introduced. When various types of molecules exist, such as in a flame at atmospheric pressure, the overall rate constant k is a summation of the specific rate constants corresponding to the various kind of particles. The general expression for the rate constant k is given by the following relation:

$$k_{21} = \sum_j n_j \sigma_j \bar{u}_j \qquad (6)$$

where n_j is the density of quenching particles of kind j, in cm^{-3}; σ_j is the effective cross section (at a given temperature T), in cm^2; and $\bar{u}_j$ is the mean relative velocity, in $cm\,s^{-1}$, of atoms and quenching particles. Remembering that

$$n_j = P_j/kT \quad \text{and} \quad \bar{u}_j = (8kT/\pi\mu_j)^{1/2} \qquad (7)$$

where P_j is the partial pressure of particles of kind j and μ_j is the reduced mass of the atom and the particle of kind j, and introducing typical values for n_j ($\sim 10^{18}\,cm^{-3}$), σ_j ($\sim 10^{-15}\,cm^2$), and $\bar{u}_j$ ($\sim 10^5\,cm\,s^{-1}$), an order-of-magnitude estimate for the quenching rate constant in a flame of $k_{21} \sim 10^8\,s^{-1}$ is obtained.

As will clearly emerge later, the quantum efficiency plays an essential role in the theoretical approach to saturation of an atomic transition in the presence of the strong radiation field provided by the laser.

4.4 BASIC FLUORESCENCE SIGNAL EXPRESSIONS

The dependence of the fluorescence signal upon the type and intensity of the excitation source, the quantum efficiency, and the concentration of absorbing atoms has been treated very extensively in the literature (4,13), and it can be generally stated that, with some unavoidable simplifying assumptions, the theoretical background of the technique has been firmly established and in most cases demonstrated experimentally.

The use of lasers as excitation source has the important consequence that the conventional photon transport equation (Beer's law) is strictly valid in the limit of zero incident light flux and is therefore an accurate approximation only for low-intensity sources. The high radiation density of a laser focused into an atomic vapor is able to completely redistribute the populations of the levels involved in the absorption process to the point where no more absorption occurs, that is, where the absorption

coefficient decreases to zero as stimulated emission balances absorption. This effect has been commonly referred to as saturation of the optical transition (16–21). The fluorescence signal will then no longer be proportional to the source irradiance and will reach a limiting value depending upon the properties of the atomic system.

We present here a general derivation of the fluorescence radiance expression based upon simple kinetic considerations. For the sake of simplicity, the atomic system is characterized as an ensemble of atoms having only two energy levels 1 and 2 without multiplet splitting, with equal statistical weights $g_1 = g_2$, separated by the energy difference $E = h\nu_0 \geq 2$ eV, and with populations (number of atoms per unit volume) n_1 and n_2, with $n_1 + n_2 = n_T$, where n_T is the total density of atoms.

Several important assumptions are made: (i) atoms are present as a trace component in a gas of molecules at thermodynamic temperature T (2000–5000 K), that is, no self-absorption effects are considered; (ii) the pulsed laser radiation does not affect the energy distribution of the gas molecules, the velocity distribution of the atoms, or the temperature T of the system; (iii) any coherence effects between absorbed and emitted photons are neglected; (iv) polarization effects are neglected; (v) the atomic system is homogeneous with regard to concentration and temperature; and finally (vi) the radiation density of the source is constant.

4.4.1 Temporal Behavior of Fluorescence Excited by a Pulsed Continuum Source

The temporal dependence of the concentration of the excited state can be represented by the following equation:

$$dn_2/dt = B\rho_{\nu_0}(n_1 - n_2) + k_{12}n_1 - n_2(A_{21} + k_{21}) \tag{8}$$

where ρ_{ν_0} stands for the uniform spectral volume energy density at $\nu = \nu_0$ (erg Hz^{-1} cm^{-3}) of the laser, assumed to act as a spectral continuum, that is, with a frequency bandwidth much larger than the absorption bandwidth; B (erg^{-1} cm^3 s^{-1} Hz) represents the Einstein coefficient for absorption and stimulated emission (in this case, $B_{12} = B_{21} = B$ because of our assumption of equal statistical weights); and all other terms have been previously defined (Sect. 4.3). Remembering that $\tau \equiv (A_{21} + k_{21})^{-1}$ and neglecting k_{12} in comparison with k_{21} because of the negligible Boltzmann factor for the transition and temperature values considered, Eq. (8) can be rearranged as follows:

$$dn_2/dt + \frac{n_2}{\tau}(2B\rho_{\nu_0}\tau + 1) = B\rho_{\nu_0}n_T \tag{9}$$

From the theory of radiation (1), the following relationship occurs:

$$L = (c/h\nu_0)\{1/(n_1 - n_2)\}\int k(\nu)\,d\nu$$

or

$$B = (c/h\nu_0)\int \sigma(\nu)\,d\nu \tag{10}$$

where $k(\nu)$ is the frequency-dependent absorption coefficient of the atomic vapor and $\sigma(\nu)$ is the frequency-dependent absorption cross section. Therefore, by substitution of Eq. (10) into Eq. (9),

$$\frac{dn_2}{dt} + \frac{n_2}{\tau}\left\{\frac{2\tau}{h\nu_0}E_{\nu_0}\left[\int \sigma(\nu)\,d\nu\right] + 1\right\} = \frac{E_{\nu_0}}{h\nu_0}\left[\int \sigma(\nu)\,d\nu\right]n_T \tag{11}$$

where use has been made of the relation $\rho_{\nu_0} = E_{\nu_0}/c$, where c is the velocity of light and E_{ν_0} (erg s^{-1} cm^{-2} Hz^{-1}) represents the spectral irradiance of the source. Equation (11) can be simplified by defining (16) the saturation parameter $E^s_{\nu_0}$ as

$$E^s_{\nu_0}/h\nu_0 \equiv 1\Big/\left\{2\tau\left[\int \sigma(\nu)\,d\nu\right]\right\} \tag{12}$$

Making use of Eq. (12), Eq. (11) becomes

$$\frac{dn_2}{dt} + \frac{n_2}{\tau}\left(1 + \frac{E_{\nu_0}}{E^s_{\nu_0}}\right) = \frac{E_{\nu_0}}{h\nu_0}n_T\left[\int \sigma(\nu)\,d\nu\right] \tag{13}$$

With the assumptions made at the beginning of this section, the proportional dependence of the fluorescence signal upon n_2 is given by

$$B_F = n_2 h\nu_0 \frac{l}{4\pi}(\tau_{sp})^{-1} \tag{14}$$

where B_F is the absolute fluorescence radiance (erg s^{-1} cm^{-2} sr^{-1}) and l (cm) denotes the depth of the homogeneous fluorescing volume in the direction of observation. By introducing this relation into Eq. (13),

$$\frac{dB_F}{dt} + \frac{B_F}{\tau}\left(1 + \frac{E_{\nu_0}}{E^s_{\nu_0}}\right) = CE_{\nu_0} \tag{15}$$

where $C \equiv (l/4\pi)(n_T/\tau_{sp})[\int \sigma(\nu)\,d\nu]$. Equation (15) describes the temporal behavior of the fluorescence radiance during the excitation when the atomic vapor is irradiated with a pulsed spectral continuum source. We may apply Eq. (15) to describe several analytically useful limiting cases.

4.4.1.1 *Low Irradiance*

In this case, $E_{\nu_0} \ll E^s_{\nu_0}$, and therefore Eq. (15) reads

$$\frac{dB_F}{dt} + \frac{B_F}{\tau} = CE_{\nu_0} \tag{16}$$

If we consider an idealized flat-topped pulse of light, of constant irradiance after time zero, that is, $\rho_{\nu_0}(t) = \rho_{\nu_0}$ at $t \geq 0$ and $\rho_{\nu_0}(t) = 0$ for $t < 0$, and with the boundary condition that B_F equals zero at time zero, we have

$$B_F = CE_{\nu_0}\tau(1 - e^{-t/\tau}) \tag{17}$$

From this equation one can see that the approaching of a steady-state condition is governed by the ratio (t/τ). If steady-state conditions are attained, which is the usual case of atomic fluorescence excited with conventional sources and conventional modulation techniques, then $dB_F/dt = 0$, and the fluorescence radiance expression becomes

$$B_F = CE_{\nu_0}\tau = (l/4\pi)(\tau/\tau_{sp})\left[\int \sigma(\nu)\, d\nu\right] E_{\nu_0} n_T \tag{18a}$$

or

$$B_F = (l/4\pi)\, Y_{21} E_{\nu_0}\left[\int k(\nu)\, d\nu\right] \tag{18b}$$

Equation (18*b*) shows the well-known *linear* dependence of the fluorescence radiance upon the source spectral irradiance and the quantum efficiency of the transition. The linear dependence upon the total atomic density holds here because of the assumption of dilute atomic vapor.

4.4.1.2 *High Irradiance*

When $E_{\nu_0}/E^s_{\nu_0}$ is no longer negligible with respect to unity, then, proceeding as in the low-intensity case, the solution of Eq. (15) gives

$$B_F = CE_{\nu_0}\tau[E^s_{\nu_0}/(E_{\nu_0} + E^s_{\nu_0})]\left[1 - \exp\left\{-\frac{t}{\tau}\left(\frac{E_{\nu_0} + E^s_{\nu_0}}{E^s_{\nu_0}}\right)\right\}\right] \tag{19a}$$

or

$$B_F = CE_{\nu_0} t_r[1 - \exp(-t/t_r)] \tag{19b}$$

where the *response time* of the system, t_r, has been introduced. This quantity is by definition given by

$$t_r \equiv \tau[E^s_{\nu_0}/(E_{\nu_0} + E^s_{\nu_0})] \tag{20}$$

One can easily see now that the attainment of steady-state conditions is governed by the ratio t/t_r and therefore also by the spectral irradiance of the source. If the spectral irradiance is much less than the saturation irradiance, then t_r is simply the effective lifetime. However, if $E_{\nu_0} \gg E^s_{\nu_0}$, then steady-state conditions might be warranted even if the width of the excitation pulse is narrow. For steady-state conditions, we have

$$B_F = CE_{\nu_0}\tau[E^s_{\nu_0}/(E_{\nu_0} + E^s_{\nu_0})]$$
$$= (l/4\pi)E_{\nu_0}[E^s_{\nu_0}/(E_{\nu_0} + E^s_{\nu_0})](\tau/\tau_{sp})n_T\left[\int \sigma(\nu)\, d\nu\right] \tag{21a}$$

or

$$B_F = (l/4\pi)\, Y_{21}\left[\int k(\nu)\, d\nu\right] E_{\nu_0}[E^s_{\nu_0}/(E_{\nu_0} + E^s_{\nu_0})] \tag{21b}$$

or

$$B_F = (l/4\pi)\, Y_{21}\left[\int k^*(\nu)\, d\nu\right] E_{\nu_0} \tag{21c}$$

where

$$k^*(\nu) = k(\nu)[E^s_{\nu_0}/(E_{\nu_0} + E^s_{\nu_0})] \tag{21d}$$

It is easy to see that when $E_{\nu_0} \ll E^s_{\nu_0}$, that is, for conventional excitation sources, Eq. (21) reduces to Eq. (18). However, for laser excitation, E_{ν_0} can approach $E^s_{\nu_0}$ and/or be much greater than $E^s_{\nu_0}$. If $E_{\nu_0} \gg E^s_{\nu_0}$, Eq. (21) becomes

$$(B_F)_{\max} = (l/4\pi)(\tau/\tau_{sp})E^s_{\nu_0} n_T\left[\int \sigma(\nu)\, d\nu\right] \tag{22}$$

and remembering Eq. (12) and that $(\tau_{sp})^{-1} \equiv A_{21}$,

$$(B_F)_{\max} = (l/4\pi)h\nu_0 A_{21}(n_T/2) \tag{23}$$

This equation gives the *maximal* fluorescence radiance obtainable for a given n_T. An *absolute* measurement of $(B_F)_{\max}$ yields the product $n_T A_{21}$, all other parameters being known. (In principle, densities of species important in diagnosis of plasmas can be measured.) The advantage of determining this product through Eq. (23) is that neither the source parameters nor the temperature of the atomic system or the value of the quantum efficiency of the transition need be known (20).

The physical significance of the saturation parameters $E^s_{\nu_0}$ clearly results from Eq. (21). When $E_{\nu_0} = E^s_{\nu_0}$, B_F becomes equal to $(B_F)_{\max}/2$. In other words, $E^s_{\nu_0}$ represents the source spectral irradiance for which the maximum attainable value of the fluorescence radiance is decreased by a

factor of 2. The experimental measurement of $E^{\circ}_{\nu_0}$ should offer a possibility of measuring the quantum efficiency of the transition (see Sect. 4.6.2).

4.4.2 Temporal Behavior of Fluorescence Excited by a Pulsed Monochromatic Source

When the laser output bandwidth is narrowed by some means to a value markedly smaller than the spectral absorption linewidth, then the first term in the right-hand side of Eq. (8), accounting for the radiatively induced processes, has to be replaced by the term $[\int B\rho(\nu)g(\nu-\nu_0)\,d\nu]\times(n_1-n_2)$. The factor $g(\nu-\nu_0)$ represents the *absorption lineshape function.* The function $g(\nu-\nu_0)\,d\nu$ can be defined as the probability that a given transition will result in the absorption (emission) of a photon whose energy lies between $h\nu$ and $h(\nu+d\nu)$. The curve $g(\nu-\nu_0)$ versus ν is normalized so that the total area under it is always unity. It is well known (1, 22) that the shape of this curve depends upon the physical processes responsible for it. See also Chapter 3.

If the absorbing atoms contribute *equally* to the absorption at any frequency within the absorption profile, then the function $g(\nu-\nu_0)$ is described by a Lorentzian profile and the broadening process is called *homogeneous.* If, on the other hand, a *particular frequency interval* in the absorption profile curve can be associated with a *particular set* of absorbing atoms, then the function $g(\nu-\nu_0)$ is described by a Gaussian profile and the broadening process responsible for it is called *inhomogeneous.* Typically, homogeneous broadening is due to collisions while inhomogeneous broadening is due to the Doppler effect. When both broadening processes are present in the atomic system, the lineshape function will be given by their convolution. With the assumption that both mechanisms act independently, the result is a convolution integral, known as the Voigt function. The profile of the absorption coefficient is therefore entirely determined by the Voigt function (1, 22).

Clearly, when the radiation density of the laser is such that the saturation regime will be approached, it is very important to know whether the laser can strongly interact with the entire atomic population. From the above definitions it follows that this will happen only if the laser bandwidth is greater than the inhomogeneous absorption line profile. On the contrary, if the laser bandwidth is much smaller than the inhomogeneously broadened absorption profile, then the atomic population may be thought as grouped in a number of Doppler intervals shifted in frequency relative to the laser frequency. In this case, the population numbers n_1 and n_2 in the derivation given for the continuum case now become $n_1(\nu)$ and $n_2(\nu)$ and refer *only* to a particular Doppler interval (18, 19).

Let the inhomogeneously broadened Doppler absorption profile be described as a superposition of many narrow subprofiles, each having a homogeneous width $\delta\nu_h$ due to collisions and spontaneous processes. The homogeneous width characterizes the bandwidth of interaction of the atoms and the monochromatic laser. The laser beam, at frequency ν, traversing the atomic system in the x direction can only be absorbed by atoms having a velocity component within the interval $v_x \pm (\delta v_x/2)$, where $v_x = (\nu-\nu_0)c/\nu_0$ and $\delta v_x = \delta\nu_h c/\nu_0$. If saturation occurs, the velocity-selective absorption process results in a "hole burning" in the population distribution of ground state atoms. The width of the hole will be given by the homogeneous width. By using two beams traversing the atomic system in opposite directions and tuning the laser across the absorption frequency of the atoms, the Doppler effect is nearly eliminated (23); this process is known as *saturation spectroscopy.*

For analytical purposes, we may formally evaluate the difference between continuum and line excitation by remembering that the definition of the absorption coefficient, for $g_1 = g_2$, is given by

$$k(\nu) = B(h\nu_0/c)(n_1-n_2)g(\nu-\nu_0) \tag{24}$$

The lineshape function, with the help of Eq. (10), therefore becomes

$$g(\nu-\nu_0) = k(\nu)\Big/\left[\int k(\nu)\,d\nu\right] \tag{25a}$$

or, at the peak frequency $\nu = \nu_0$,

$$g(\nu_0) = k(\nu_0)\Big/\left[\int k(\nu)\,d\nu\right] \tag{25b}$$

where the integration extends over all frequencies for which the absorption coefficient differs noticeably from zero.

For *pure* Lorentzian and Gaussian shapes it is known that

$$[g(\nu_0)]_L = 2/\pi\delta\nu_L = 0.637/\delta\nu_L \tag{26a}$$

and

$$[g(\nu_0)]_D = (2/\delta\nu_D)(\sqrt{\ln 2}/\sqrt{\pi}) = 0.939/\delta\nu_D \tag{26b}$$

where $\delta\nu_L$ and $\delta\nu_D$ are the Lorentzian and Doppler half-widths, respectively. Therefore, the excitation rate evaluated at the peak frequency $\nu = \nu_0$ becomes

$$\rho B g(\nu_0) \equiv \rho B\left\{k(\nu_0)\Big/\left[\int k(\nu)\,d\nu\right]\right\} \tag{27a}$$

where $\rho \equiv \int \rho(\nu)\,d\nu$ represents now the integrated spectral density of the source, where the integration extends over the whole spectral width of the

exciting line. By introducing now the quantity

$$\delta\nu_{\text{eff}} \equiv \left[\int k(\nu)\, d\nu\right] \Big/ k(\nu_0) \tag{27b}$$

as the effective width of the absorption line (12,15), we have

$$\delta\nu_{\text{eff}} = 1.571\delta\nu_L \tag{28a}$$

in the case of a purely broadened Lorentzian line and

$$\delta\nu_{\text{eff}} = 1.064\delta\nu_D \tag{28b}$$

in the case of a purely broadened Doppler line. In the case of combined Doppler and Lorentzian absorption profiles, $\delta\nu_{\text{eff}}$ will range somewhere between these two limiting values.

In the case of a line excitation, we may therefore replace ρ_{ν_0}, the spectral energy density of the continuum source, by $(\rho/\delta\nu_{\text{eff}})$. This leads to the conclusion that a continuum source, whose irradiance within the limiting spectral bandpass (i.e., $\rho_{\nu_0}\delta\nu_s$, where $\delta\nu_s$ is the bandpass of the quasi-continuum laser or any spectrometric device used between the source and the flame, depending upon which bandpass is the smaller) equals the integral irradiance of a line source (i.e., $\rho = \int \rho_\nu\, d\nu \sim \rho'_{\nu_0}\delta\nu_{\text{eff}}$, where ρ'_{ν_0} is the peak line source spectral density) will be *less* effective in exciting the atomic fluorescence by a factor equal to $\delta\nu_{\text{eff}}/\delta\nu_s$. While this is well known for conventional low-irradiance sources, it does not hold for a laser if saturation is already achieved with a continuum laser source. However, it is clear that, for a given atomic system, the laser power needed to attain a certain degree of saturation decreases by a factor $\delta\nu_{\text{eff}}/\delta\nu_s$ when the laser bandwidth is very narrow.

If we can disregard frequency fluctuations of the monochromatic output, a narrow band laser is to be preferred over a broad band one in the case of scattering problems, which are definitely more severe with continuum excitation.

4.4.3 Numerical Evaluation of Nonlinear Fluorescence Behavior

It is now useful to give a quantitative estimation of the experimental conditions necessary to approach saturation in atomic fluorescence spectrometry (20). When Eq. (8) is solved for the ratio of the atomic populations, n_2/n_1, with the assumption of steady-state conditions, the following expression is obtained:

$$\frac{n_2 g_1}{n_1 g_2} = \frac{k_{12} + B_{12}\rho_{\nu_0}}{k_{12}\exp(E/kT) + (D + \rho_{\nu_0})B_{12}} \tag{29}$$

where the statistical weights of the levels have now been considered and use has been made of the detailed balance relationship between the collisional rate constants and of the relations

$$A_{21} = B_{21}(8\pi h\nu_0^3/c^3) \equiv B_{21}D \tag{30}$$

and

$$B_{21}g_2 = B_{12}g_1 \tag{30a}$$

From the Stern-Volmer equation for the fluorescence quantum efficiency Y_{21},

$$k_{21} = A_{21}(1 - Y_{21})/Y_{21} \tag{31}$$

Combining the above equations, the following value for k_{12} is obtained:

$$k_{12} = B_{12}D[(1 - Y_{21})/Y_{21}]\exp(-E/kT) \tag{32}$$

which, after substitution into Eq. (29), gives the following general expression:

$$\frac{n_2 g_1}{n_1 g_2} = \frac{D[(1 - Y_{21})/Y_{21}]\exp(-E/kT) + \rho_{\nu_0}}{(D/Y_{21}) + \rho_{\nu_0}} \tag{33}$$

The general validity of Eq. (33) can be realized as follows: (i) When $\rho_{\nu_0} = 0$, i.e., in the absence of external radiation, the ratio of the populations deviates from the Boltzmann equilibrium ratio by the factor $1 - Y_{21}$; this factor is well known to account for radiative disequilibrium. (ii) The Boltzmann equilibrium ratio is obtained when ρ_{ν_0} is given by $D[\exp(E/kT) - 1]^{-1}$, i.e., when ρ_{ν_0} represents the Planck radiation density at the temperature T. (iii) When ρ_{ν_0} grows very large, n_2 is no more linearly related to the source density ρ_{ν_0}; and when ρ_{ν_0} approaches infinity, n_2/n_1 approaches unity; with the assumption of equal statistical weights, n_2 approaches half of the total population density.

Let us now approximate the laser to a spectral continuum source traversing the atomic vapor as homogeneous beam of cross section S (in cm^2) and characterized by a radiant flux Φ (in erg s^{-1}) and a spectral width $\delta\nu_s$ (in Hz) much larger than the absorption spectral linewidth. Therefore,

$$\rho_{\nu_0} = \frac{E_{\nu_0}}{c} = \frac{\Phi}{\delta\nu_s Sc} \tag{34}$$

where c (cm s^{-1}) is the speed of light. Using this equation, expressing D numerically and converting frequencies into wavelengths (in nm), Eq. (33) now reads

$$\frac{n_2 g_1}{n_1 g_2} = \frac{(1 - Y_{21})\exp(-E/kT) + z}{1 + z} \tag{35}$$

where $z = 6.6\times10^{-25} Y_{21}\Phi\lambda_0^5/\delta\lambda_s S$ or $z \equiv 6.6\times10^{-25} Y_{21}\lambda_0^5 E_{\lambda_0}$, where the units are erg s^{-1} for Φ, nm for λ_0, nm for $\delta\lambda_s$, cm^2 for S, and erg s^{-1} cm^{-2} nm^{-1} for E_{λ_0}. If the laser bandwidth is narrow, E_{λ_0} must be replaced by $E/\delta\lambda_{\text{eff}}$, where E is the line integral irradiance (in W cm^{-2}) of the laser and $\delta\lambda_{\text{eff}}$ will be an intermediate value between those given by Eqs. (28*a*) and (28*b*).

The parameter z clearly defines the nonlinear optical behavior of the fluorescence signal. If z is much less than unity, the linear case applies, while if z is much greater than unity, saturation is approached (if $z > 10$, saturation is reached for all practical purposes). It is important to stress here that the saturation behavior is governed by the *product* $\Phi \cdot Y_{21}$ and therefore depends upon the medium in which atoms are present. If strong quenching occurs, Y_{21} will be very low and more source power will be needed to saturate the optical transition. On the other hand, the outcome of Eq. (23), that is, the removal of the Y_{21} dependence when saturation is reached and the maximal fluorescence radiance is attained, clearly results also from Eq. (35) when z is very large because of Φ being *above* a certain threshold value.

As an example of calculation in practical situations, the following parameters were measured (20) for a tunable dye laser: $\Phi = 7.0 \pm 0.7$ kW, $\delta\lambda_s = 3.5 \pm 0.3$ Å, $S = 0.4 \pm 0.1$ mm^2. Thus, for the thallium transition at 377.6 nm in an air–acetylene flame ($Y = 0.03$), $z = 7.64$, that is, saturation was approached within 12%.

As already stated, the saturation spectral irradiance $E^s_{\nu_0}$ is defined as the spectral irradiance for which the fluorescence radiance is within a factor of 2 of the maximum possible fluorescence. This parameter is related to the atomic system via Eq. (12). From the classical theory of radiation,

$$\int \sigma(\nu)\, d\nu = (\pi e^2/mc) f_{12} \tag{36}$$

and

$$(\tau_{sp})^{-1} = (8\pi^2 \nu_0^2 e^2/mc^3) f_{12} \tag{37}$$

where e and m are the charge and mass of the electron respectively, and f_{12} is the absorption oscillator strength. Therefore,

$$E^s_{\nu_0} = (4\pi h\nu_0^3/c^2)(\tau_{sp}/\tau) = (4\pi h\nu_0^3/c^2)(Y_{21})^{-1} \tag{38}$$

or, converting again frequencies to wavelengths (in nm),

$$E^s_{\lambda_0} = 7.6\times10^{23}(\lambda_0)^{-5}(Y_{21})^{-1} \tag{39}$$

If line excitation is used, $\delta\lambda_{\text{eff}}$ has to be taken into account, as shown before.

It is finally instructive to evaluate the radiative transition rates as compared to the collisional (quenching) rates estimated in Sect. 4.3. For a continuum source, the radiational rate constant will be given by the product $B\rho_{\nu_0}$. Expressing ρ_{ν_0} in terms of E_{ν_0}, see Eq. (34), and using the relationship between B and τ_{sp}, Eq. (30), as well as that between τ_{sp} and f_{12}, Eq. (37), the following expression is obtained:

$$B\rho_{\nu_0} = 4.4\times10^3 \lambda^3 E_{\lambda_0} f_{12} \tag{40}$$

Again, $\delta\lambda_{\text{eff}}$ has to be considered for a line source.

Now if we take the experimental laser parameters used for the calculation of z (20), we estimate that, for wavelengths in the visible near-ultraviolet and for strong lines ($f \approx 1$), the excitation rate constant is of the order of 10^{11} s^{-1}, that is, at least three orders of magnitude larger than the quenching rate constant in a flame at atmospheric pressure.

4.4.4 Extension to Multilevel Atomic Systems

The theory developed in the previous sections was aimed at emphasizing as simply as possible the fundamental outcome of the influence of the laser radiation upon a two-level atomic system. Clearly, a more general approach is needed in most experimental situations in atomic fluorescence spectroscopy, because very few, if any, systems can be approximated as two-level systems. *The presence of one or more additional levels modifies the equations given, with the important consequence that the value of the laser radiation density necessary to achieve a certain degree of saturation and the limiting value of the excited atom fraction in respect to the total atomic population are changed.* We assume here that the laser excitation still couples two levels, which we indicate as level p (ground state) and level s (one of the possible excited states); but we also consider the presence of a level manifold of energy greater than s, designated as q, and of a level manifold, designated as r, whose energy is intermediate between levels p and s. By considering all possible processes of excitation and deexcitation of level s, we may write for the rate of change of the population n_s, in the *absence* of laser excitation, the following general equation:

$$dn_s/dt = \left[n_p k_{ps} + \sum_{q>s} n_q(k_{qs} + A_{qs}) + \sum_{r<s} n_r k_{rs}\right] + \\ -n_s\left[(k_{sp} + A_{sp}) + \sum_{s>r}(k_{sr} + A_{sr}) + \sum_{s<q} k_{sq}\right] \tag{41}$$

The first term on the right-hand side gives the total (collisional plus spontaneous radiative) rate of population of level s, while the second term

takes into account all possible channels of depopulation for level s. When the laser-induced radiation rates are considered, we have to add an extra term given by

$$B_{ps}\rho_{\nu_{ps}}(n_p - n_s)$$

in the case of spectral continuum excitation, or

$$B_{ps}\left[\int \rho(\nu)\, g(\nu - \nu_0)\, d\nu\right](n_p - n_s)$$

for narrowband excitation. Correspondingly, we can write a similar equation for the temporal dependence of the population of the ground state p as well as the intermediate state s.

In order to present the results in a reasonably simple way, we restrict ourselves to the case of a three-level system (see Fig. 4.7). Here, levels 1 and 3 are coupled by the laser excitation while level 2 is an intermediate level. For the sake of generality, level 2 can be radiatively coupled with level 1 only, with level 3 only, or with both. Again, we consider the laser radiation as a spectral continuum at frequency ν_{13}.

According to Eq. (41),

$$dn_3/dt = R_{13}n_1 + R_{23}n_2 - n_3(R_{32} + R_{31}) \tag{42}$$

and

$$dn_2/dt = R_{12}n_1 + R_{32}n_3 - n_2(R_{23} + R_{21}) \tag{43}$$

where, in the case of radiative coupling of level 2 with both levels 3 and 1, the following expressions hold:

$$\begin{aligned} R_{13} &\equiv k_{13} + B_{13}\rho_{\nu_0} \\ R_{23} &\equiv k_{23} \\ R_{32} &\equiv k_{32} + A_{32} \\ R_{31} &\equiv k_{31} + A_{31} + B_{31}\rho_{\nu_0} \\ R_{12} &\equiv k_{12} \\ R_{21} &\equiv k_{21} + A_{21} \end{aligned} \tag{44}$$

As mentioned before, level 2 can be coupled radiatively with level 1 only

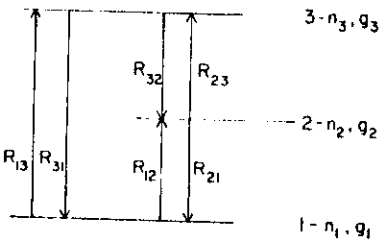

Fig. 4.7. Oversimplified sketch of a three level system, where levels can be coupled both radiationally and collisionally.

($A_{32} = 0$) or with level 3 only ($A_{21} = 0$), and the R values change accordingly. Solving for n_1, n_2, and n_3, assuming photostationary conditions,

$$\begin{aligned} n_1 &= R_{21}R_{32} + R_{31}(R_{21} + R_{23}) \\ n_2 &= R_{31}R_{12} + R_{32}(R_{13} + R_{12}) \\ n_3 &= R_{12}R_{23} + R_{13}(R_{21} + R_{23}) \end{aligned} \tag{45}$$

Since we are interested in the behavior of the system under the influence of a powerful laser beam, we can further simplify the equations by safely assuming that the collisional excitation rates to level 3 from levels 1 and 2 (i.e., k_{13} and k_{23}) are negligible with respect to the radiatively induced rates. With these simplifications, the use of Eqs. (45) and (44) gives the following ratio for the population densities:

$$\frac{n_3}{n_1} = \frac{B_{13}\rho_{\nu 0}}{B_{31}\rho_{\nu 0} + (k_{32} + A_{32} + k_{31} + A_{31})} \tag{46}$$

If we define the quantum efficiency Y_{31} as

$$Y_{31} = \frac{A_{31}}{(A_{31} + k_{31} + A_{32} + k_{32})} \tag{47}$$

then, with the help of Eq. (30),

$$\frac{n_3 g_1}{n_1 g_3} = \frac{\rho_{\nu_0} Y_{31}}{D + \rho_{\nu_0} Y_{31}} \tag{48}$$

At the limit of infinite radiation density, the laser is therefore again able to completely redistribute the populations of levels 1 and 3. However, because of the *lower* value of Y_{31} as compared with that of a two-level system, *the power needed to achieve a certain degree of saturation is increased.* This is in accordance with the definition of saturation irradiance given by Eq. (39). Therefore, *in this particular case*, neglecting an intermediate level would lead to underestimate the laser power necessary to approach saturation.

Another consequence can be derived if we consider the fraction of excited atoms in level 3 with regard to the *total* atomic density (18). From Eqs. (45) and (44), we have

$$\begin{aligned} \frac{n_3}{n_T} &\equiv \frac{n_3}{n_1 + n_2 + n_3} \\ &= \frac{B_{13}\rho_{\nu_0}(k_{21} + A_{21})}{B_{13}\rho_{\nu_0}(k_{21} + A_{21}) + (k_{31} + A_{31} + B_{31}\rho_{\nu_0})k_{12} + (k_{32} + A_{32}) \times} \\ &\quad \times (B_{13}\rho_{\nu_0} + k_{12}) + (k_{21} + A_{21})(k_{32} + A_{32} + k_{31} + A_{31} + B_{31}\rho_{\nu_0}) \end{aligned} \tag{49}$$

Equation (49), after rearranging, becomes

$$\frac{n_3}{n_T}=\frac{(B_{13}\rho_{\nu_0})\Big/\left(1+\dfrac{k_{12}}{A_{21}+k_{21}}\right)}{B_{31}\rho_{\nu_0}+(A_{31}+k_{31}+A_{32}+k_{32})+ +B_{13}\rho_{\nu_0}\left(1+\dfrac{A_{32}+k_{32}}{A_{21}+k_{21}}\right)\Big/\left(1+\dfrac{k_{12}}{A_{21}+k_{21}}\right)\Bigg]} \tag{49a}$$

and again, using Eqs. (47) and (30),

$$\frac{n_3}{n_T}=\frac{(g_3/g_1)\rho_{\nu_0}Y_{31}\Big/\left(1+\dfrac{k_{12}}{k_{21}+A_{21}}\right)}{D+\rho_{\nu_0}Y_{31}[1+(g_3/g_1)M]} \tag{50}$$

where

$$M\equiv[1+(A_{32}+k_{32})/(A_{21}+k_{21})]/[1+k_{12}/(k_{21}+A_{21})] \tag{50a}$$

In the limit of extremely high radiation density, one can see that the ratio n_3/n_T will now reach the limiting value $g_3/(g_1+g_3)$, that is, 0.5 if $g_1=g_3$, *only* if both ratios contained in Eq. (50*a*) are negligible with respect to unity.

The error made in considering a three-level system as a two-level system can be also estimated as follows. Let $n_1+n_2+n_3=n_T$, so that $n_1=n_T-n_3(1+n_2/n_3)$. Thus, it can be seen that neglecting level 2 leads to an error which depends upon the ratio n_2/n_3. This ratio can be expressed by means of Eqs. (45) and (44) as

$$\frac{n_2}{n_3}=\frac{k_{12}(k_{31}+A_{31}+k_{32}+A_{32})+k_{12}B_{31}\rho_{\nu_0}+B_{13}\rho_{\nu_0}(k_{32}+A_{32})}{B_{13}\rho_{\nu_0}(k_{21}+A_{21})} \tag{i}$$

In the limit of ρ_{ν_0} approaching infinity, Eq. (i) becomes

$$\frac{n_2}{n_3}=\frac{(g_1/g_3)k_{12}+(k_{32}+A_{32})}{k_{21}+A_{21}}=(g_1/g_3)\frac{k_{12}}{k_{21}+A_{21}}+\frac{k_{32}+A_{32}}{k_{21}+A_{21}} \tag{ii}$$

where use has been made of the relation $B_{31}=(g_1/g_3)B_{13}$. It is easy to see that

$$\frac{k_{12}}{k_{21}+A_{21}}=(1-Y_{21})(g_2/g_1)\exp(-E_2/kT) \tag{iii}$$

and therefore the error made by neglecting level 2 is given by

$$\frac{n_2}{n_3}=(1-Y_{21})(g_2/g_3)\exp(-E_2/kT)+[(k_{32}+A_{32})/(k_{21}+A_{21})] \tag{iv}$$

4.5 SHAPE OF CURVES OF GROWTH

The analytical practice of atomic fluorescence spectroscopy, and in general of all spectroscopic techniques, relies entirely upon the construction of the experimental curve of growth, which represents the plot of the analytical signal, or the log of the signal, versus the element concentration, or the log of the concentration. Extensive literature exists on the shape of such curves in atomic fluorescence (4,13,24). Generally, the lack of information on some experimental parameters does not allow the prediction of the exact shape of the curve. However, its general behavior is clearly understood; and therefore to perform the measurements in optimal conditions, the analyst should be aware of the shape that the curve of growth is expected to take.

Ideally, at low atomic concentrations (low optical densities) the integrated radiance of the fluorescence signal is linearly related to the atomic concentration, and this holds for continuum as well as for line sources of excitation. At high atomic concentrations (high optical densities), the relationship between the integrated fluorescence radiance and the atomic concentration becomes complex, the essential feature of the curve being a zero slope in the case of a continuum source and a negative slope in the case of a line source. An additional complication, which is typical of the fluorescence technique, derives from the geometry of illumination[4] and observation. A prefilter effect may be present because of the weakening of the excitation beam in a region that is not observed by the detector. Likewise, a postfilter effect occurs if there is an unexposed region between the illuminated volume and the detector, this effect being also called *self-reversal* (see Fig. 4.8). The worst case is of course given by the presence of both effects, which therefore alter the shapes of the curves of growth.

To describe the influence of the laser radiation upon the form of the analytical fluorescence curve on a qualitative basis, it is not necessary to complicate the treatment by taking into account pre- and postfilter effects. Therefore, only the phenomenon of self-absorption will be considered, with the idealized illumination geometry depicted in Fig. 4.9, where the absorption path L is restricted to a vanishingly small interval while the fluorescence emission path l toward the detector can be arbitrarily long. The assumption of homogeneity of atomic concentration

[4] In the present case, only right-angle illumination–observation is considered. However, front-surface illumination–observation (13) prevents such effects as prefilter and postfilter losses. Because the treatment given in reference 13 is generally satisfactory for laser excitation and because nothing is added to the present discussion to consider other geometries, only the conventional right-angle case is considered here.

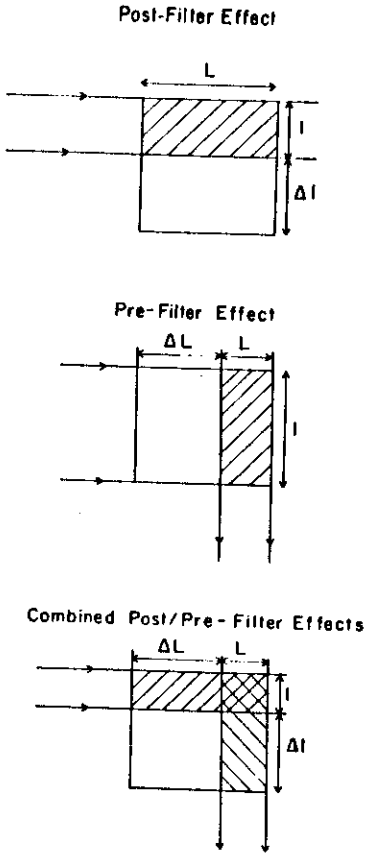

Fig. 4.8. Prefilter and postfilter effects in atomic fluorescence.

and source radiation throughout the observed region are retained, however.

Referring to Fig. 4.9, the contribution of section dx to the fluorescence spectral radiance is given by

$$dB_{l'}(\nu,x) = (A_{21}n_2h\nu/4\pi)g(\nu-\nu_0)\exp[-k(\nu)x]\,dx \tag{51}$$

Integration of this equation over x yields for the spectral radiance of the outgoing fluorescence radiation at frequency ν

$$B_{l'}(\nu) = (A_{21}n_2h\nu/4\pi)g(\nu-\nu_0)\{1-\exp[-k(\nu)l]\}/k(\nu) \tag{52}$$

Substitution for $k(\nu)$ in the denominator of the right-hand side of Eq. (52) the expression given by Eq. (24) gives

$$B_F(\nu) = (C/4\pi)(A_{21}/B)[n_2/(n_1-n_2)]\{1-\exp[-k(\nu)l]\} \tag{53}$$

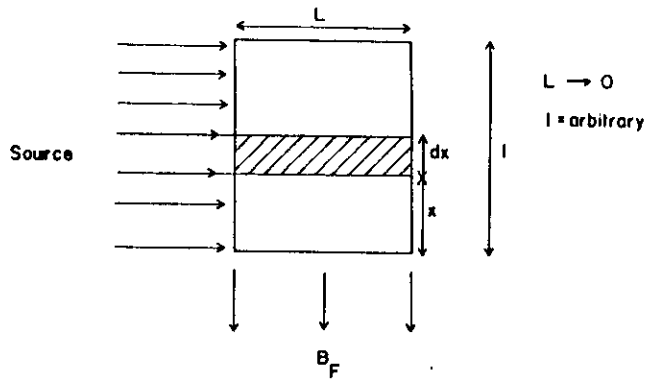

Fig. 4.9. Idealized geometry of illumination and observation of fluorescence radiance.

Integrating over frequency ν, the fluorescence radiance of the whole atom line is given by

$$B_F = \int B_F(\nu)\,d\nu = (C/4\pi)(A_{21}/B)[n_2/(n_1-n_2)]A_t \tag{54}$$

where A_t is called the total absorption factor and is defined as

$$A_t \equiv \int_{\text{line}} \{1-\exp[-k(\nu)l]\}\,d\nu \tag{55}$$

Equation (54) describes the influence of self-absorption on the radiance of the outgoing fluorescence radiation. When the laser radiation density is very high, the populations of the two levels coupled by the laser equalize, that is, $n_1 = n_2$. In this case, the absorption coefficient $k(\nu)$ will approach zero; compare Eq. (24). A series expansion of the factor A_t then gives, at the limit of $k(\nu)l \to 0$,

$$A_t = l\int k(\nu)\,d\nu \tag{56}$$

and Eq. (54) becomes

$$B_F = (C/4\pi)(A_{21}/B)[n_2/(n_1-n_2)]l\int k(\nu)\,d\nu \tag{57}$$

or, with the help of Eq. (10),

$$B_F = (l/4\pi)n_2h\nu A_{21} = (l/4\pi)h\nu A_{21}(n_T/2) \tag{58}$$

where the second expression holds for a two-level system with equal statistical weights.

In conclusion, if the system holds at saturation *for any value of the total atom concentration* n_t, the vapor becomes transparent to the resonance line radiation, and therefore the *same expressions given in the case of negligible self-absorption result.*

These theoretical predictions have been qualitatively borne out experimentally using tunable dye lasers (25, 26). Figures 4.10 and 4.11 show the effect of decreasing the laser irradiance on the atomic fluorescence curves for thallium, indium, and strontium aspirated in an air–acetylene flame. Note from the insert in Fig. 4.10 that the laser beam was focused at the edge of the flame so as to minimize self-reversal effects, which if present

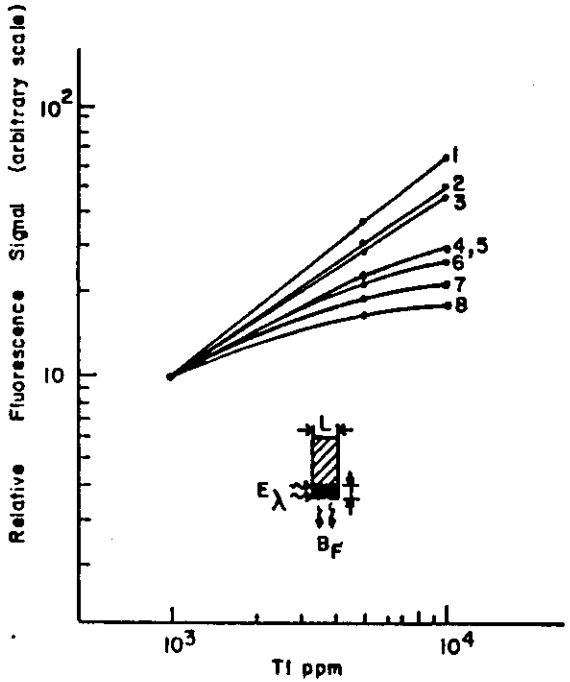

Fig. 4.10. Effect of source irradiance on the shape of resonance fluorescence curves for thallium (illumination geometry shown by insert). The fluorescence signals for each curve are relative to the signal from 1000 ppm of Tl for that specific irradiance: (1) focusing lens, no filters; (2) focusing lens, 50% transmittance filter between source and sample; (3) focusing lens, 10% transmittance filter between source and sample; (4) focusing lens, 0.1% transmittance filter between source and sample; (5) no lens, no filters; (6) no lens, 50% transmittance filter between source and sample; (7) no lens, 10% transmittance filter between source and sample; (8) no lens, 0.1% transmittance filter between source and sample. From N. Omenetto, L. P. Hart, P. Benetti, and J. D. Winefordner, *Spectrochim. Acta*, **28B**, 30 (1973). Reproduced by permission.

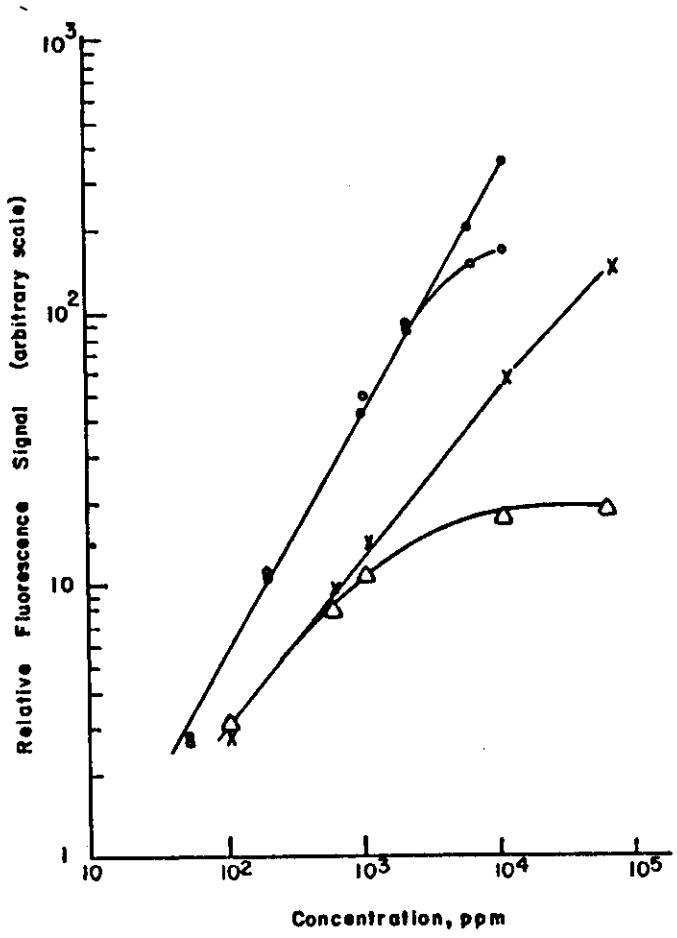

Fig. 4.11. Resonance fluorescence calibration curves for indium and strontium. The fluorescence signals for the different curves are not reported on the same scale: (●) indium, focusing lens; (○) indium, no lens; (×) strontium, focusing lens; (△) strontium, no lens. From N. Omenetto, L. P. Hart, P. Benetti, and J. D. Winefordner, *Spectrochim. Acta*, **28B**, 301 (1973). Reproduced by permission.

would have hindered the observation of the phenomenon. The same effect is shown in Fig. 4.12, which demonstrates the occurrence of saturation for magnesium atoms in an air–acetylene flame. As one can see, because of self-absorption the fluorescence due to 10 ppm is *higher* than that given by 100 ppm if the irradiance level is kept below 0.1 kW cm^{-2}. At higher irradiances the opposite holds, demonstrating that the influence of self-absorption decreases.

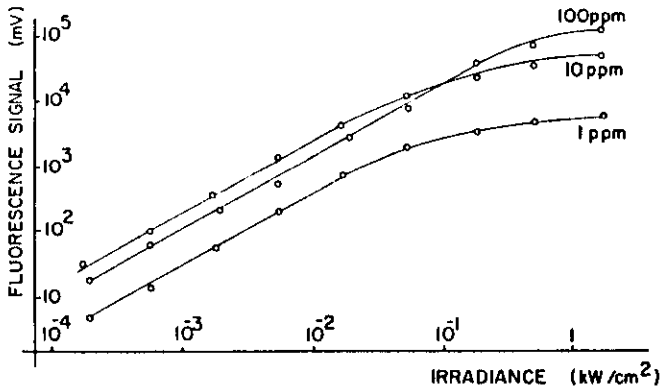

Fig. 4.12. Effect of laser irradiance on shape of saturation curve of magnesium at three different concentration levels. From J. Kuhl and H. Spitschan, *Opt. Commun.*, **7**, 256 (1973). Reproduced by permission.

4.6 LOCALIZED DIAGNOSTICS

Physical characterization of a plasma requires the knowledge of several fundamental parameters such as the plasma temperature, electron, ion and radical concentration, and so on. Most of the diagnostic techniques available use stainless steel or silica probes placed somewhere in the combustion mixture and coupled with conventional systems of analysis such as gas chromatography, infrared spectroscopy, and mass spectrometry. The insertion of a probe into the plasma allows for detailed spatial resolution of its state since sampling of a small volume can be realized. This is mandatory whenever strong inhomogeneities in composition and temperature exist due to the very nature of the combustion process.

Emission and absorption methods can be used to provide average "line of sight" measurements from which the measured quantity can be derived by somewhat elaborate procedures, such as the Abel inversion method (27). In principle, the fluorescence technique has to be considered a local sampling technique because only the region at the intersection of the excitation beam and the optical path of the detector is sampled. If the source and the observation region are narrow, the sampled volume can be very small, say, less than 1 mm^3. Early in 1962, fluorescence excited by a powerful thin electron beam (up to 30 keV) was used as a tool for local density measurements in a rarefied gas flow. The selected fluorescence volume was approximately equal to 1 mm^3 (28).

The advent of lasers tunable over most of the near-ultraviolet and visible range has opened new possibilities in the field of plasma diagnostics

(29–31). Raman spectroscopy has been successfully used as a means of investigating gaseous flame combustion products (32). Fluorescence from the (0,0) band of the $A^2\Delta$–$X^2\Pi$ electronic transition of CH in an oxyacetylene flame at atmospheric pressure was reported (33). Low concentrations of other radicals such as OH, CN, and SH have been also detected by resonance fluorescence excited with tunable dye lasers (34–36), and it is easy to foresee attractive analytical applications of molecular fluorescence in flames at atmospheric pressure (39).

The application of laser-excited fluorescence as a powerful tool for flame diagnostics is somewhat beyond the scope of the present chapter. However, it is interesting to speculate about the possibility of measuring the flame temperature and the quantum efficiency of atoms in flames by simply referring to the theory outlined in the previous paragraphs. Also, the measurement of spatial densities will be briefly discussed.

4.6.1 Flame Temperature

It has been demonstrated (37, 38) that the ratio of the anti-Stokes to the Stokes direct-line fluorescence signals obtained when a thallium solution is aspirated into a flame irradiated by a continuum source of excitation allows the calculation of the flame temperature. This method requires the calibration of the electro-optical setup as well as knowledge of the source spectral irradiances at the wavelengths of interest. If we use a laser whose power at both excitation wavelengths is sufficient to saturate the transitions, then the populations of both levels coupled by the laser will remain locked to the ratio of their respective degeneracies, and no knowledge of the source power is needed. Furthermore, if the laser is pulsed and we can measure the *peak of the time-resolved fluorescence waveform*, that is, at the point where $dB_F/dt = 0$, then the ratio of the signals emitted as resonance and anti-Stokes fluorescence yields directly the flame temperature.

Referring to Fig. 4.13, let the (homogeneous) laser beam, whose bandwidth is much larger than the absorption linewidth, be tuned to the transition $1 \rightarrow 3$ (377.6 nm), the fluorescence being measured at the same wavelength (resonance fluorescence). Under saturation conditions,

$$n_3 g_1 / n_1 g_3 = 1 \tag{59a}$$

and

$$n_1 + n_3 = (n_1)_{th} \tag{59b}$$

where $(n_1)_{th}$ is the population of the ground level *prior* to the laser irradiation. Equation (59a) then becomes

$$n_3 = [g_3/(g_1 + g_3)](n_1)_{th} \tag{60}$$

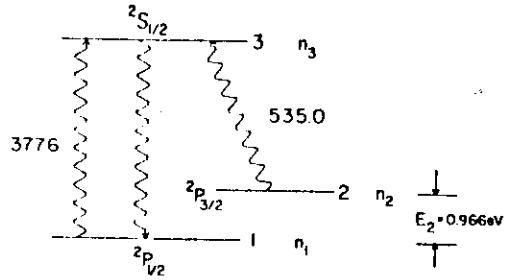

Fig. 4.13. Oversimplified sketch indicating the thallium transitions used for flame temperature measurements.

Now let the laser be tuned to the transition $2 \rightarrow 3$ (535.0 nm) while the fluorescence is still measured at 377.6 nm (anti-Stokes direct-line fluorescence). Again, for saturation conditions, the laser will equalize the weighted populations of levels 2 and 3, therefore giving

$$n'_3 g_2 / n_2 g_3 = 1 \tag{61a}$$

and

$$n'_3 = [g_3/(g_2 + g_3)](n_2)_{th} \tag{61b}$$

where n'_3 is now the population of level 3 induced by excitation at ν_{23} and $(n_2)_{th}$ is again the population of level 2 *prior* to the laser irradiation. If the system is in thermodynamic equilibrium before the irradiation, the ratio of Eqs. (60) and (61b) gives

$$n_3/n'_3 = (g_2 + g_3)/(g_1 + g_3)(g_1/g_2) \exp(E_2/kT) \tag{62}$$

The left-hand side of Eq. (62) is simply the ratio of the resonance fluorescence signals to the anti-Stokes direct-line fluorescence signals. Because the same frequency is involved, no calibration of the electro-optical detection system is required. A similar scheme, involving the fluorescence of barium ion, was proposed by Measures as a means of evaluating the electron temperature of a low-temperature plasma ($\leq$5000 K) early in 1968 (29).

It is worth stressing again here that this method can be applied only *if saturation occurs and if the fluorescence waveform can be resolved by the detection system. When the entire fluorescence waveform is integrated, as for example in a measurement with a boxcar whose gate aperture is similar to or larger than the fluorescence pulse, the usual complications arise because of the collisional terms which have to be taken into account in deriving a final relationship.* Preliminary attempts to obtain *relative* temperature profiles in nonshielded air–acetylene and nitrous oxide–acetylene flames at atmospheric pressure have been reported, demonstrating the

expected existence of significant thermal gradients toward the outer, cooler zones of the flame (39).

If the three-level system of thallium is treated as in Sect. 4.4.4 and the collisional (de-)activation of level 2 with level 1 is considered, we come to the following approximate relationship:

$$n_3/n_3 = (k_{21}/k_{12})\left[\left(1 + \frac{k_{31} + A_{31}}{k_{21}}\right)\Big/\left(2 + \frac{k_{12} + A_{32}}{k_{21}}\right)\right] \tag{i}$$

where, for the sake of simplicity, the statistical weights have been taken as equal, that is, $g_1 = g_2 = g_3$. Equation (i) still shows the temperature dependence of the fluorescence ratio n_3/n'_3 via the ratio

$$k_{21}/k_{12} = \exp(E_2/kT) \tag{ii}$$

However, in this case it would not be possible to obtain an *absolute* value for T because the collisional rate constants k_{21}, k_{31}, and k_{32} are not known.

4.6.2 Quantum Efficiency

It has been shown in Sect. 4.4.3, see Eq. (35), that the saturation parameter z contains the product of the laser spectral irradiance times the quantum efficiency of the transition. From Eq. (35), if z is much greater than the first term in the numerator, it is easy to show that

$$n_T/n_2 = (g_1/g_2)(1/z) + [(g_1 + g_2)/g_2] \tag{63}$$

It follows that the plot of $(B_F)^{-1}$, proportional to $(n_2)^{-1}$, as a function of Φ^{-1}, proportional to z^{-1}, should yield a straight line whose slope varies with Y^{-1}. Moreover, the ordinate axis of this plot can be simply scaled in *absolute* values of n_T/n_2 because, for z approaching infinity, n_T/n_2 approaches the ratio $(g_1 + g_2)/g_2$.

Again, for a three-level system, expressing n_1 as a function of $n_T = n_1 + n_2 + n_3$ and proceeding as in Sect. 4.4.4, we have to modify Eq. (63) as follows:

$$(n_T/n_3) = (g_1/g_3)(1/z) + \left[\frac{(g_1 + g_3)}{g_3} + (1 - Y_{21})\frac{g_2}{g_3}\exp(-E_2/kT) + \frac{(k_{32} + A_{32})}{k_{21}}\right]$$

As a consequence, it is not possible to scale the ordinate values of this plot in absolute quantities because of our lack of knowledge of the collisional rate constants involving level 2 with the other two levels.

A similar possibility derives from Eq. (39), which shows that the quantum efficiency is inversely proportional to the saturation spectral irradiance of the source. If we make a plot of the fluorescence radiance

versus laser power up to saturation, it is only necessary to interpolate to the power needed to reduce the maximal fluorescence radiance to one half. The quantum efficiency can therefore be calculated from Eq. (39), provided the spectral bandwidth of the laser and its cross section in the atomic system are known.

4.6.3 Concentrations

As shown before, see Eq. (23), it is possible to measure concentrations (species cm^{-3}) within the flame gases provided that saturation has been reached and the maximal fluorescence radiance is measured in absolute units. The same can be done with transient fluorescent signals, as speculated by Daily (40), who called the technique *pulsed resonance spectroscopy* (PRS). This technique has been utilized by Haas (41) for low-pressure laboratory plasma diagnostics. When the fluorescence waveform is observed, the measurement of the decay time will give the quenching rate constant (assuming a two-level system and a simple exponential decay) while the measurement of the time-integrated signal will give the atomic concentration.

Daily (40) also derived an expression for the concentration, n_T, in terms of S/N ratio, assuming that this ratio depends exclusively on the uncertainty in time in the estimation of the decay constant. Under these conditions, the detection limit was given by the following relationship:

$$(n_T)_{\text{lim}} \cong \left(\frac{2\pi}{\epsilon\eta\Omega V}\right)\left(\frac{g_1+g_2}{g_2}\right)\left(\frac{k_{21}+A_{21}}{A_{21}}\right)\left(\frac{S}{N}\right)^3_{\text{lim}} \quad (64)$$

where $(S/N)_{\text{lim}}$ is the limiting detectable S/N ratio, ϵ is the quantum efficiency of the photocathode of the detector, η is the overall optical transfer efficiency, Ω is the solid angle of the collection optics, and V is the effective focal volume of the collection optics. Typical values of these parameters, for $S/N = 10$, result in the possibility of detecting $\geq 10^9$ species cm^{-3} via electronic (UV-visible fluorescence) resonance spectroscopy and $\geq 10^{13}$ species cm^{-3} via vibrational (IR fluorescence) resonance spectroscopy. Therefore, PRS appears quite useful for concentration measurements of atoms and molecules in flames.

4.7 INSTRUMENTATION

4.7.1 Dye Laser Characteristics

Analytical studies using laser excitation have been carried out with both pulsed and cw lasers. We emphasize here the use of pulsed tunable dye lasers, since cw results are reported elsewhere in this book (Chapter 8). Tunable dye lasers may be pumped by a flashlamp or by another laser. Typical values obtainable in terms of power, duty cycle, and spectral bandwidth are shown in Table 4.2, where the approximate ranges of tunability achieved with the most important classes of dyes are also reported. From this table one can see that the pulse characteristics are usually determined by the pumping source. With nitrogen, ruby, and neodymium lasers, the pulse length is short, few tens of nanoseconds and even less than 10 ns for nitrogen, while flash lamp excitation gives more energy per pulse due to the increased length of the pulse itself. However, with nitrogen laser excitation, the repetition rate can be much higher.

The laser used by Winefordner et al. (10, 11, 20) consisted of a commercial dye laser unit (AVCO Everett Research Laboratory, Massachusetts) with a grating in the cavity replacing one laser mirror, pumped by a nitrogen laser. The parameters characterizing the laser output were as follows: Nitrogen laser (337.1 nm): 120 kW peak power, pulse width 8–10 ns, repetition rate 1–100 Hz, beam size 3.2×51 mm, time jitter 1–2 ns. Dye laser: tunability range 357–650 nm, with ten interchangeable

TABLE 4.2
Typical Values of Dye Laser Performances[a]

Pumping mode	Power, W: Peak	Power, W: Mean	Bandwidth, cm^{-1} [b]	Pulse length, ns	Repetition rate, s^{-1}	Duty cycle
Nitrogen	10^4–10^5	<0.05	10^{-2}–10^{-1}	3–10	100–500	$<2\times10^{-6}$
Ruby-Sh	10^4–10^6	$<10^{-3}$	10^{-2}–10^{-1}	10–30	<0.1	$\approx10^{-9}$
Nd-Sh	10^5–10^7	$<10^{-3}$	10^{-2}–10^{-1}	10–30	<0.1	$\approx10^{-9}$
Ruby	10^5–10^8	$<10^{-3}$	10^{-2}–10^{-1}	10–30	<0.1	$\approx10^{-9}$
Nd	10^4–10^7	$<10^{-3}$	10^{-2}–10^{-1}	10–30	<0.1	$\approx10^{-9}$
Flash lamp (50 ns)	10^3–10^5	$<10^{-3}$	10^{-2}–10^{-1}	100–200	<0.1	$\approx10^{-9}$
Flash lamp (200 ns)	10^4–10^5	0.05–0.5	10^{-3}–10^{-1}	300–1000	5–20	$\sim10^{-5}$
Argon (cw)	—	0.02–1	10^{-5}–10^{-3}	—	—	—

0.3 0.4 0.5 0.6 0.7 0.8 0.9 1.
λ, μm
—— scintillator dyes
——— coumarines
———— rhodamines
————— cresyl violet
—————— cyanines

[a] Values given in the Table do not represent ultimate performances achievable. Flash lamp pumping results are given both for 50 ns and 200 ns lamp rise times. Output characteristics of a cw argon ion laser are included for comparison purposes.

[b] $\Delta\bar{\nu}(cm^{-1})\times\lambda^2(cm^2)\times10^7(nm\,cm^{-1}) = \Delta\lambda(nm)$
$\Delta\bar{\nu}(cm^{-1})\times3\times10^{10}(cm\,s^{-1}) = \Delta\nu(s^{-1})$

TABLE 4.3
Laser Spectral Output with Rhodamine 6G, $2.5 \times 10^{-4} M$ Solution in Methanol, Pump Energy 8.5 J, Reflectivity of the Laser Mirrors 99.8 and 50%

Laser cavity filter	Spectral half-width (FWHM), Å	Peak power, kW	Spectral peak power density, kW Å^{-1}
No frequency-selective elements in the cavity	61	17.5	0.29
Interference filter (FWHM = 60 Å, peak transmission 96%)	7	11.4	1.63
Interference filter + Fabry-Perot etalon	$<10^{-2}$	7.6	>760
Interference filter (FWHM = 6 Å, peak transmission 84%)	1	6.1	6.1
Interference filter + Fabry-Perot etalon	$<10^{-2}$	5.9	>590

[a] Data taken from J. Kuhl, G. Marowsky, P. Kunstmann, and W. Schmidt, *Z. Naturforsch.*, **27A**, 601 (1972). Reproduced by permission.

dyes, peak power greater than 10 kW, pulse width 2–8 ns, spectral half-width ranging from 0.1 to 1 nm, therefore justifying the assumption made (20) that the source could be assimilated to a spectral continuum. In most experiments, 10 Hz was used as the repetition rate.

The laser used by Kuhl et al. (40–42) was a flash lamp-pumped dye laser (Carl Zeiss, Oberkochen, West Germany) providing approximately 10 kW peak power with 200 ns pulse width for a $5 \times 10^{-5} M$ solution of rhodamine 6G in methanol. Care was taken by these authors to reduce the spectral bandwidth of the laser output by inserting frequency-selective elements in the laser cavity. Table 4.3 summarizes their results of power and linewidth measurements. As one can see, at the expense of a factor of 2–3 only for the output power, the spectral power density increased considerably. The emitted intensity per unit frequency interval was raised by a factor of 21 by the insertion of the interference filter alone and by at least 2000 when the filter and the Fabry-Perot interferometer were both present in the cavity. Compared to a grating, the interference filter in the cavity has the advantage of providing a high value of angular dispersion and negligible adjustment demands (42). With this system, laser bandwidths as small as 5×10^{-4} nm were obtained.

It is known that, because of strong absorption of the fluorescence emission by molecules in the excited singlet state, it is impossible to find a highly efficient laser dye for wavelengths shorter than 300 nm. Because of this, all experiments requiring an excitation below 300 nm take advantage

of the properties of nonlinear crystals such as ADP (ammonium dihydrogen phosphate) and KDP (potassium dihydrogen phosphate) to generate the second harmonic when visible laser radiation impinges on these crystals. Because this is a nonlinear process, the second harmonic output power goes with the square of the power in the fundamental frequency. When the beam spread of the laser is reduced by mode selection, peak power conversion efficiencies between 10 and 18% can be achieved even for laser output powers as low as 15–25 kW (43). With 10 kW peak power at 566.6 nm, the use of a KDP crystal 38 mm long, cut and polished for $\lambda = 560$ nm, resulted in the generation of the second harmonic at 283.3 nm with a peak power of 400 W (44). (The alternative to doubling the dye laser output is to utilize multiphoton excitation, that is, doubling within the sample cell itself.)

4.7.2 Atomizers

Atomizers used in analytical atomic fluorescence excited by conventional low-intensity sources include flames and electrothermal devices such as graphite cuvettes, carbon rods, and so on. One of the practical disadvantages of the fluorescence technique often stressed in the pertinent literature (4,13) is that high quantum efficiency flames have to be used to maximize the fluorescence signals. Therefore, combustion mixtures containing argon as a diluent, for example, oxygen–argon–hydrogen flames, have been preferred because of the small quenching cross section of argon. However, compared to air–acetylene and nitrous oxide–acetylene mixtures, the argon-diluted flames containing hydrogen as fuel have a relatively low atomization capability that can cause severe scattering[5] problems when analysis of practical samples is attempted by means of resonance fluorescence. On the other hand, even in the absence of

[5] It should be stressed that scattering occurs not only from particles in the flame gases as well as dust particles but also occurs from Rayleigh scattering of radiation from molecules and atoms, and therefore the latter phenomenon represents a fundamental limit of resonance fluorescence measurements. The Rayleigh scattering cross sections increase as λ_i^{-4}, where λ_i is the incident laser wavelength. The Rayleigh scattering (due to atoms and molecules) contribution in flames corresponds to ~200–2000 counts s^{-1} for a typical fluorescence setup in which a 150-W EIMAC cw conventional xenon arc lamp is used as the source of excitation. Therefore, assuming a 10-s integration, and assuming shot noise due to the scatter is limiting, the noise is ~100 counts, which is typically the limiting noise level in convent onal AF with conventional light sources, particularly in the UV region. Of course, in the visible region (≥300 nm), flame background noise may even exceed scatter noise in some spectral regions. In any event, the magnitude of scatter noise inherent in any fluorescent technique is sufficient to justify extensive studies of nonresonance fluorescence for analysis.

scattering, conventional lock-in detection does not allow taking full advantage of the good atomization efficiency of a high-temperature flame, such as the nitrous oxide–acetylene flame (~2900°K) for refractory elements (Al, V, Mo, etc.) because the prohibitive flame background in certain spectral regions results in highly noisy signals.

The use of a pulsed laser and gated detection (see below) should permit full exploitation of such atomization capabilities, and this despite the low value of the quantum efficiency of the fluorescence.

Flames used in laser experiments include air–hydrogen, air–acetylene, and nitrous oxide–acetylene mixtures, supported by conventional circularly or rectangularly shaped burners. Results have also been reported for carbon rod atomization (44).

4.7.3 Detection Systems and Signal-to-Noise Considerations

Detection systems for laser-excited fluorescence have consisted of photomultiplier tubes coupled with either a sampling oscilloscope or a boxcar integrator. It has been stressed (11,45,46) that photomultipliers suitable for pulsed operation must possess certain specific requirements such as short transit time of the electron cloud, small transit time spread, short rise time, and minimal parasitic capacitance. In addition, the tube should also be capable of sustaining high-peak anodic currents. For pulsed work, the dynode chain typical of normal operation is modified by placing capacitors between the dynodes. The laser output is usually monitored by a photodiode or a photocell. If the detector is calibrated, power measurements can be performed with the use of neutral density filters. Signals are fed into an oscilloscope and into a boxcar integrator.

The boxcar (45–47) is the analogue of a sampling oscilloscope with all the gadgets and flexibility that one might add externally for signal processing. Both "scan mode" of operation and "single point" measurements are possible with commercially available boxcars. Basically, the instrument performs a sample and hold operation, the sampling time being determined by an appropriate reference pulse that bears a definite relationship to the signal of interest. When pulse measurements are performed, the timing and width of the sampling window are adjusted so as to coincide with the occurrence of the fluorescence pulse. More details of boxcar operation and measurements are discussed in Chapter 7.

This gated operation results in a significant improvement in signal-to-noise ratio if the system under study is background noise[6] limited, since the detector is "on" only during the laser "on" time, (or a short delay

[6] The background must not be source induced such as molecular fluorescence.

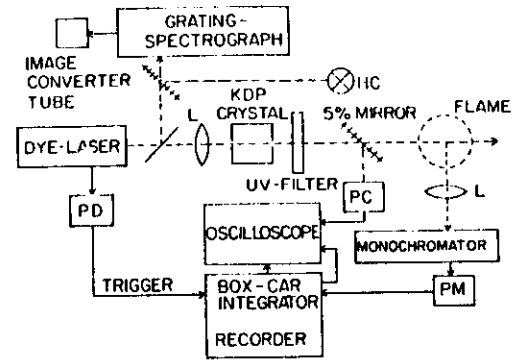

Fig. 4.14. Schematic diagram of a typical experimental setup for laser-excited fluorescence studies. J. Kuhl and H. Spitschan, *Opt. Commun.*, **7**, 256 (1973). Reproduced by permission.

after), so that background noise (shot and fluctuation), which is also measured only during this short time interval, will be greatly diminished. It has been shown (48) that if shot noise (source and background) dominates over fluctuation noise (source and background), the gain obtained when the S/N ratio given by pulsing the source and gating the detector (po/go) over that obtained with cw sources and cw operation (cw/cw) is given by the relations

$$\psi\frac{\text{po/go}}{\text{cw/cw}} = \{B^{s,p}_{ave}/B^{s}_{ave}\}\{1/(ft_p)\}^{1/2} = (B^{s}_{peak}/B^{s}_{ave})(ft_p)^{1/2} \qquad (65a)$$

and

$$\psi\frac{\text{po/go}}{\text{cw/cw}} = (B^{s,p}_{ave}/B^{s}_{ave})^{1/2} \qquad (65b)$$

where $B^{s,p}_{ave}$ represents the average radiance of the pulsed source, B^{s}_{ave} is the average radiance of the cw source, f is the repetition rate, t_p is the duration of the light pulse, and B^{s}_{peak} is the peak radiance of the pulsed source.

Equation (65a) holds if the system is background noise limited, while Eq. (65b) results when the limiting noise is source carried, that is, fluorescence or scattering. Clearly, no advantage will be obtained if the fluorescence measurements are plagued by scattering. Moreover, the equations derived assume that the fluorescence signal does follow linearly the source radiance, that is, no limiting value to the fluorescence due to the occurrence of saturation was considered.

Figure 4.14 shows a complete experimental setup for laser-induced flame fluorescence measurements. The flash lamp-pumped dye laser

output is frequency doubled by a KDP crystal. A photodiode (PD) serves for triggering purposes. Beam splitters are used to either monitor the laser output power with a photocell (PC) or for spectral tuning of the generated ultraviolet radiation by observing the emission spectrum of a hollow-cathode lamp (HC) and that of the laser in the focal plane of a 1.5-m Czerny-Turner grating spectrograph by means of an UV image converter tube. The fluorescence signals are isolated by a monochromator, measured with a fast-response photomultiplier, and fed to a boxcar integrator.

4.8 ANALYTICAL RESULTS

It is helpful at this point to stress the analytical implications of the theory outlined in the previous paragraphs. Characteristic features of laser-excited fluorescence should include the following:

1. *Extended tunability* over most of the UV-visible range with a spectral bandwidth variable from 1 nm down to less than 10^{-4} nm. This implies that the strongest absorption lines of most elements can be reached with approximately the same peak power (no filters are needed) and that scattering can be eliminated whenever nonresonance transitions are intense enough to be analytically useful. An example is shown in Fig. 4.15 for the atomic fluorescence of niobium excited in a nitrous oxide–acetylene flame, demonstrating the potential utility of fluorescence lines *other than* the resonance line where strong scattering would indeed significantly deteriorate the analytical results or even make the analysis impossible.

2. *Independence of fluorescence signal upon source stability* if saturation is achieved. This outcome has been qualitatively seen in flames (20) where the peak-to-peak noise in the fluorescence signal obtained enlarging the beam into the flame (and therefore decreasing the source irradiance) compared with that given when the laser spot was focused (saturation more closely approached) increased more than the value which one would have predicted by taking into account the relative magnitude of the signals. However, this was not the case for electrothermal atomization (44) of lead where the relative standard deviation of the fluorescence signal, as high as 37%, did not show a significant decrease at high irradiances. This latter behavior was partially attributed to the pronounced inhomogeneity of the atomic cloud distribution during the carbon rod atomization cycle, with the result that clusters of analyte atoms were vaporized at different times causing rapid fluctuations in the fluorescence signal, which were resolved because of the short time constant (<0.1 μs) of the detection system. Moreover, considering the laser

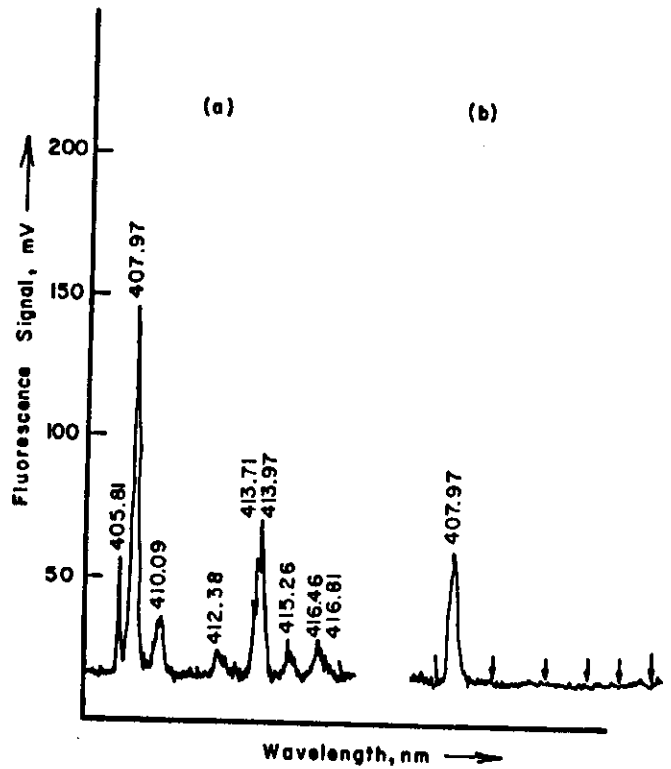

Fig. 4.15. Atomic fluorescence of niobium-wavelength scanning: 200 μm slit (0.4 nm spectral band width). (*a*) Laser excitation set at 407.97 nm, 1000 ppm Nb; the intensity of the 407.97 nm line has been decreased 2.5 times as compared to the intensity of the other lines; (*b*) laser excitation set at 407.97 nm, 1000 ppm W; the intensity scattered at 407.97 nm has been also decreased 2.5 times and is therefore directly comparable to the Nb signal observed in (*a*) at the same wavelength. From N. Omenetto, N. N. Hatch, L. M. Fraser, and J. D. Winefordner, *Spectrochim. Acta*, **28B**, 65 (1973). Reproduced by permission.

bandwidth (<0.002 nm) and the length of the laser cavity, an estimation of the lead absorption linewidth of 0.0006 nm corresponded to roughly six mode spacings of a total of about 20 longitudinal modes. Since the oscillatory strength of these modes varied considerably from shot to shot and some may even have vanished, this caused the irradiance to vary considerably over the absorption linewidth.

3. *Less stringent dependence on the quantum efficiency of fluorescence.* This has been shown theoretically to hold for a two-level system and for a three-level system if a given definition of quantum efficiency is considered, compare Eqs. (47)–(48). The importance of such a consequence is obvious since it means that one can use atomizers with high atomization

efficiencies even if strong quenching is present. With reference to flames, it means, for example, that the fluorescence signal is not expected to be greater in an oxygen–hydrogen flame diluted with argon than the signal obtained in hydrocarbon flames containing nitrogen as the major constituent. This point, which clearly assumes identical atomization efficiencies for the two combustion mixtures, has not yet been proved experimentally.

4. *Improved linearity of the calibration curves.* As shown in Sect. 4.5, if the source irradiance is such that the atomic system is saturated at any value of the population density, the absorption coefficient goes to zero and no self-absorption occurs, thus making the calibration curve obtained under idealized illumination conditions linear over all concentration ranges. This holds for a continuum as well as for a line source of excitation. However, unavoidable tradeoffs in practical situations do not allow the observation of such extended linearity. For example, when the laser beam is focused at the center of the atomizer, postfilter (self-reversal) effects in the observation path toward the detector have to be certainly included to account for the observed shape of the curve. If the beam is defocused to illuminate a larger volume of atoms, the irradiance can decrease to the point where saturation is no more approached, and therefore the shape of the curve will resemble that obtained with conventional sources of excitation. Linear dynamic ranges of three to five orders of magnitude are common for laser-excited fluorescence. Figure 4.16 compares relative fluorescence curves of growth obtained when lead vapor from a carbon rod atomizer is excited with a hollow-cathode lamp, an electrodeless discharge lamp, and a dye laser. The linear range, defined as the ratio of upper to lower concentration limits, found here was 1.25×10^5, 3.33×10^3, and 1×10^3 for dye laser, electrodeless discharge lamp, and hollow-cathode excitation, respectively. The lower concentration limit corresponds to the detection limit while the upper limit was defined as the lead concentration resulting in a signal whose deviation from linearity did not exceed 5%.

Table 4.4 summarizes the limits of detection obtained with laser excitation in flames and compares them with those obtained by other conventional sources operated in the pulsed mode and with the ones given by cw sources. Limits of detection are usually defined on the basis of a *S/N* (rms) ratio of 2.

The column giving the laser results in Table 4.4 has more entries than the other columns; this is due to the fact that several elements such as the rare earths and some transition elements were never studied before by conventional fluorescence because they required both the nitrous oxide–acetylene flame and high-intensity sources, most of which were not

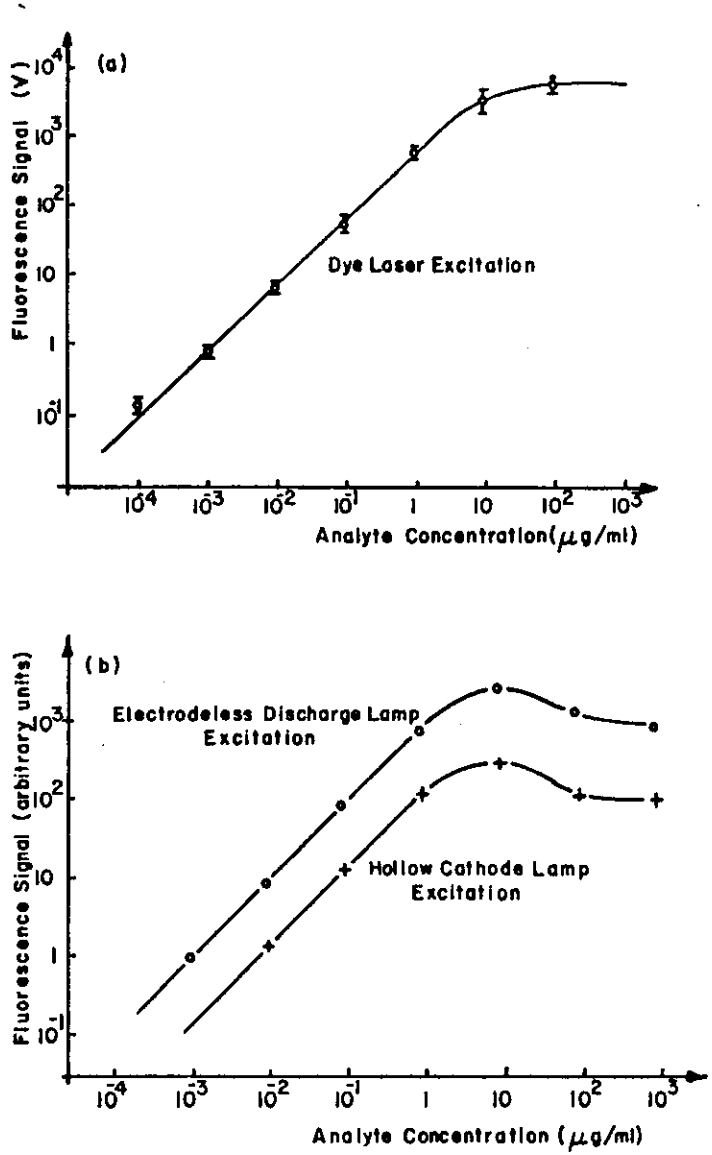

Fig. 4.16. Analytical curves for flameless atomic fluorescence of lead. Exciting light sources: (*a*) dye laser; (*b*) EDL and HCL. From S. Neumann and M. Kriese, *Spectrochim. Acta*, **29B**, 127 (1974). Reproduced by permission.

TABLE 4.4

Comparison Between Detection Limits Obtained with Dye Lasers and Conventional Sources in Atomic Fluorescence Flame Spectrometry[a]

	Limits of detection, $\mu g\ ml^{-1}$				
	Pulsed sources			cw Sources	
Element	Laser	Line	Continuum	Line	Continuum (Eimac 150 W)
Ag	—	0.004	0.02	0.0001	0.006
Al	0.005	0.07	—	0.1	0.2
Au	—	—	—	0.003	—
Be	—	—	0.2	0.01	0.07
Ca	0.005	0.0003	—	0.02	—
Cd	—	0.004	0.03	0.000001	0.01
Ce	0.5(I)	—	—	—	—
Co	0.2	0.007	0.1	0.005	0.02
Cr	0.02	0.004	—	0.05	0.01
Cu	—	0.002	—	0.0005	—
Dy	0.3(I)	—	—	—	—
Er	0.5	—	—	—	—
Eu	0.02	—	—	—	—
Fe	0.3	0.008	—	0.008	—
Ga	0.02	—	—	0.01	—
Gd	0.8(I)	—	—	—	—
Hf	100.	—	—	—	—
Ho	0.1	—	—	—	—
In	0.002	—	—	0.1	—
Lu	3.	—	—	—	—
Mg	0.0003	0.001	0.004	0.001	0.0003
Mn	0.01	0.002	0.03	0.006	0.004
Mo	0.3	0.06	—	0.5	0.2
Nb	1.	—	—	—	—
Nd	2.	—	—	—	—
Ni	0.05	0.02	—	0.003	—
Os	150.	—	—	—	—
Pb	0.03	0.07	—	0.01	—
Pr	1(I)	—	—	—	—
Rh	0.1	—	—	3.	—
Ru	0.5	—	—	—	—
Sb	—	0.05	—	0.05	—
Sc	0.01	—	—	—	—
Se	—	1.	—	0.04	3.
Sm	0.1(I)	—	—	—	—
Sn	—	0.2	—	0.05	—
Sr	0.01	0.01	—	0.03	—
Tb	0.5(I)	—	—	—	—
Ti	0.1	—	—	4.	0.9
Tl	0.02	—	—	0.008	—
Tm	0.1	—	—	—	—
V	0.5	0.2	—	0.07	0.1
Yb	0.01	—	—	—	—
Zn	—	0.003	0.1	0.00001	0.006

[a] Table reprinted with permission from N. Omenetto, *Anal. Chem.* **48**, 75A (1976). Copyright by the American Chemical Society. Values are for analyte in aqueous solutions; (I) means ionic fluorescence.

available. On the other hand, it can be seen that the laser detection limits are not so spectacular as one would have predicted. The erratic quality of these results needs careful interpretation on the basis of parameters such as laser output variations (sometimes up to 25%) if saturation is not approached and limiting noise in the system. Unlike the fluorescence, the scattering signal keeps increasing with the laser irradiance, and therefore a compromise must be reached between scattering and signal stability. It is important to stress that most of the laser limits reported in Table 4.4 were obtained on nonresonance transitions, and this is a definite advantage from the scattering point of view. Another point is that in several cases (e.g., Mn, Co, Fe, Ni, Os, Ru, Rh, etc.), the most sensitive *absorption* lines could not be reached because frequency doubling was not available.

Certainly, more experimental work is needed in this respect, and far better results would be achieved if the range of tunability could be extended down into the 200–300 nm region. When resonance fluorescence is the only possibility, the use of a narrow bandwidth laser output is to be preferred. In this way, scattering can be compensated by recording the signal at two wavelengths, one tuned at the center and the other just outside the absorption profile.

4.9 CONCLUDING REMARKS

As we have repeatedly pointed out in the appropriate paragraphs, the theory given in this chapter *accounts only for the basic features* of the results obtained experimentally. Indeed, no quantitative agreement between theory and experimental results could be claimed in most cases. It is essential to stress that this is so because many complicating effects have been purposely neglected in the derivation given. Although a number of concomitant effects induced by extremely high radiation densities ($>10^7\ W\ cm^{-2}$), such as self-focusing of the laser beam, multiple photon absorption, pulse shape distortion, and so on, would probably not alter the experimental results for flames, the parameters characterizing the laser output power do certainly require a more realistic evaluation. For example, it was always assumed that the laser beam was homogeneous and of constant irradiance while traversing the atomic vapor. In practice, however, the laser has both a *spatial* and a *temporal* profile with extremely large gradients. This causes the saturation effects to occur at different times and at different radii of the excited atom volume. Saturation of the transition will initially take place along the laser axis, where the power density is greatest, and then expand radially as the power increases. As a consequence, although the temporal variation of the

fluorescence signal depends only on the local laser power and the local conditions of the atomic system, the signal detected by the photomultiplier will be due to the average effect over the whole observed excited volume (49). Therefore, *different* results are to be expected when time-integrated measurements are compared with signals measured at the peak of the time-resolved fluorescence waveform. In addition, the theory was considered for idealized geometries of excitation and observation of the fluorescence signals. It is almost impossible to exclude completely prefilter as well as postfilter effects in practical measurements when the concentration of the analyte becomes significant.

Doubtlessly, more experiments are needed to gain full insight into the physics of the process and to unambiguously compare theoretical predictions with experimental results. Up to now, analytical papers on laser-excited atomic fluorescence as a means of chemical analysis are still scanty, both because of the high cost required to set up on a laboratory scale a dye laser tunable over the whole spectral range of interest (strong commercial competition might improve this situation now) and because the results obtained for flames at atmospheric pressure are not significantly superior to those already achieved by conventional atomic absorption and emission spectroscopy.

Nevertheless, quite spectacular results have been achieved for cw laser excitation (see Chapter 8), and research on efficient frequency doubling down to 200 nm is under way.[7] Therefore, this field will receive increasing attention, and new results are expected in the future.

References

1. A. C. G. Mitchell and M. W. Zemansky, *Resonance Radiation and Excited Atoms*, Cambridge University Press, New York, (1971).
2. C. Th. J. Alkemade, Proc. 10th CSI, Spartan Books, Washington, D.C. (1963), p. 143.
3. J. D. Winefordner and T. J. Vickers, *Anal. Chem.*, **36,** 161 (1964).
4. V. Sychra, V. Svoboda, and I. Rubeška, *Atomic Fluorescence Spectroscopy*, Van Nostrand-Reinhold, New York (1975).
5. R. F. Browner, B. M. Patel, T. H. Glenn, M. E. Rietta, and J. D. Winefordner, *Spectrosc. Lett.*, **5,** 311 (1972).
6. J. P. Webb, *Anal. Chem.*, **44,** 30A (1972).
7. J. R. Allkins, *Anal. Chem.*, **47,** 752A (1975).
8. J. I. Steinfeld, MIT Report, 1975; *CRC Crit. Rev. Anal. Chem.*, **5,** 225 (1975).
9. N. Omenetto and J. D. Winefordner, *Appl. Spectrosc.*, **26,** 555 (1972).

[7] The use of a KPB (potassium pentaborate) crystal allows tuning below 250 nm.

10. N. Omenetto, N. N. Hatch, L. M. Fraser, and J. D. Winefordner, *Spectrochim. Acta*, **28B,** 65 (1973).
11. L. M. Fraser and J. D. Winefordner, *Anal. Chem.*, **44,** 1444 (1972).
12. C. Th. J. Alkemade and P. J. Th. Zeegers, in *Spectrochemical Methods of Analysis*, J. D. Winefordner, Ed., Wiley, New York (1971).
13. J. D. Winefordner, S. G. Schulman, and T. C. O'Haver, "Luminescence Spectrometry in Analytical Chemistry," in *Chemical Analysis*, Vol. 38, P. J. Elving, J. D. Winefordner, Eds., Wiley, New York (1972).
14. P. L. Lijnse and R. J. Elsenaar, *J. Quant. Spectrosc. Radiat. Transfer*, **12,** 1125 (1972).
15. C. Th. J. Alkemade, *Pure Appl. Chem.*, **23,** 73 (1970).
16. M. Hercher, *Appl. Opt.*, **6,** 947 (1967).
17. L. Huff and L. G. DeShazer, *J. Opt. Soc. Amer.*, **60,** 157 (1970).
18. E. H. Piepmeier, *Spectrochim. Acta*, **27B,** 431 (1972).
19. E. H. Piepmeier, *Spectrochim. Acta*, **27B,** 445 (1972).
20. N. Omenetto, P. Benetti, L. P. Hart, J. D. Winefordner, and C. Th. J. Alkemade, *Spectrochim. Acta*, **28B,** 289 (1973).
21. J. Kuhl, S. Neuman, and M. Kriese, *Z. Naturforsch.*, **28A,** 273 (1973).
22. L. de Galan and H. C. Wagenaar, *Meth. Phys. Anal.*, 10 (Sept. 1971).
23. W. Lange, J. Luther, and A. Stendel, *Adv. Atom. Mol. Phys.*, **10,** 173 (1974).
24. H. P. Hooymayers, *Spectrochim. Acta*, **23B,** 567 (1968).
25. N. Omenetto, L. P. Hart, P. Benetti, and J. D. Winefordner, *Spectrochim. Acta*, **28B,** 301 (1973).
26. J. Kuhl and H. Spitschan, *Opt. Commun.*, **7,** 256 (1973).
27. H. R. Griem, *Plasma Spectroscopy*, McGraw-Hill, New York (1964).
28. E. O. Gadamer, UTIAS Report No. 83 *Institute of Aerophysics, University of Toronto* (March 1962).
29. R. M. Measures, *J. Appl. Phys.*, **39,** 5232 (1968).
30. D. E. Jensen and B. E. L. Travers, paper given at IUPAC International Symposium on Plasma Chemistry, Kiel, Germany (September 1973).
31. S. S. Penner and T. Jerskey, *Ann. Rev. Fluid Mech.*, **5,** 9 (1973).
32. W. M. Arden, T. B. Hirschfeld, S. M. Klainer, and W. A. Mueller, *Appl. Spectrosc.*, **28,** 554 (1974).
33. R. H. Barnes, C. E. Moeller, J. F. Kircher, and C. M. Verber, *Appl. Opt.*, **12,** 2531 (1973).
34. K. H. Becker, D. Haaks, and T. Tatarczyk, *Z. Naturforsch.*, **27A,** 1520 (1972).
35. K. H. Becker, D. Haaks, and T. Tatarczyk, *Z. Naturforsch.*, **28A,** 829 (1974).
36. C. C. Wang and L. J. Davis, Jr., *Appl. Phys. Lett.*, **25,** 34 (1974).

37. N. Omenetto, P. Benetti, and G. Rossi, *Spectrochim. Acta*, **27B**, 453 (1972).
38. N. Omenetto, R. F. Browner, J. D. Winefordner, G. Rossi, and P. Benetti, *Anal. Chem.*, **44**, 1683 (1972).
39. N. Omenetto, Plenary Lecture Given at 5th International Conference on Atomic Spectroscopy, Melbourne (August 1975).
40. J. W. Daily, *Appl. Opt.*, **15**, 955 (1976).
41. Y. Haas, Lawrence Berkeley Laboratory Report No. 14035, University of California, Berkeley (1975).
42. J. Kuhl, G. Marowsky, P. Kunstmann, and W. Schmidt, *Z. Naturforsch.*, **27A**, 601 (1972).
43. J. Kuhl and H. Spitschan, *Opt. Commun.* **5**, 382 (1972).
44. S. Neumann and M. Kriese, *Spectrochim. Acta*, **29B**, 127 (1974).
45. F. E. Lytle, *Anal. Chem.*, **46**, 545A (1974).
46. F. E. Lytle, *Anal. Chem.*, **46**, 817A (1974).
47. J. D. W. Abernethy, *Wireless World* (December 1970).
48. N. Omenetto, L. M. Fraser, and J. D. Winefordner, in *Applied Spectroscopy Reviews*, Vol. 7, E. G. Brame, Ed., Marcel Dekker, New York (1973), p. 147.
49. A. B. Rodrigo and R. M. Measures, *IEEE QE*, **9**, 972 (1973).
50. N. Omenetto, *Anal. Chem.*, **48**, 75A (1976).

Additional References

Several interesting papers have appeared in the literature since the writing of this chapter and are reported below. Theoretical writings on laser-induced fluorescence deal with the spectral distribution of the light emitted under intense field excitation (51–56), with the derivation of a fluorescence expression under selfabsorption conditions (57), with the applicability of the rate equations approach to describing the optical interaction (58), with the saturation of the sodium fluorescence (59–61), with the feasibility of the technique in the field of plasma diagnostics (61–63), with its analytical sensitivity (64–65) and with the time and wavelength dependence of the fluorescence signal (66). A comparison between pulsed and continuous wave fluorescence in terms of analytical results has been given (67), and the fluorescence behavior of iron and lead has been discussed (68, 69).

51. R. E. Grove, F. Y. Wu, and S. Ezekiel, *Phys. Rev.* **A, 15,** 227 (1977).
52. E. Courtens and A. Szöke, *Phys. Rev.* **A, 15,** 1588 (1977).
53. P. Avan and C. Cohen-Tannoudji, *J. Phys. B: Atom. Mol. Phys.*, **10,** 155 (1977).
54. B. Renaud, R. M. Whitley, and C. R. Stroud Jr., *J. Phys. B: Atom. Mol. Phys.*, **10,** 19 (1977).
55. J. L. Carlsten, A. Szöke, and M. G. Raymer, *Phys. Rev.* **A, 15,** 1029 (1977).
56. C. Cohen-Tannoudji and S. Reynaud, *J. Phys. B: Atom. Mol. Phys.*, **10,** 345 (1977)
57. N. Omenetto, J. D. Winefordner, and C. Th. J. Alkemade, *Spectrochim. Acta*, **30B,** 335 (1975).
58. J. W. Daily, *Appl. Opt.*, **16,** 2322 (1977).
59. D. D. Burgess and M. J. Eckart, *J. Phys. B: Atom. Molec. Physics*, **9,** L519 (1976).
60. B. L. Sharp and A. Goldwasser, *Spectroch. Acta*, **31B,** 431 (1976).
61. B. Smith, J. D. Winefordner, and N. Omenetto, *J. Appl. Phys.*, **48,** 2676 (1977).
62. J. W. Daily, *Appl. Opt.* **16,** 568 (1977).
63. A. P. Baronavski and J. R. McDonald, *Appl. Opt.*, **16,** 1897 (1977).
64. J. P. Hchimer and P. J. Hargis Jr., *Appl. Phys. Lett.*, **30,** 344 (1977).
65. J. A. Gelbwachs, C. F. Klein, and J. E. Wessel, *Appl. Phys. Lett.*, **30,** 344 (1977).
66. H. L. Brod and E. S. Yeung, *Anal. Chem.*, **48,** 344 (1976).
67. N. Omenetto, G. D. Boutilier, S. J. Weeks, B. W. Smith, and J. D. Winefordner, *Anal. Chem.*, **49,** 1076 (1977).
68. M. A. Bolshov, A. V. Zybin, L. A. Zybina, V. G. Koloshnikov, and I. A. Majorov. *Spectrochim. Acta*, **31B,** 493 (1976).
69. M. A. Bolshov, A. V. Zybin, V. G. Koloshnikov, and K. N. Koshelev, *Spectrochim. Acta*, **32B,** 279 (1977).

Spectrochimica Acta, Vol. 30B, pp. 335 to 341. Pergamon Press, 1975. Printed in Northern Ireland

An expression for the atomic fluorescence and thermal-emission intensity under conditions of near saturation and arbitrary self-absorption

N. Omenetto,
Institute of Inorganic and General Chemistry, University of Pavia, Viale Taramelli 12, 27100 Pavia, Italy

J. D. Winefordner
Department of Chemistry, University of Florida, Gainesville, Florida 32611

and

C. Th. J. Alkemade
Fysisch Laboratorium der Rijksuniversiteit, Sorbonnelaan 4, Utrecht, The Netherlands. U.S.A.

(*Received* 9 *December* 1974. *Revised* 7 *March* 1975)

Abstract—An expression for the effect of self-absorption on the fluorescence and thermal emission intensities is derived by taking into account stimulated emission. A simple, idealized case is considered, consisting of a two level atomic system, in a flame, homogeneous with respect to temperature and composition, and uniformly illuminated by an external quasi-continuum radiation source.

Introduction

The effect of self-absorption on the outgoing radiation intensity in a uniformly excited atomic vapor present in a flame of uniform temperature and composition, can be described in a most simple and elegant way by introducing the integral absorption, A_i(in s^{-1}). This applies for both the thermal-emission intensity [1–5] and the fluorescence intensity of a resonance line [4]. The expression for A_i, which is the integral of the absorption factor over the whole line profile, reads according to Beer's law

$$A_i = \int_{\text{line}} [1 - \exp\{-k(\nu)l\}]\, d\nu \qquad (1)$$

where $k(\nu)$ (in cm^{-1}) is the absorption coefficient at frequency ν and l (in cm) is the flame thickness along the line of observation. In the usual expression for $k(\nu)$, the effect of stimulated emission is neglected, which seems justified for spectral lines in the u.v. visible regions, excited by conventional light sources or thermally-excited in analytical flames with temperatures, T_f, up to about 3000 K.

[1] J. D. Winefordner, W. W. McGee, J. M. Mansfield, M. L. Parsons and K. E. Zacha, *Anal. Chim. Acta* **36**, 25 (1966).
[2] C. Th. J. Alkemade, E. R. Lippincott and M. Margoshes, *Proc. of the Xth Colloquium Spectroscopicum Internationale*. Spartan Books, Washington 1963.
[3] C. Th. J. Alkemade and P. J. Th. Zeegers, In *Spectrochemical Methods of Analysis*. (Edited by J. D. Winefordner). Wiley, New York 1971.
[4] C. Th. J. Alkemade, *Pure Appl. Chem.* **23**, 73 (1970).
[5] T. Hollander, *Self-absorption, Ionization and Dissociation of Metal Vapours in Flames*. PhD Thesis, University of Utrecht, 1961.

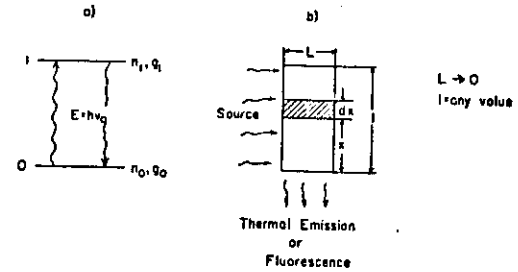

Fig. 1. Representation of Simple Two-Level Atomic System and Illumination Geometry. a. Energy Level Diagram b. Geometry of illumination and observation (diagrams apply to either emission or fluorescence processes).

The advent of intense (tunable) laser sources has made it possible to nearly saturate atom lines in the flame [6–9]. Under such conditions, (self-) absorption is accompanied by stimulated emission, which reduces the *net* absorption coefficient as measured, e.g., in a direction perpendicular to the laser beam. Stimulated emission induced by photons that are re-emitted as fluorescence in a direction perpendicular to the laser beam (see Fig. 1b) will thus partly offset the reduction of the fluorescence intensity due to self-absorption.

For a simple, idealized case, an expression will be derived for the effect of self-absorption on the fluorescence and thermal-emission intensities, while taking into account stimulated emission.

Theory

A simple atomic system (see Fig. 1a) will be considered having only two energy levels (0 refers to the ground state), statistical weights g_0 and g_1, and an energy separation $E = h\nu_0$, where ν_0 is the central frequency (in Hz) of the optical transition. In the case of fluorescence excitation by an external light source, the geometry of illumination and observation is as depicted in Fig. 1b. In order to avoid mathematical complications due to the gradual weakening of the primary light beam along its path through the flame or due to self-reversal of the fluorescence line [4, 10], it will be assumed that the whole flame section observed is uniformly illuminated. (This may be realized, for a given atom concentration, by keeping L sufficiently small and by choosing the width of the primary beam equal to l, which is itself not restricted; see Fig. 1b).

[6] E. H. Piepmeier, *Spectrochim. Acta* **27B**, 431 (1972).
[7] E. H. Piepmeier, *ibid*, 445 (1972).
[8] N. Omenetto, P. Benetti, L. P. Hart, J. D. Winefordner and C. Th. J. Alkemade, *Spectrochim. Acta* **28B**, 289 (1973).
[9] J. Kuhl, S. Neumann and M. Kriese, *Z. Naturforsch* **28A**, 273 (1973).
[10] N. Omenetto, L. P. Hart, P. Benetti and J. D. Winefordner, *Spectrochim. Acta* **28B**, 301 (1973).

Furthermore, the simplification will be made that the flame is homogeneous as to temperature and composition, and that the atom concentration is uniform throughout the illuminated region in the flame. (The more general case of a non-uniform atom concentration will be dealt with separately in the Appendix.) The product of atom concentration and flame depth l is, however, not restricted, so that the extent of self-absorption of the outgoing fluorescence or thermal radiation may be arbitrarily high (assuming negligible radiation diffusion).

General expression

Referring to Fig. 1b, the contribution of section dx to the spectral radiance, $\mathrm{d}B_\nu(\nu, x)$ (expressed in erg s^{-1} cm^{-2} sr^{-1} Hz^{-1}) of the outgoing radiation at frequency ν observed along the x-axis is given by

$$\mathrm{d}B_\nu(\nu, x) = (A_{10} n_1 h\nu/4\pi) S_\nu(\nu) \exp\left\{\int_0^x -k^*(\nu)\,\mathrm{d}x'\right\} \mathrm{d}x \tag{2}$$

where n_1 is the number density of excited atoms (in cm^{-3}), A_{10} is the Einstein transition probability for spontaneous emission (in s^{-1}), h is Planck's constant, $S_\nu(\nu)$ is the normalized spectral distribution function (in Hz^{-1}) of photons emitted by a downward transition $1 \to 0$ ($\int_{\text{line}} S_\nu(\nu)\,\mathrm{d}\nu = 1$), and $k^*(\nu)$ is the *net* absorption coefficient of the atomic vapor at vapor frequency ν. The exponential factor in Equation (2) accounts for the attenuation of the atomic radiation generated at place x, due to the *net* effect of self-absorption and stimulated emission, when travelling over a path length x. From Einstein's radiation theory [11, 12],

$$k^*(\nu) = (B_{01} h\nu/c) S_\nu(\nu)\{n_0 - (g_0/g_1) n_1\}, \tag{3a}$$

or

$$k^*(\nu) = (B_{01} h\nu/c) S_\nu(\nu) n_0 \{1 - (g_0/g_1)(n_1/n_0)\} \tag{3b}$$

where B_{01} is the Einstein coefficient for absorption (in erg^{-1} cm^3 s^{-1} Hz), which equals the Einstein coefficient for stimulated emission, B_{10}, multiplied by (g_1/g_0), c is the velocity of light (in cm s^{-1}), and n_0 is the number density of ground-state atoms (in cm^{-3}). In Equations (3), we have indirectly assumed that the normalized spectral distribution function of photons absorbed (from a hypothetical continuum radiation field), is the same as that for spontaneous emission, $S_\nu(\nu)$; this assumption implies that coherence effects between absorbed and re-emitted photons are neglected which seems to be justified in flames at 1 atm pressure [13]. We have also neglected radiation diffusion effects in assuming that a photon re-absorbed at place $x'(0 < x' < x)$ on its way out, will have a negligible chance to leave the flame in the same direction after being re-emitted and re-absorbed in succession a number of times; this latter assumption seems to be justified if the efficiency of resonance fluorescence Γ, is not too close to unity.

[11] A. C. G. Mitchell and M. W. Zemansky, *Resonance Radiation and Excited Atoms*. University Press, Cambridge, (1961).
[12] R. Mavrodineanu and H. Boiteux, *Flame Spectroscopy*. Wiley, New York 1964).
[13] H. P. Hooymayers and C. Th. J. Alkemade, *J. Quant. Spectros. Radiative Transf.*, **6**, 847 (1966).

With conventional external light sources and/or under usual flame conditions in atomic fluorescence and flame emission spectrometry, the second term between brackets { } in Equation (3b) is much less than unity. This is tantamount to assuming that stimulated emission is negligble in comparison with (real) absorption, and so to a good approximation

$$k^*(\nu) \approx k(\nu) \equiv (B_{01} h\nu/c) S_\nu(\nu) n_0. \tag{4}$$

Under (near-) saturation conditions, however, the (exact) equation for $k^*(\nu)$ (Equations (3a, b) instead of Equation (4)) must be applied.

From the general assumptions made, it can be concluded that n_0, n_1, $S_\nu(\nu)$ and thus $k^*(\nu)$ [see Equations (3a, b] are independent of position, x. Therefore from Equations (2), $\mathrm{d}B_\nu(\nu, x)$ is given by

$$\mathrm{d}B_\nu(\nu, x) = (A_{10} n_1 h\nu/4\pi) S_\nu(\nu) \exp\{-k^*(\nu)x\}\,\mathrm{d}x. \tag{5}$$

Integration of the latter equation over x then yields for the spectral radiance $B_\nu(\nu)$ of the outgoing radiation at frequency ν

$$B_\nu(\nu) = (A_{10} n_1 h\nu/4\pi) S_\nu(\nu)\,[1 - \exp\{-k^*(\nu)l\}]/k^*(\nu) \tag{6}$$

Substituting the expression for $k^*(\nu)$ given by Equation (3a) in the denominator of the right-hand side of Equation (6), gives

$$B_\nu(\nu) = \left(\frac{c}{4\pi}\right)\left(\frac{A_{10}}{B_{01}}\right)\left(\frac{n_1}{n_0 - (g_0/g_1)n_1}\right)[1 - \exp\{-k^*(\nu)l\}]. \tag{7}$$

Making use of the general relationship between A_{10} and B_{01} [11, 12] and substituting into Equation (7) gives

$$B_\nu(\nu) = \left(\frac{2h\nu_0^3}{c^2}\right)\left(\frac{n_1(g_0/g_1)}{n_0 - (g_0/g_1)n_1}\right)[1 - \exp\{-k^*(\nu)l\}] \tag{8}$$

The radiance, B, (in erg s^{-1} cm^{-2} sr^{-1}) of the whole atom line is obtained by integrating Equation (8) over frequency and so

$$B = \int_{\text{line}} B_\nu(\nu)\,\mathrm{d}\nu = \left(\frac{2h\nu_0^3}{c^2}\right)\left(\frac{n_1(g_0/g_1)}{n_0 - (g_0/g_1)n_1}\right) A_t^*, \tag{9}$$

where the *net* integral absorption A_t^* is defined by

$$A_t^* \equiv \int_{\text{line}} [1 - \exp\{k^*(\nu)l\}]\,\mathrm{d}\nu \tag{10}$$

Equations (9) and (10) describe the influence of self-absorption on the radiance of the outgoing radiation, *while taking the contribution of stimulated emission exactly into account*. These equations replace the previously derived expression for the self-absorption of fluorescence radiation. This previous expression is again found from Equations (9) and (10) by neglecting the term $(g_0/g_1)n_1$ with respect to n_0 in Equation (9) as well as in the expression for $k^*(\nu)$ given by Equation (3a).

Case of fluorescence

When the atomic vapor is uniformly illuminated by a quasi continuum source with spectral irradiance E_{ν_0} (in erg s^{-1} cm^{-2} Hz^{-1}) at $\nu \approx \nu_0$ and with a spectral

bandwidth much larger than the atomic line-width, then [8]

$$\frac{n_1(g_0/g_1)}{n_0 - (g_0/g_1)n_1} = \frac{1}{2}\left(\frac{E_{\nu_0}}{E^s_{\nu_0}}\right) \tag{11}$$

if thermal excitation is neglected; $E^s_{\nu_0}$ is the "saturation parameter" (expressed as spectral irradiance) defined [8] by

$$B^s_{\nu_0} \equiv 4\pi h\nu_0^3/c^2 Y \tag{12}$$

where Y = quantum efficiency of fluorescence. Substitution of Equations (11) and (12) in Equation (9) yields

$$B = (Y/4\pi)E_{\nu_0}A_t^*. \tag{13}$$

The factor A_t^* is, in general, dependent on E_{ν_0} too, as A_t^* contains $k^*(\nu)$ which again depends on the degree of saturation through the factor $\{n_0 - (g_0/g_1)n_1\}$ occurring in Equation (3a). The latter factor is found from Equation (11) to be given by

$$n_0 - (g_0/g_1)n_1 = n_t/\{1 + \tfrac{1}{2}(E_{\nu_0}/E^s_{\nu_0})(g_1 + g_0)/g_0\} \tag{14}$$

where $n_t (\equiv n_1 + n_0)$ is the total number density of atoms.

With conventional light sources, $E_{\nu_0} \ll E^s_{\nu_0}$, so that $k^*(\nu)$ and thus A_t^* can be approximated by $k(\nu)$ and A_t, respectively, which are independent of E_{ν_0}. Therefore, according to Equation (13), the fluorescence intensity is simply proportional to the source intensity. The dependence of fluorescence intensity on $(n_0 l)$ is then described by the usual curve-of-growth theory through the factor A_t.

With very high intensity sources, $E_{\nu_0}/E^s_{\nu_0} \to \infty$, it can be seen from Equation (3a) and (14) that, for a given n_t, $k^*(\nu) \to 0$. But $k^*(\nu) \to 0$ implies that self-absorption is removed, that is, A_t^* becomes simply proportional to n_t [which is found from the usual series expansion [3, 10] of the exponential term in Equation (10)]. This was to be expected; under saturation conditions, the atomic vapor becomes transparent to the resonance line radiation which has great analytical value [10].

Case of thermal emission radiation

Equation (9) for the outgoing radiation intensity is valid irrespectively of the particular process(es) by which the atoms are actually excited. It can thus also be applied in order to derive an *exact* expression for the thermal emission radiation intensity (i.e., without external light source); in which case, the effects of self-absorption as well as stimulated emission are taken into account. For this case, it is only necessary to replace the ratio n_1/n_0 in Equation (9) by the thermal equilibrium ratio as given by Boltzmann's law*

$$\frac{n_1{}^{\text{th}}}{n_0{}^{\text{th}}} = \frac{g_1}{g_0}\exp\{-E/kT_f\} \tag{15}$$

* This law is obeyed exactly only if the flame were placed inside a cavity at the same temperature. In practical flames, it is obeyed in reasonable approximation at any atom concentration, if the fluorescence efficiency is not higher than, say 10% [3, 13].

From Equations (9) and (15) and substituting $E = h\nu_0$, the thermal radiance is given by

$$B^{\text{th}} = (2h\nu_0{}^3/c^2)\left(\frac{\exp\{-h\nu_0/kT_f\}}{1 - \exp\{-h\nu_0/kT_f\}}\right)A_t^*$$

$$= (2h\nu_0{}^3/c^2)[\exp\{h\nu_0/kT_f\} - 1]^{-1}A_t^*. \tag{16}$$

According to Planck's law, the spectral radiance of a blackbody at temperature T_f and frequency ν_0 is given by

$$B_{\nu_0}{}^{Pl}(T_f) = (2h\nu_0{}^3/c^2)[\exp\{h\nu_0/kT_f\} - 1]^{-1} \tag{17}$$

Combining Equations (16) and (17), B^{th} is given by

$$B^{\text{th}} = A_t^* B_{\nu_0}{}^{Pl}(T_f) \tag{18a}$$

Thus, in the thermal case, the effect of stimulated emission is *exactly* taken into account, if Equations (3b) and (15) are used in the calculation of $k^*(\nu)$, and Equation (10) is used in the calculation of A_t^*, while using Planck's law [Equation (17)] for the blackbody spectral radiance. The criterion for the applicability of the approximate Wien's law, instead of Planck's law, results when $\exp\{h\nu_0/kT_f\} \gg 1$, and holds generally in analytical flame emission spectroscopy. But the same criterion also holds for the replacement of $k^*(\nu)$ by $k(\nu)$, while neglecting in Equation (3b) the term $(g_0/g_1)(i_1{}^{\text{th}}/n_0{}^{\text{th}}) = \exp\{-h\nu_0/kT_f\}$ with respect to unity. The presence of the (-1) term in the denominator of the right-hand side of Equation (17) is intrinsically related to the occurrence of stimulated emission transitions. If $\exp\{h\nu_0/kT_f\} \gg 1$, then the (-1) term as well as stimulated emission can be neglected, and instead of Equation (18a) the more common approximative expression for B^{th} is obtained

$$B^{\text{th}} \approx A_t B_{\nu_0}{}^{W}(T_f) \tag{18b}$$

where the superscript index W refers to Wiens's law.

By series expansion of A_t^* and A_t to first order of $(n_0 l)$ (i.e., for $n_0 l \to 0$), Equations (18a) and (18b) become, in fact identical. This does not hold, however, to higher orders of approximation. Therefore, it is suggested that whenever we use the term A_t instead of the exact term A_t^*, we should consistently replace Planck's law by Wien's law, too.

Appendix

Derivation of Equation (7) for non-uniform atom distribution

When n_0 and n_1 are assumed to be arbitrary functions of the position coordinate, x, then also the net absorption coefficient $k^*(\nu)$ will vary with x [compare Equation (3b)]. If, however, the other initial assumptions are retained (uniform illumination, flame temperature and composition), $S_\nu(\nu)$ as well as the ratio $n_1(x)/n_0(x)$ are independent of place and the same as before.

Instead of Equations (5) and (6), the appropriate expressions for $dB_\nu(r, x)$ and $B_\nu(r)$ are now

$$dB_\nu(r, x) = (A_{10}h\nu/4\pi)S_\nu(\nu)n_1(x) \exp\{-\int_0^x k^*(r, x')\,dx'\}\,dx \qquad (A\text{-}1)$$

and

$$B_\nu(r) = (A_{10}h\nu/4\pi)S_\nu(\nu)\int_0^l n_1(x) \exp\{-\int_0^x k^*(r, x')\,dx'\}\,dx \qquad (A\text{-}2)$$

respectively. The latter equation can be solved by putting: $y(x) = \int_0^x k^*(r, x')\,dx'$, so that $y'(= dy/dx) = k^*(r, x)$. Equation (A-2) then becomes

$$B_\nu(r) = (A_{10}h\nu/4\pi)S_\nu(\nu)\{n_1(x)/k^*(r, x)\}\int_0^l \exp\{-y\}y'\,dx \qquad (A\text{-}3)$$

where according to Equation (3b)

$$n_1(x)/k^*(r, x) = \frac{c\{n_1(x)/n_0(x)\}}{B_{01}h\nu S_\nu(\nu)[1 - (g_0/g_1)\{n_1(x)/n_0(x)\}]} \qquad (A\text{-}4)$$

which is independent of x, (because $n_1(x)/n_0(x)$ is independent of x see above). The integral:

$$\int_0^l \exp\{-y\}y'\,dx$$

can be solved by choosing y as a new integration variable with $y'\,dx = dy$. The integral then becomes

$$\int_0^{y(l)} \exp\{-y\}\,dy = 1 - \exp\{-y(l)\} = 1 \exp\{-\int_0^l k^*(r, x')\,dx'\} \qquad (A\text{-}5)$$

Substituting Equations (A-4) and (A-5), into Equation (A-3), Equation (7) and all equations after Equation (7) result again except that $\exp\{-k^*(\nu)l\}$ is now replaced everywhere by: $\exp\{-\int_0^l k^*(r, x')\,dx'\}$.

Offprints from:
Analytical Applications of Lasers
Edited by Edward H. Piepmeier

CHAPTER

2

LASER-EXCITED ATOMIC AND IONIC FLUORESCENCE IN FLAMES AND PLASMAS

J. D. WINEFORDNER

Department of Chemistry
University of Florida
Gainesville, Florida

N. OMENETTO

CCR, European Community Center
Stabilimento di Ispra
Analytical Chemistry Division
Ispra, Italy

Work supported by AFOSR-F49620-80-C-0005.

1. INTRODUCTION

Atomic fluorescence spectrometry (AFS) is based upon radiational excitation of atoms (produced in a suitable atomizer) and measurement of the consequent radiational deactivation (called fluorescence). Laser-excited AFS (LEAFS) involves the same processes except that the source of excitation is a laser, and in most cases of analytical interest, a dye laser. Atomic fluorescence spectrometry has been of considerable interest to researchers in atomic spectrometry because of its use for analytical and diagnostical purposes. However, no commercial AFS instruments are currently available except for the Baird hollow cathode lamp-excited inductively coupled plasma (HCL-ICP-AFS) system. There are no commercial analytical LEAFS instruments.

This chapter is concerned strictly with LEAFS. To facilitate the discussion of principles, instrumentation, analytical figures of merit, and applications of LEAFS and to conform to rather limited space requirements, the authors will use primarily figures and tables with minimal textual discussions. The authors have attempted to give a rather comprehensive survey of the literature available (up to about January 1, 1984). The references are divided into three main groups: Reviews (R); Fundamentals (F) of fluorescence; and Instrumentation and Methodologies (I) of LEAFS.

The reader is referred to the previous reviews (see references) on LEAFS. The considerable interest in LEAFS is apparent when one considers that it is within the realm of possibility to detect *selectively* single atoms in complex real-world samples. Alkemade (F52) in a *classic* paper has given an overview of the principles and achievements of various laser-based methods for single-atom detection (called SAD). He showed the ultimate detection limit is an intrinsic value dependent on the statistical fluctuations of the atoms within the observation volume. The intrinsic detection limit is ultimately the limit to quantitative trace analysis. Various experimentalists have approached, and in fact exceeded, single-atom detection within an observation volume that consists of either a beam oven or a pure vapor vessel, that is, a cell system often not of analytical importance. In more analytically significant cells such as flames, but especially electrothermal atomizers, detection limits of under 100 atoms/cm^3 are obtained and have been predicted by Omenetto and Winefordner (F33) and by Falk (F57).

LEAFS is not only a technique with high detection power but also one with high *spectral selectivity*. The high spectral selectivity is achieved because it is possible to excite the atomic vapor with a single, narrow-bandwidth line, thus minimizing problems associated with spectral interferences and stray light that often plague other atomic methods, for example, plasma atomic emission methods. LEAFS is certainly a technique worthy of consideration by analytical chemists, and it is hoped that this chapter will provide an impetus to others to work in this area of research.

In Tables 2.1 and 2.2, a brief review is given of the considerations concerning

Table 2.1. Why Are Dye Lasers of Interest in Atomic Fluorescence Spectrometry?

1. High spectral irradiance

   Optical saturation possible (especially in the fundamental region, >350 nm), and consequently:
   a. Improved limits of detection (assuming noise is not related to source intensity)
   b. Increased linear dynamic range (because of reduced self-absorption and prefilter effects)
   c. Increased precision (because of increased signal levels)
   d. Freedom from quenching effects

2. Narrow spectral bandwidth

   a. Stray light is minimal
   b. Spectral interferences are minimal since it is easy to excite *only* the wavelength of the element of interest and also to select the fluorescence wavelength.

3. Small beam size, beam collimation, narrow temporal pulses

   a. Optimal for small atom reservoirs, e.g., furnace
   b. Optimal for spatial profile of atoms in flames, plasmas, etc.

Table 2.2. Why Are No Commercial Laser-excited Atomic Fluorescence Spectrometers Available?

1. Complexity of dye lasers
   Frequency doubling, frequency narrowing, frequency mixing, Raman shifting, spatial matching, temporal matching, etc.
2. Expense of dye laser
   Equipment costs of ~$50,000–$120,000

   Operational costs of ~$1,000–$20,000/year depending on amount and kind of dye used, part replacement such as thyratrons, capacitors, etc.
3. Stability (amplitude) of dye lasers (pulsed)
   Pulse to pulse stability can be poor.
4. Wavelength scan difficulties
   Difficult to scan wavelength over more than one dye
5. Low UV spectral irradiances, E_λ
   In the ultraviolet region, where doubling techniques (for Raman shifting) must be used

   E_λ is in general less than that necessary to reach optical saturation
6. Size and special conditions
   Dye laser systems are often bulky, nonmobile, and demanding in terms of utilities (cooling and power requirements)

Table 2.3. Selected Projects on Fundamental Aspects of Laser-excited Fluorescence Spectrometry

Reference	Intensity Expressions	Source[a]	Ys and ks	τs and ks	$n_T s$	Line Broadening	Other[b]
F1	—	Both	—	—	—	—	Fundamentals
F2	—	Both	—	—	—	—	Fundamentals
F3	—	Both	—	—	—	—	Fundamentals
F4	Yes	Both	Yes	Yes	Yes	Yes	Fundamentals
F5	Yes	Both	Yes	Yes	Yes	Yes	Edited book
F6	—	Both	—	—	—	—	Fundamentals
F7	Yes	Both	Yes	Yes	Yes	Yes	Edited book
F8	—	Both	—	—	—	—	Fundamentals
F9	Yes	Both	Yes	Yes	Yes	Yes	Key paper
F10	Yes	Cont	Yes	Yes	Yes	No	Key paper
F11	Yes	Cont	Yes	Yes	Yes	No	—
F12	Yes	Line	Yes	No	Yes	No	Key paper
F13	Yes	Line	Yes	No	Yes	No	Key paper
F14	No	No	No	No	No	No	Designation of AF transitions
F15	Yes	Cont	Yes	No	Yes	No	Key paper
F16	Yes	Cont	Yes	No	Yes	No	Shapes of curves of growth
F17	Yes	Line	Yes	No	Yes	No	—
F18	Yes	Cont	Yes	No	Yes	No	—
F19	No	Both	No	Yes	Yes	Yes	Key paper
F20	Yes	Cont	Yes	No	Yes	No	—
F21	Yes	Cont	Yes	Yes	Yes	No	Key paper
F22	Yes	Cont	Yes	No	Yes	No	Exptal verification
F23	Yes	Cont	Yes	No	Yes	No	Exptal study
F24	No	Cont	No	No	No	Yes	Excitation profile
F25	No	None	No	No	No	No	S/N expressions for AFS
F26	Yes	Cont	Yes	No	Yes	No	—
F27	Yes	Cont	Yes	No	Yes	No	General paper
F28	Yes	Cont	Yes	No	Yes	No	—
F29	No	Cont	No	No	No	No	—
F30	Yes	Cont	Yes	No	Yes	No	Derivation of two-level/three-level intensities
F31	No	Line	No	No	No	Yes	Laser saturation broadening
F32	Yes	Cont	Yes	No	Yes	No	—
F33	Yes	Both	Yes	Yes	Yes	Yes	General treatment of AFS
F34	Yes	Both	Yes	—	Yes	—	Saturated absorption profiles
F35	No	Cont	Yes	No	No	Yes	—
F36	Yes	Cont	Yes	Yes	Yes	No	Saturation curves
F37	Yes	Cont	Yes	No	Yes	No	Exptal study on Ne microwave discharge
F38	Yes	Cont	Yes	No	Yes	No	Ionization in flames
F39	Yes	Cont	Yes	No	Yes	No	Ionization in flames
F40	Yes	Cont	Yes	No	Yes	No	—
F41	Yes	Cont	Yes	No	Yes	No	—
F42	Yes	Cont	Yes	Yes	Yes	No	Exptal verification
F43	Yes	Cont	Yes	No	No	No	Fluorescence ratio of Na-D lines
F44	Yes	Cont	Yes	No	Yes	No	Compound formation in excited state
F45	Yes	Cont	Yes	No	Yes	No	OH studies
F46	Yes	Cont	Yes	No	Yes	No	OH studies
F47	Yes	Cont	Yes	No	No	Yes	Laser saturation broadening

Table 2.3. (*Continued*)

Reference	Intensity Expressions	Source[a]	Ys and ks	τs and ks	$n_1 s$	Line Broadening	Other[b]
F48	Yes	Cont	No	No	No	No	Ionization by one and two photons
F49	Yes	Cont	Yes	No	No	No	Extended model for saturation in two-level atom
F50	Yes	Cont	Yes	No	Yes	No	Experimental verification
F51	Yes	Both	Yes	No	Yes	No	Ionization of vapors
F52	No	Both	No	No	Yes	No	Single-atom detection Key paper
F53	No	Cont	Yes	No	No	No	Response time to steplike excitation
F54	No	Cont	Yes	No	Yes	No	Experimental verification
F55	Yes	Cont	Yes	No	No	No	Saturation parameter in two- and three-level atoms
F56, F58	No	Cont	Yes	Yes	No	No	Lifetimes and Y's as function of height in ICP
F57	Yes	Both	Yes	No	Yes	No	Comparison of methods

[a]Cont = Continuum source, Line = Line source, Both = Line or continuum source.
[b]Fundamental means that principles of excitation, deexcitation, broadening, etc., are given. Key paper means papers that have stimulated considerable *analytical* interest (opinion of authors).

why dye lasers are of interest in AFS and why no LEAFS system are commercially available. These considerations will be discussed at numerous points throughout this chapter.

Table 2.3, in addition to a few selected books and chapters, lists a number of papers that have had, in the author's opinion, a significant impact in the analytical development of the technique.

2. PRINCIPLES

2.1. Atomic Fluorescence Transitions

The possible types of AFS transitions with the appropriate designations (F14) have been described several times in the literature and are shown again in Fig. 2.1 for the sake of completeness. Essentially, all processes shown in Fig. 2.1 have been observed in LEAFS. It should be stressed that the analytical interest in nonresonance transitions (either direct line fluorescence, DLF, or stepwise line fluorescence, SLF) exists because of the freedom from scattering problems (background, background noise). Scatter can be either *elastic*, for example, Rayleigh scatter from atoms and molecules or Mie scatter from particles much larger than the excitation wavelength, or *inelastic*, for example, atomic and molecular fluorescence and Raman scatter. It should be emphasized here that the use of laser excitation for resonance fluorescence, assuming optical saturation occurs, will degrade analytical figures of merit since the fluorescence signal will reach a plateau with an increase in source intensity, but the scatter signal *and* scatter noise will continue to increase.

2.2. Comparison of Sources of Excitation for AFS

In Table 2.4, a comparison is given of several of the characteristics (figures of merit) of three major types of dye lasers (excimer laser-pumped dye laser, nitrogen laser-pumped dye laser, synchronously pumped, mode-locked dye laser), a conventional light (line) source, and an Eimac xenon arc lamp (300 W). Footnotes are given to describe the characteristics in the right side of the table. It is apparent that dye lasers have much higher spectral irradiances (peak values) than conventional sources, by factors of 10^5–10^{12}, which will allow optical saturation in the visible (fundamental region of the dye laser) region and in some cases in the UV (doubled fundamental of the dye laser). In addition, their use will result in far fewer spectral interferences than a conventional continuum source (Eimac xenon arc lamp) or a conventional line source (electrodeless lamp or hollow cathode discharge lamp). On the other hand, dye lasers are

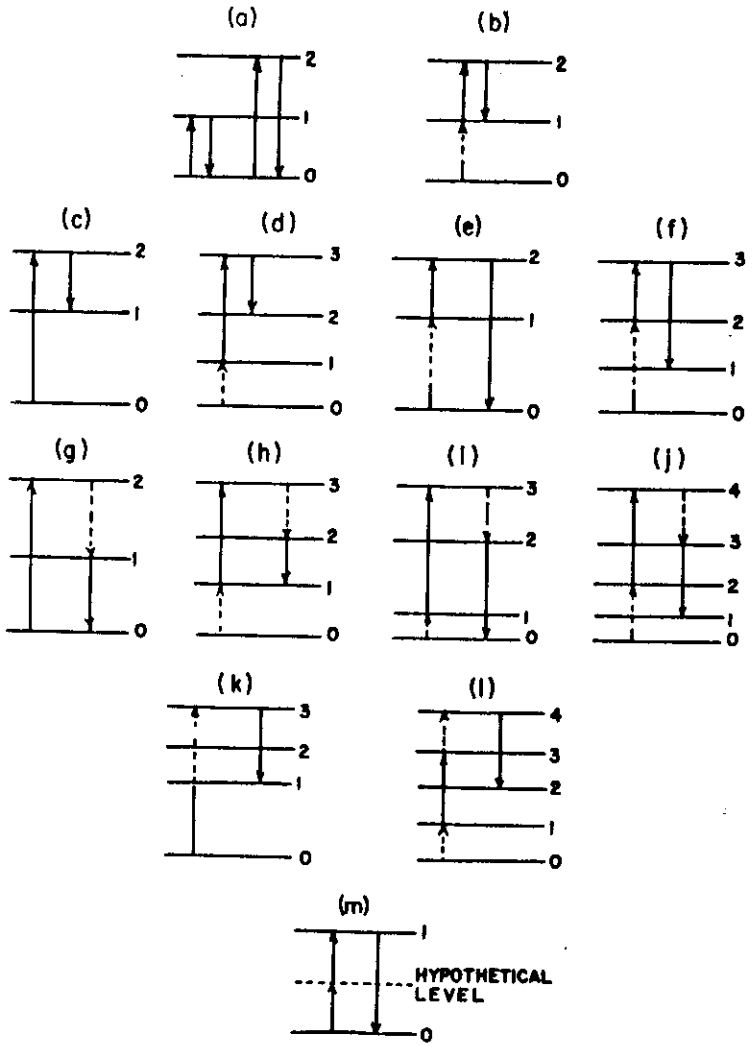

Fig. 2.1. Types of atomic fluorescence transitions (the spacing between atomic levels is not indicative of any specific atom). (a) RF resonance fluorescence (either process); (b) ERF, excited-state resonance fluorescence; (c) SDLF, Stokes direct line fluorescence; (d) ESDLF, excited-state Stokes direct line fluorescence; (e) ASDLF, anti-Stokes direct line fluorescence; (f) EASDLF, excited-state anti-Stokes direct line fluorescence; (g) SSLF, Stokes stepwise line fluorescence; (h) ESSLF, excited-state Stokes stepwise line fluorescence; (i) ASSLF, anti-Stokes stepwise line fluorescence; (j) EASSLF or ESSLF, excited-state anti-Stokes or Stokes stepwise line fluorescence; (k) TASSLF or TAASSLF, thermally assisted Stokes or anti-Stokes stepwise line fluorescence (depending on whether the absorbed radiation has shorter or longer wavelengths, respectively, than the fluorescent radiation); (l) ETASSLF or ETASSSLF, excited-state thermally assisted Stokes or anti-Stokes stepwise line fluorescence (depending on whether the absorbed radiation has shorter or longer wavelengths, respectively, than the fluorescence radiation); (m) TPF, two-photon excitation fluorescence (multiphoton processes involving more than two identical photons are even less probable than the two-photon processes).

more expensive to purchase and operate, more difficult to use, and of poorer stability than conventinal sources.

2.3. Atomic Fluorescence Radiance

Expressions for the atomic fluorescence radiance, B_F, in J s^{-1} cm^{-2} sr^{-1}, in the limiting cases of low source intensity (said to be the *linear case*) and of high source intensity (called *optical saturation*) are given in Table 2.5, with definitions of symbols. The reader is referred to numerous articles (F4, F9, F15, F27, F30, F33) where the above expressions have been derived and discussed.

Several conclusions or comments can be made based upon the radiance expressions in Table 2.5:

1. In all cases, B_F is proportional to the analyte concentration.
2. In linear AFS (low-intensity source cases), B_F is proportional to the source spectral irradiance, $E_\nu(\nu_0)$ and to the quantum efficiency, Y, of the fluorescence process.
3. In nonlinear AFS (high-intensity source cases), B_F is independent of source spectral irradiance, $E_\nu(\nu_0)$.
4. For two-level atoms and for nonlinear AFS, B_F is also independent of Y and, a simple expression results.
5. For a three-level Na-like atom and for nonlinear AFS, B_F will be independent of the collisional rate coefficients provided that the mixing between levels 2 and 3 is very effective, that is, k_{32} or $k_{23} \gg (A_{21} + k_{21})$ for $1 \rightarrow 3$ excitation and k_{32} (or k_{23}) $\gg (A_{31} + k_{31})$ for $1 \rightarrow 2$ excitation.
6. For a three-level Tl-like atom and for nonlinear AFS, B_F will depend also on the gas temperature, T, although the dependency is small for the $1 \rightarrow 3$ excitation process since $\exp(-E_{12}/kT) \ll 1$, but is significant for the $2 \rightarrow 3$ excitation since $\exp(E_{12}/kT) \gg 1$.
7. It is possible to determine *absolute concentrations of atoms* (atoms/cm^3) via saturated fluorescence (F21–23, F29–31, F37–39, F40, F44, F46) as long as the atoms within the observation volume are optically saturated, and B_F is measured in absolute units (use of a calibrated spectrometer-detector). However, in the case of a three-level atom, the collisional rate coefficients should be known or their effect should be negligible. In addition, such measurements require critical attention to the spatial, spectral, and temporal characteristics of the laser beam and the excited-state processes, including compound formation, ionization, and so on (see Table 2.3, especially references F4, F29, F32, F35, F36, F38, F39, F44).

Table 2.4. Comparison of Excitation Sources in Atomic Fluorescence Spectrometry[a]

Source	Peak Spectral Irradiance (W cm^{-2} nm^{-1})		Pulse Width (ns)	Optical Saturation	Wavelength Range	Ease of Use		Spectral	Cost	
	Fundamental	Doubled		Vis, UV	Vis, UV	Vis, UV	Stability	Interferences[b]	Initial	Operation
Excimer dye laser	10^9–10^{10}	10^7–10^9	5–20	Yes, ?	Yes, ≲215 nm	F_1, F_2	Go	VL	Mo_2	Mo_2
N_2 dye laser	10^8–10^{10}	10^6–10^8	3–10	Yes, ?	Yes, ≲215 nm	F_1, F_2	Go	VL	Mo_1	Mo_1
Synch pump dye laser	10^5–10^7	10^4–10^5	0.005–0.05	?, ?	Yes, 285–315 nm	F_3, F_3	Go	VL	Hi	Hi
Eimac arc	10^{-1}–10^0	10^{-2}–10^{-1}	cw	No, No	Yes, Yes	E, E	Ex	Gr	Lo_1	Lo_1
Electrodeless discharge lamp	10^{-3}–10^{-5}	10^{-3}–10^{-5}	cw	No, No	Yes, Yes	E, E	Ex	L	Lo_2	Lo_2

[a] E = easy, F_1 = difficult, F_2 = more difficult, F_3 = most difficult, Go = good, Ex = excellent, VL = very low, Gr = great, L = low, Hi = high, Mo_2 = moderate but still high, Mo_1 = moderate but low; Lo_1 = lowest, Lo_2 = low (higher than Lo_1).
[b] Spectral interferences correspond to those expected when the source is used to execute atoms in a flame or an ICP

2.4. Saturation Steady-State Spectral Irradiance, E^s_ν

The saturation steady state-spectral irradiance E^s_ν is the value of the source spectral irradiance, E_ν, where $B_F = 50\%$ of the maximum possible value (optically saturated) plateau value. Expressions for E^s_λ are given in Table 2.6. The saturation spectral irradiance, E^s_ν (J s^{-1} cm^{-2} nm^{-1}) is related to E^s_ν (J s^{-1} cm^{-2} Hz^{-1}) by

$$E^s_\lambda(\lambda_0) = E^s_\nu(\nu_0)\frac{c}{\lambda_0^2}10^{-7} = \left(\frac{3 \times 10^3}{\lambda_0^2}\right)E^s_\nu$$

where λ_0 is the wavelength of excitation (in centimeters). In Table 2.7, saturation spectral irradiance values (E^s_λ) for a two-level atom are given for excitation wavelengths from 200 to 800 nm in 100-nm intervals. It is apparent that optical saturation occurs more readily as the quantum efficiency increases (toward unity) and the wavelength increases (E^s_λ is proportional to $\lambda_0^{-5}\,Y^{-1}$).

The importance of the saturation parameter as well as the pitfalls associated with its determination from the experimental saturation curves have received much attention (see especially references F4, F19, F36, F49 and F55).

2.5. Signal-to-Noise Ratio in AFS

The signal-to-noise (S/N) ratios in AFS have been described in detail by Omenetto and Winefordner (R14 and R17) and so will be treated only briefly here.

The noise in LEAFS is determined by the following sources: background (flame, ICP, furnace) shot and flicker noise; source scatter (resonance case only) shot and flicker noise; background radical fluorescence shot and flicker noise; analyte fluorescence (and emission) shot and flicker noises; and interferent fluorescence (and emission) shot and flicker noises. In Table 2.8, some of the flame gas radicals and molecular analyte species that have been found to fluoresce in flames are given. As an example, Fig. 2.2 shows a typical molecular fluorescence spectrum of manganese in an air–acetylene flame. If the analyte excitation–emission combination is chosen properly, then interferent fluorescence and molecular fluorescence of flame radicals can generally be avoided. If the analyte concentration is low (as near the limit of detection), then the analyte-related noises are minimal. If nonresonance fluorescence is measured, then the scatter noises (except in cases where stray light could cause problems) are negligible. If the source is modulated or pulsed and a phase-sensitive or boxcar detection system used, the background flicker noises can be minimized. Therefore, the ultimate limiting noise at the powers of detection experimentally measured in LEAFS (and in AFS, in general) is cell background emission shot noise. In Table 2.9, detection limits and other analytical figures of merit of LEAFS and several other atomic methods are given. The detection limits were estimated as discussed in the footnotes and based upon general calculations by Omenetto and Winefordner (F33) and by Falk (F57).

Source pulsing and gated detection will often lead to improved detection limits (and S/N ratios at concentrations above the detection limits) compared to continuous-wave (cw) operation of the source and detector. Based on work described in references (R1) and (F25), the expressions and gain factors reported

General Expression

$$B_F = \frac{\ell}{4\pi} h\nu_{ul} A_{ul} n_u$$

Two-Level Atom

Low-excitation irradiance

$$B_F = \frac{\ell}{4\pi} Y_{21} E_\nu(\nu_0) \int k(\nu)\, d\nu$$

High-excitation irradiance

$$B_F = \frac{\ell}{4\pi} h\nu_{ul} A_{21} n_T \frac{g_u}{g_u + g_l}$$

Three-Level Atom

The three levels are indicated here as 1, 2, and 3 in order of increasing energy, 1 being the ground state. The levels not coupled by radiation are levels 2 and 3 for sodiumlike atoms, and levels 2 and 1 for thalliumlike atoms. The subscripts for B_F refer to the fluorescence and absorption transitions, e.g., $B_{F_{1\to3}}$ means that laser excitation is set at λ_{13} and fluorescence is measured at λ_{21}.

Na atom type

Low-excitation irradiance (resonance fluorescence)

$$B_{F_{1\to3}} = \frac{\ell}{4\pi} A_{31} h\nu_{31} n_T \frac{g_3}{g_1} \frac{E_\nu(\nu_{31})}{E^*_\nu(\nu_{31})}$$

High-excitation irradiance (resonance fluorescence)

$$B_{F_{1\to3}} = \frac{\ell}{4\pi} A_{31} h\nu_{31} n_T \left(1 + \frac{g_1}{g_3} + \frac{k_{32}}{A_{21} + k_{21} + k_{23}}\right)^{-1}$$

High-excitation irradiance (Stokes stepwise line fluorescence)

$$B_{F_{1\to3}} = \frac{\ell}{4\pi} A_{21} h\nu_{21} n_T \frac{g_3 k_{32} E_\nu(\nu_{31})}{g_1(A_{21} + k_{23} + k_{21})\, E^*_\nu(\nu_{31})}$$

High-excitation irradiance (stepwise line fluorescence)

$$B_{F_{1\to3}} = \frac{\ell}{4\pi} A_{21} h\nu_{21} n_T \left[1 + \frac{A_{21} + k_{21} + k_{23}}{k_{32}} + \left(1 + \frac{g_1}{g_3}\right)\right]^{-1}$$

[Note: for the opposite cases, where excitation is at $1 \to 2$, replace all 2's by 3's and all 3's by 2's.]

Three-Level Atom

Tl atom type

Low-excitation irradiance (resonance fluorescence)

$$B_{F_{1\to3}} = \frac{\ell}{4\pi} A_{31} h\nu_{31} n_T \frac{g_3(E_\nu(\nu_{31})}{g_1 E^*_\nu(\nu_{31})\,[1 + (g_2/g_1)\, e^{-E_{12}/kT}]}$$

High-excitation irradiance (resonance fluorescence)

$$B_{F_{1\to3}} = \frac{\ell}{4\pi} A_{31} h\nu_{31} n_T \left(1 + \frac{g_1}{g_3} + \frac{g_2}{g_3} e^{-E_{12}/kT} + \frac{A_{32} + k_{32}}{k_{21}}\right)^{-1}$$

Low-excitation irradiance (Stokes direct line fluorescence)

$$B_{F_{1\to3}} = \frac{\ell}{4\pi} A_{32} h\nu_{32} n_T \frac{g_3 E_\nu(\nu_{31})}{g_1 E^*_\nu(\nu_{31})\,[1 + (g_2/g_1)\, e^{-E_{12}/kT}]}$$

High-excitation irradiance (Stokes direct line fluorescence)

$$B_{F_{1\to3}} = \frac{\ell}{4\pi} A_{32} h\nu_{32} n_T \left(1 + \frac{g_1}{g_3} + \frac{g_2}{g_3} e^{-E_{12}/kT} + \frac{A_{32} + k_{32}}{k_{21}}\right)^{-1}$$

[Note: for the opposite cases, where excitation is at $2 \to 3$, replace all 2's by 1's and all 1's by 2's and replace E_{12} by $-E_{12}$.]

Key to Symbols

ℓ = emission (fluorescence path length), m
$h\nu_{ul}$ = energy of emission photon, J
n_u = upper (radiative) level population density, m^{-3}
n_T = total population density of *all* electronic states of same atom, m^{-3}
g_l, g_u = statistical weights of lower and upper levels, respectively
$k(\nu)$ = atomic absorption coefficient at frequency ν, m
$E_\nu(\nu_{ul})$ = source spectral irradiance at ν_{ul}, J s^{-1} m^{-2} Hz^{-1}
$E^*_\nu(\nu_{ul})$ = modified saturation spectral irradiance at ν_{ul}, J s^{-1} m^{-2} Hz^{-1}

$$= \frac{cA_{ul}}{B_{ul}Y_{ul}} = \frac{8\pi h\nu^3_{ul}}{c^2 Y_{ul}}$$

B_{ul} = Einstein coefficient of induced emission, s^{-1} $(J/m^3\ Hz)^{-1}$
k = pseudo-first-order radiationless rate coefficient between levels shown, s^{-1}
A = Einstein coefficient of spontaneous emission between levels shown, s^{-1}
E_{12} = energy separation between levels 1 and 2, J
k = Boltzmann constant, J K^{-1} $atom^{-1}$
T = temperature of gas, K
c = velocity of light in vacuum, m s^{-1}

Table 2.5 (*Continued*)

Assumptions Necessary to Obtain Expressions

1. All expressions are for low optical densities of analyte (no self-absorption).
2. Prefilter and postfilter (self-reversal) effects are absent.
3. Rate equations approach is valid (no coherent effects).
4. Analyte atom concentration and cell temperature are constant over the cell (e.g., flame) dimensions.
5. Source of excitation is a continuum with respect to the absorption line width ($\delta\lambda_s > \delta\lambda_a$).

Quantum Efficiencies, Y

Two-level atom

$$Y_{21} = \frac{A_{21}}{k_{21} + A_{21}}$$

Three-level atom Na-like

$$Y_{31} = \frac{A_{31}}{(A_{31} + k_{31} + k_{32})\left(1 - \dfrac{k_{32}k_{23}}{(A_{31} + k_{31} + k_{32})(A_{21} + k_{21} + k_{23})}\right)}$$

$$Y_{21} = \frac{A_{21}}{(A_{21} + k_{21} + k_{23})\left(1 - \dfrac{k_{32}k_{23}}{(A_{32} + k_{31} + k_{32})(A_{21} + k_{21} + k_{23})}\right)}$$

Three-level atom Tl-like

$$Y_{31} = \frac{A_{31}}{A_{31} + A_{32} + k_{32} + k_{31}} \qquad Y_{32} = \frac{A_{32}}{A_{31} + A_{32} + k_{32} + k_{31}}$$

Table 2.6. Saturation Steady-State Spectral Irradiance $E^s_\nu(\nu_0)$[a]

Two-level atom

$$E^s_{\nu_{12}} = \left(\frac{c}{B_{21}}\right)\left(\frac{g_1}{g_1 + g_2}\right)(k_{21} + A_{21}) = \left(\frac{g_1}{g_1 + g_3}\right)E^*_{\nu_{12}}$$

Three-level Na-like atom

$$E^s_{\nu_{13}} = E^*_{\nu_{13}}\frac{g_1}{g_3}\left(1 + \frac{g_1}{g_3} + \frac{k_{32}}{k_{23} + k_{21} + A_{21}}\right)^{-1}$$

Three-level Tl-like atom

$$E^s_{\nu_{13}} = E^*_{\nu_{13}}\frac{g_1}{g_3}\left(1 + \frac{g_1}{g_3} + \frac{A_{32} + k_{32}}{k_{21}}\right)^{-1}$$

[a] See Table 2.5 for definition of all terms and units.

Table 2.7. Saturation Steady-State Spectral Irradiance Values for a Two-level Atom ($g_1 = g_2$)[a]

λ_0 (nm)	$E^s_\lambda(\lambda_0)$ (J s^{-1}/ cm^{-2}/ nm^{-1})
200	$2.5 \times 10^5/Y_{21}$
300	$3.0 \times 10^4/Y_{21}$
400	$7.0 \times 10^3/Y_{21}$
500	$2.5 \times 10^3/Y_{21}$
600	$1.0 \times 10^3/Y_{21}$
700	$4.5 \times 10^2/Y_{21}$
800	$2.0 \times 10^2/Y_{21}$

[a] Y_{21} = fluorescence quantum efficiency.

Table 2.8. Molecular Fluorescence Observed in Flames with Laser Excitation

Species	Excitation (nm)	Fluorescence (nm)	Transition	Reference
C_2	473.7, 516.5, 563.4	500–670	$A^3\Pi \leftarrow X^3\Pi$	*a*
CH	387.2, 431.2	390–450	$B^2\Sigma \leftarrow X^2\Pi$	*a*
	387.2, 431.2	420–500	$A^2\Delta \leftarrow X^2\Pi$	*a*
CN	388.3, 421.6	300–700	$B^2\Sigma \leftarrow X^2\Pi$	*a*
OH	306.4	280–350	$A^2\Sigma \leftarrow X^2\Pi$	*a*
BaCl	506–532	506–532	$C^2\Pi \leftarrow X^2\Sigma$	*b*
BaO	480–540	480–560	$A^1\Sigma \leftarrow X^1\Sigma$	*b*
BaOH	480–540	470–550		*b*
		700–850		
CaOH	540–560	540–660	$B^2X \leftarrow X^2\Sigma$	*c*
	590–650	540–660	$A^2\Pi \leftarrow X^2\Sigma$	
SrOH	620–630	600–700	$B^2X \leftarrow X^2\Sigma$	*c*
			$A^2\Pi \leftarrow X^2\Sigma$	
CrO	570–605	605–680	$A^5\Pi \leftarrow X^5\Sigma$	*c*
MnO	585–591	585–591		*c*
YO	$A^2\Pi_{3/2,1/2} \leftarrow X^2\Sigma$	594–628	$A^2\Pi \rightarrow X^2\Sigma$	*d*
	Q (1, 1) and Q (0, 0)			

[a] K. Fujiwara, N. Omenetto, J. D. Bradshaw, J. N. Bower, S. Nikdel, and J. D. Winefordner, *Spectrochim. Acta*, **34B**, 317 (1979), and references therein cited.
[b] H. Haraguchi, S. J. Weeks, and J. D. Winefordner, *Spectrochim. Acta*, **35A**, 391 (1979), and references therein cited.
[c] M. B. Blackburn, J. M. Mermet, and J. D. Winefordner, *Spectrochim. Acta*, **34A**, 847 (1978), and references therein cited.
[d] T. Wijchers, H. A. Dijkerman, P. J. Th. Zeegers, and C. Th. J. Alkemade, *Spectrochim. Acta*, **35B**, 271 (1980).

11.40

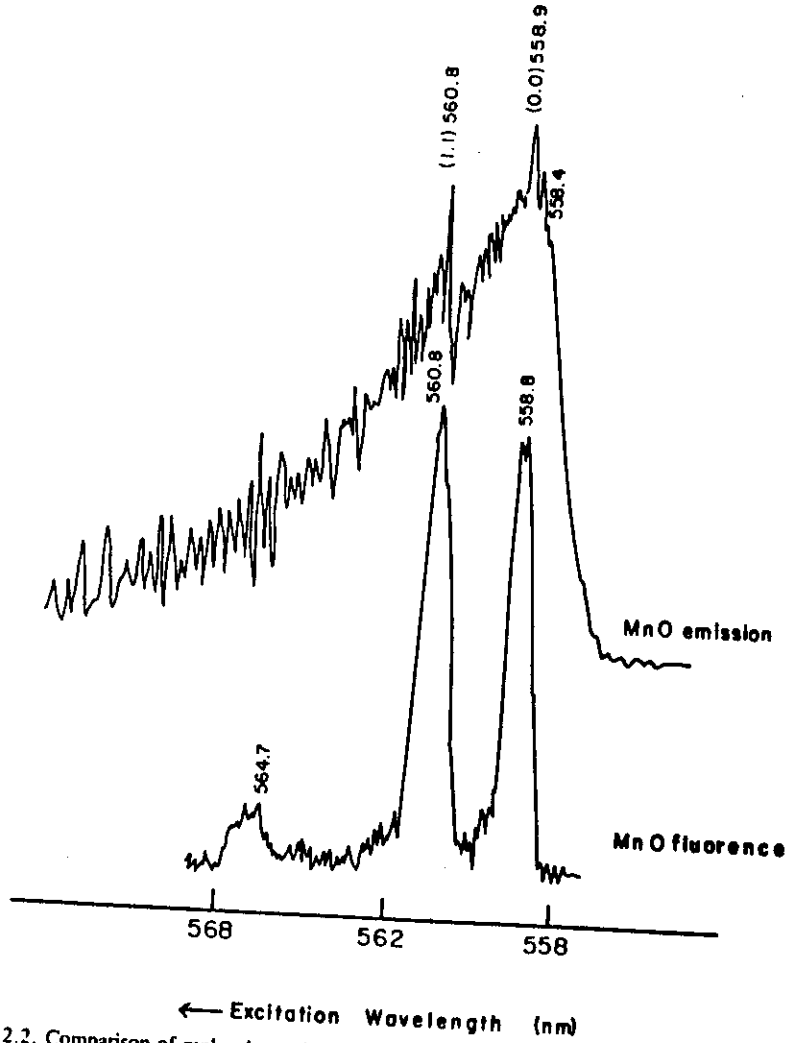

Fig. 2.2. Comparison of molecular emission and molecular fluorescence of MnO in an Ar-O_2-H_2 flame (Table 2.8, ref. c). MnO flame emission; MnO flame fluorescence (laser excitation at 587.9 nm).

in Table 2.10 have been derived. In general, in those cases where the noise is determined predominately by the cell background, it is possible to obtain an appreciable gain by source pulsing and detector gating if one assumes that the same average source power as in cw operation can be obtained and if no deleterious effects such as those described in footnote *f* of Table 2.10 are present.

Table 2.9. Comparison of Laser-excited Atomic Fluorescence Spectrometry with Other Atomic Methods

Method[a]	Cell	LOD[b] (atoms/cm^3)	LDR[c]	Spectral[d] Interferences	Matrix[e] Interferences	Comments
LEAFS	Flame	$\sim 10^5$	$\sim 10^6 X$	+	++	Background shot noise
	ICP	$\sim 10^5$	$\sim 10^6 X$	+	+	
	furnace	$\sim 10^5$	$\sim 10^5 X$	+	++++	
XEAFS	Flame	$\sim 10^9$	$\sim 10^5 X$	+++	++	Background shot noise
HCAFS[f]	ICP	$\sim 10^7$	$\sim 10^5 X$	++	+	Background shot noise
LEIS	Flame	$\sim 10^5$	$\sim 10^6 X$	++	+++	Background current shot noise
AAS	Flame	$\sim 10^8$	$\sim 10^2 X$	++	++	Source Shot noise
	Furnace	$\sim 10^8$	$\sim 10^2 X$	++	++++	Source shot noise
AES	ICP	$\sim 10^5$	$\sim 10^6 X$	++++	+	Background shot noise

[a]LEAFS = Laser-excited atomic fluorescence spectrometry with flame or ICP as cell
XEAFS = Xenon-excited atomic fluorescence spectrometry with flame cell
HCAFS = Pulsed hollow cathode lamp AFS with ICP cell
LEIS = Laser-enhanced ionization spectroscopy in flame cell
AAS = Atomic absorption spectrometry with flame or furnace cell; source could be hollow cathode lamp or xenon arc with high-resolution spectrometer (echelle)
AES = Atomic emission spectrometry with ICP source/cell.
[b]LOD = Limit of detection in atoms/cm^3. Values calculated by Omenetto and Winefordner (F33) and by Falk (F57). Values are averages of those obtained for typical experimental conditions.
[c]LDR = Linear dynamic range, i.e., range of linearity of calibration curve = C_u/C_l where C_u = upper concentration which is within 5% of linearity and C_l = limit of detection. The LDR values represent experimental values.
[d]Spectral interferences = selectivity of method to spectral interferences. ++++ = many spectral interferences and + = few spectral interferences.
[e]Matrix interferences = selectivity of method to matrix interferences. ++++ = many matrix interferences and + = few matrix interferences. In case of furnace AAS, some of the newer methods (platform vaporization, probe vaporization, and capacitative discharge represent ways to minimize such intereferences).
[f]The LOD was estimated by assuming the same conditions as in (F33) for the electrodeless discharge lamp excitation except that the duty cycle was taken as $\frac{1}{12}$ and the average hollow cathode irradiance was assumed to be the same as in the dc operated lamp used for the calculations in (F33).

Table 2.10. Benefit of Using Pulsed Sources and Various Detection in Atomic Fluorescence Spectrometry

Case	Source Type[a]	Detector Type[b]	Noise Type[c]	S/N[d]	Gain Factor[e]	Assumptions[f]
I	cw	cw	Source/bkgnd-shot	$K_1\bar{E}_{s,cw}/\sqrt{\bar{E}_{s,cw}+\bar{E}_b}$	1 (Refn)	—
I	pu	ga	Source/bkgnd-shot	$K_1E_{s,pu}/\sqrt{\bar{E}_{s,pu}+ft_p\bar{E}_b}$	$\bar{E}_{s,pu}/\bar{E}_{s,cw}\sqrt{ft_p}\rightarrow\frac{1}{\sqrt{ft_p}}$	$\bar{E}_b > \bar{E}_{s,cw}$ or $\bar{E}_{s,pu}$
I	pu	ga	Source/bkgnd-shot	$K_1\bar{E}_{s,pu}/\sqrt{\bar{E}_{s,pu}+ft_p\bar{E}_b}$	$\sqrt{\bar{E}_{s,pu}/\bar{E}_{s,cw}}\rightarrow 1$	$\bar{E}_{s,cw}\approx\bar{E}_{s,pu}$ $\bar{E}_b < \bar{E}_{s,cw}$ or $\bar{E}_{s,pu}$ $\bar{E}_{s,cw}\approx\bar{E}_{s,pu}$
II	cw	cw	Bkgnd-flicker	$K_2\bar{E}_{s,cw}/\xi_b\bar{E}_b$	1 (Refn)	—
II	pu	ga	Bkgnd-flicker	$K_2\bar{E}_{s,pu}/\xi_b ft_p\bar{E}_b$	$\bar{E}_{s,pu}/\bar{E}_{s,cw}ft_p\rightarrow\frac{1}{ft_p}$	$\bar{E}_{s,cw}\approx\bar{E}_{s,pu}$
III	cw	cw	Source-flicker	$\bar{E}_{s,cw}/\xi_s\bar{E}_{s,cw}$	1 (Refn)	—
III	pu	ga	Source-flicker	$\bar{E}_{s,pu}/\xi\bar{E}_{s,pu}$	1	

[a] cw = continuous wave source (on all of the time); pu = pulsed source.
[b] cw = continuous wave detector (on all of the time); ga = gated detector.
[c] source/bkgnd-shot = source and background shot noise; source-flicker = source flicker noise; bkgnd-flicker = background flicker noise.
[d] $\bar{E}_{s,cw}$ = average excitation irradiance of cw source; $\bar{E}_{s,pu}$ = average excitation irradiance of pulsed source = $ft_p\bar{E}_{s,peak}$ (assuming a rectangular pulse of width t_p, seconds, and a repetition rate of f, Hz); $\bar{E}_{s,peak}$ = peak pulsed source irradiance; $\bar{E}_b$ = average background irradiance; ξ_s = flicker noise factor for source related noise; K = proportionality factors accounting for optical throughput.
[e] Gain factor is always with respect to the cw/cw case for each type of noise.
[f] There are other inherent assumptions concerning pulsing. (i) the pulsed source with a duty cycle of ft_p can be pulsed at sufficient power so that $E_{s,pu} = E_{s,cw}$; (ii) the pulsing does not cause self-reversal, shift in the spectral line or assymetry; (iii) saturation is not reached or else source scatter would increase faster with $\bar{E}_s$ than the fluorescence. Also, the value of $\bar{E}_{s,pu}$ necessary to achieve saturation represents the maximum value to be substituted in the above equations.

No gain (enhancement) of S/N ratio occurs for those cases where the noise is associated with the analyte fluorescence and/or with the source intensity (e.g., analyte fluorescence, scatter, interferent fluorescence, flame radical fluorescence).

2.6. Fluorescence Growth Curves

Although no expressions were given in the fluorescence radiance section for high optical densities of the analyte, it is well known (F4, F9, F33) that, because of self-absorption, a plot of log B_F versus log n_T (where n_T is the total atomic population density, Table 2.5) will have a slope of zero at high optical densities if the excitation source is a spectral continuum with regards to the absorption profile, which is the case of the dye laser considered here (and of most dye lasers). It is clear that the linearity of the analytical fluorescence growth curve will be extended when using a laser compared to a conventional source because the detection limit, when the noise is not source related, will be reduced, and because, if optical saturation can be achieved, self-absorption is minimized. Therefore, it is not unreasonable for an analytical growth curve to extend over 6–8 orders of magnitude for LEAFS as compared to 4–7 orders of magnitude for the same excitation wavelength and the same element in the case of conventional (linear) source AFS.

Of course, experimental analytical growth curves are plots of S_F, that is, the fluorescence signal due to B_F versus C, which is the analyte concentration introduced as a nebulized aerosol into the atomization cell (flame or an ICP). The log S_F versus log C curves generally do not extend over as many decades (perhaps 5–7) as the log B_F versus log n_T curves because: (i) detector saturation may occur at large B_F values and (ii) the analyte concentration in the cell, n_T, may not be linear with the sample concentration C in the solution. In the case of flame and ICP atomization, this is due to a decrease in nebulization efficiency, solution transport rate, and solute vaporization efficiency with increased concentration of sample solution. For electrothermal atomizers, it is due to a decreased atomization time and decreased vaporization and atomization efficiencies.

3. INSTRUMENTAL AND METHODOLOGICAL CONSIDERATIONS

3.1. Instrumentation

A LEAFS instrument is basically an AFS system with a dye laser source. There are two major types of LEAFS instruments: a pulsed dye laser, cell, emission monochromator–photomultiplier tube with boxcar averager (see Figs. 2.3a and 2.3b) and a modulated cw dye laser (usually Ar laser-pumped dye laser), cell,

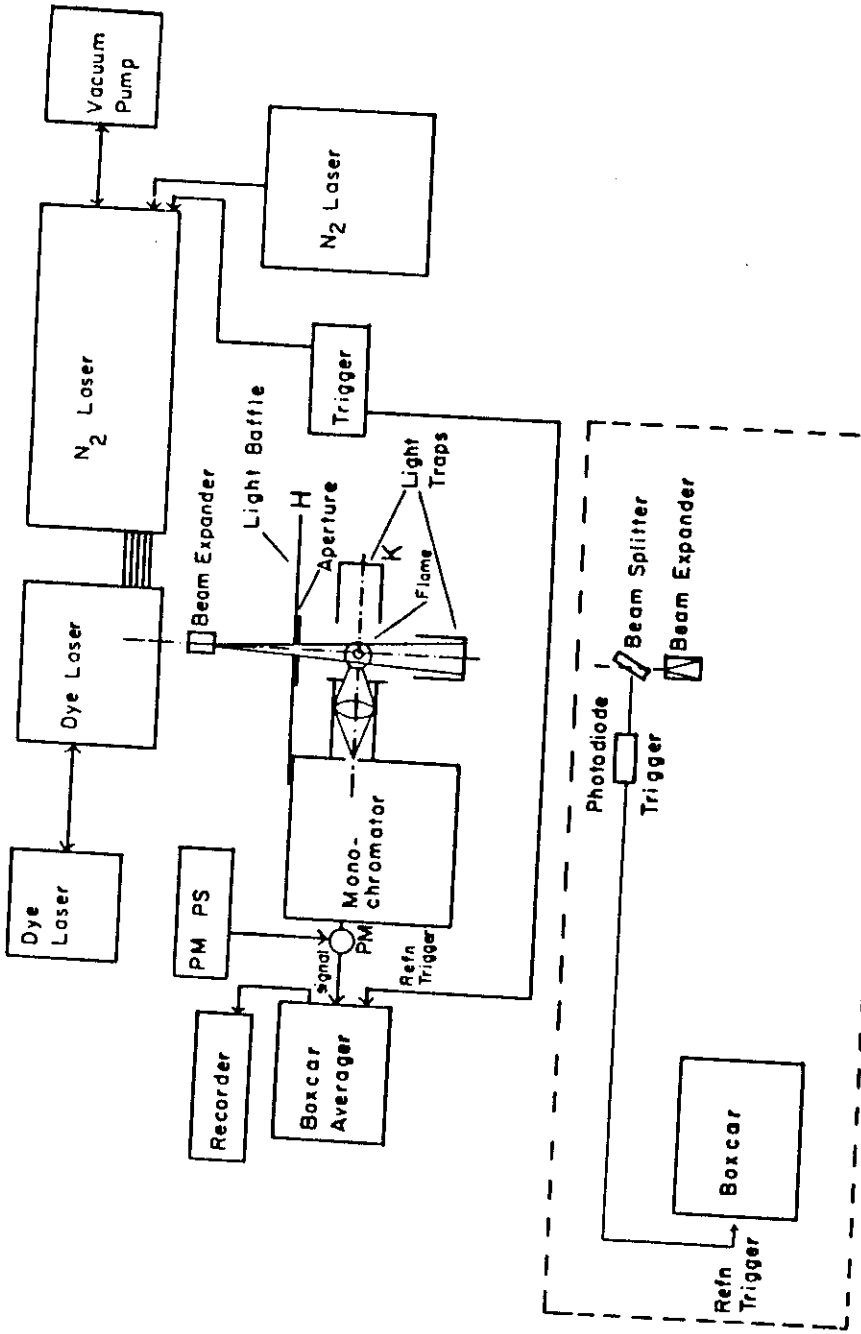

Fig. 2.3a. Schematic diagram of pulsed laser LEAFS instrument. Laser is a pulsed N_2 dye laser or a pulsed excimer dye laser or a pulsed Nd:YAG dye laser. Both external and optical triggering (with a photodiode) are indicated.

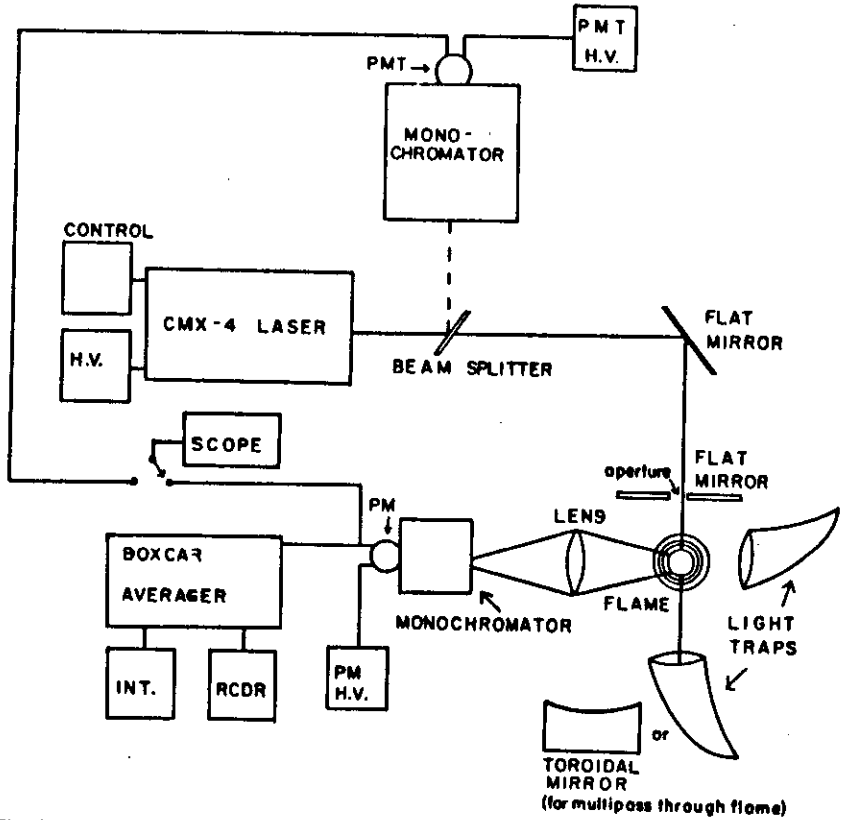

Fig. 2.3b. Schematic diagram of pulsed laser LEAFS instrument. Laser is a flashlamp dye laser.

emission monochromator–photomultiplier tube with phase-sensitive detection (see Fig. 2.4). No attempt will be made here to describe the operation of pulsed or modulation systems, or of detection systems; the reader is referred to other references.

3.2. Analytical Figures of Merit LEAFS

Table 2.11 collects several experimental papers on LEAFS. In addition to the instrumental components used in each reference, the types of analytically significant results, such as the number of elements measured, the presence of limits of detection, linear dynamic ranges (calibration curves), and the application to real samples are also given.

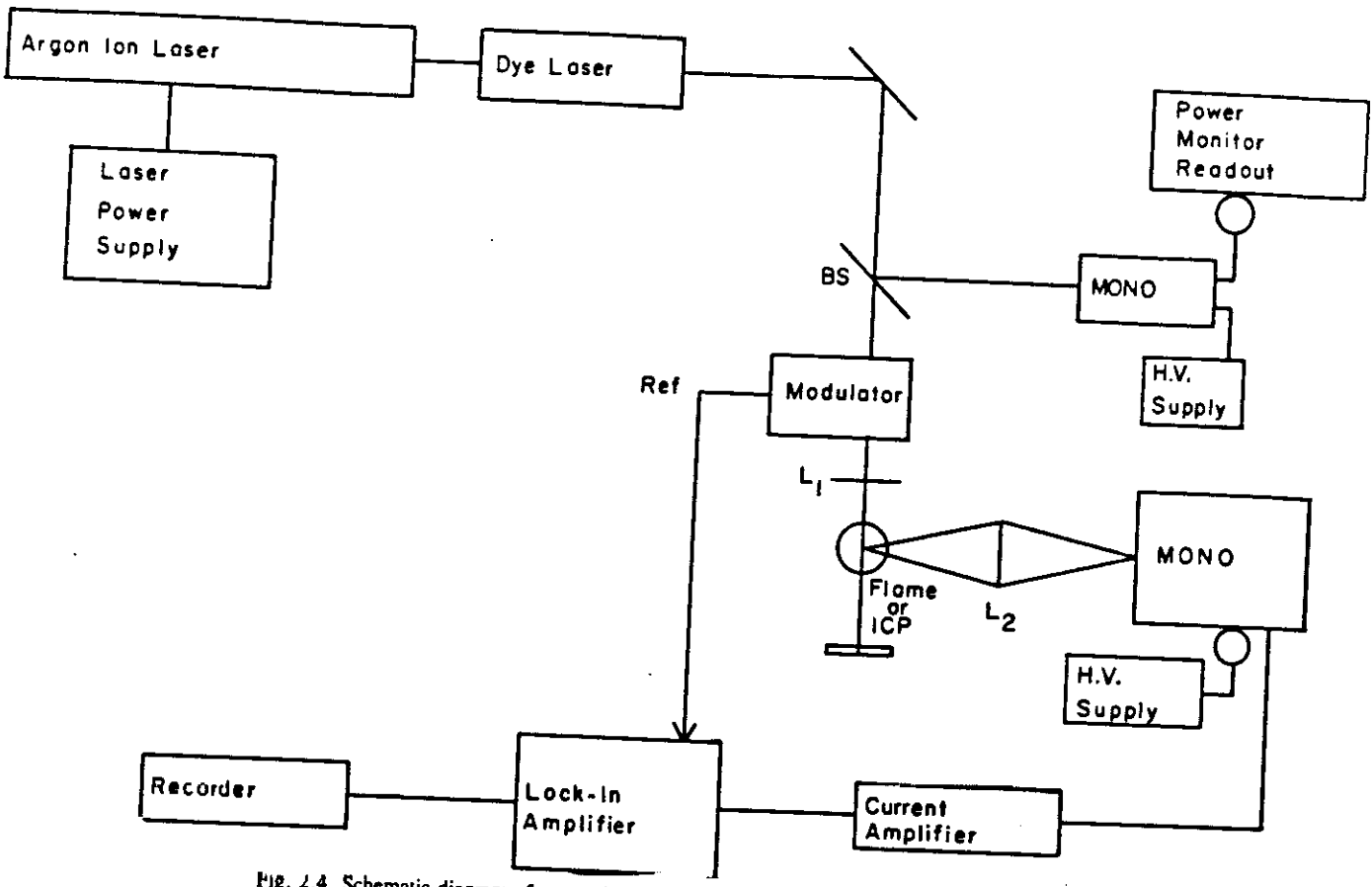

Fig. 2.4. Schematic diagram of an amplitude-modulated cw dye laser LEAFS instrument.

Table 2.11. Experimental Studies in Laser-excited Analytical Atomic Fluorescence Spectrometry

References	Laser System[a]	Cell	Modulation–Detection	Analytical Results				
				Elements	LOD	LDR	Applic.	Comments
I1	Ruby-DL	Flame	Amp-Osc	Ba	Yes	Yes	No	First paper
I2	N_2-DL	Flame	Boxcar	Many	Yes	Yes	No	First paper
I3	FDL	Na cell	Lock-in	Na	Yes	Yes	No	—
I4	N_2-DL	Flame	Boxcar	Many	Yes	Yes	No	—
I5	N_2-DL	Flame	Boxcar	Rare earth	Yes	Yes	No	Ionic fluorescence
I6	N_2-DL	Flame	Boxcar	Trans. elem.	Yes	No	No	Nonresonance fluorescence
I7	FDL	Flame	Boxcar	Na	Yes	Yes	No	—
I8	FDL	Flame	Boxcar	Mg, Ni, Pb	Yes	Yes	No	—
I9	FDL	Graphite rod	Lock-in	Pb	Yes	Yes	No	—
I10	NDL	Quartz cell	Photon counting	Alkali metals	No	No	No	Compared sensitized to resonance fluorescence
I11	ADL	Quartz cell	Lock-in	Na	Yes	Yes	No	—
I12	ADL	Quartz cell	Lock-in	Na	Yes	Yes	No	—
I13	FDL	Quartz cell	Filter + osc	Na	Yes	Yes	No	Fundamental study
I14	ADL	Flame	Lock-in	Ba, Na	Yes	Yes	No	—
I15	FDL	Quartz cell	Amp-Osc	Na	Yes	Yes	No	—
I16	ADL	Quartz cell	Lock-in	Na	Yes	No	No	—
I17	FDL	Sputtering cell	Boxcar	Fe	No	No	No	—
I18	YAG-DL	Graphite furnace	Filter + osc	Fe, Pb	Yes	Yes	No	—
I19	FDL	Flame	Boxcar	Na	Yes	No	No	Nonresonance fluorescence
I20	NDL	Flame	Boxcar	Sr, Mn, Na, Ca, In	No	No	No	Microprocessor-controlled scanning

Table 2.11. (*Continued*)

References	Laser System[a]	Cell	Modulation–Detection	Analytical Results				
				Elements	LOD	LDR	Applic.	Comments
I21	NDL	Flame	Boxcar	Na	No	No	No	Saturation study
I22	ADL	Flame	Lock-in	Na, V, B, Sr, Mo	Yes	Yes	No	—
I23	YAG-DL	Graphite furnace	Filter + osc	Pb	No	No	No	Fundamental studies
I24	FDL	Quartz cell	Boxcar	Na	Yes	Yes	No	Single-atom detector
I25	FDL	Flame	Boxcar	Na, MgO	Yes	Yes	No	Dye laser
I26	NDL	Flame	Boxcar	Many	Yes	Yes	No	—
I27	NDL	Graphite furnace	Boxcar	Tl	Yes	Yes	No	—
I28	ADL	Flame	Lock-in	Ba	Yes	Yes	No	Used wavelength modulator
I29	YAG-DL	Flame	Boxcar	Na	Yes	Yes	No	—
I30	YAG-DL	Flame	Boxcar	Na	Yes	Yes	No	—
I31	YAG-DL	Flame	Boxcar	Na	Yes	No	No	Comparison with photoionization
I32	ADL	Interactivity ABS cell	Fluorescence detector	I_2	Yes	Yes	No	Isotope detect.
I33	ADL	ICP	Lock-in	Na, Ba, Li, V	Yes	Yes	No	—
I34	NDL	Ablation chamber	Boxcar	Cr	Yes	Yes	Yes	Ruby laser used to ablate sample
I35	NDL	Ablation chamber	Boxcar	Cr	Yes	Yes	Yes	Ruby laser used to ablate sample
I36	?	Quartz cell	?	Na	Yes	?	No	Single-atom detector
I37	NDL	U-oven	Transient recorder	U	No	No	No	Spectra only
I38	FDL	Flame	Boxcar	Fe	Yes	Yes	Yes	Multipass cell
I39	FDL or NDL	ICP	Boxcar	Fe, Sn, Ba, In	Yes	No	No	—
I40	FDL	Flame	Boxcar	Sn, Ni	Yes	Yes	Yes	—
I41	ADL	Low-pressure cell	Lock-in	Na	Yes	No	No	Single-atom detector
I42	Resonance line	Flame	Boxcar	Tl, Na	Yes	No	No	Resonance line lasers, photoionization detection
I43	ADL	Flame	Lock-in	Na	Yes	No	No	Scatter correction
I44	NDL or ADL	Flame	Boxcar/lock-in	Na	No	No	No	Chemical rx's in exc. state
I45	YAG-DL	Furnace	Amp/disc/counter	Pb	Yes	Yes	No	—
I46	YAG-DL	Quartz cell	Amp/disc/counter	Hg	Yes	No	No	Multiphoton ioniz. & recomb.
I47	NDL	Flame	Boxcar	Ca, Sr, Mg, Pb, Fe	Yes	No	Yes	—
I48	YAG-DL	Quartz cell/furnace	Boxcar	Pb	Yes	Yes	No	—
I49	YAG-DL	Graphite furnace	Boxcar	Pb, Fe, Na, Pt, Ir, Eu, Ca, Ag, Co, Mn	Yes	Yes	Yes	—
I50	YAG-DL	Low-pressure discharge	Boxcar	Cl	No	No	No	—
I51	YAG-DL	Flame	Boxcar	?	Yes	No	No	Single-atom detector
I52	YAG-DL	Quartz cell	Photon counting	Hg	Yes	Yes	No	Projected use for atmosphere
I53	NDL	ICP	Boxcar	Tl, Ba, Ca, V, Y, Mo, Pb	Yes	Yes	No	Short torch
I54	NDL	ICP	Boxcar	Many	Yes	Yes	No	Long Torch

S+·II

Table 2.11. (*Continued*)

References	Laser System[a]	Cell	Modulation–Detection	Analytical Results				
				Elements	LOD	LDR	Applic.	Comments
I55	Exc-DL	Flame, furnace ICP	Boxcar	—				General considerations
I56	Exc-DL	ICP, flame	Boxcar	Al, B, Ba, Ga, Mo, Pb, Si, Sn, Ti, Tl, V, Y, Zr	Yes	No	No	Short torch
I57	Exc-DL	ICP	Boxcar					
I58	Exc-DL	Flame	Boxcar	Pb	Yes	No	Yes	Direct determination in blood
I59	ADL	Flame	Lock-in	Na	No	No	No	Scattering correction
I60	NDL	Graphite cuvette	Boxcar	Many	Yes	No	No	
I61	ADL	Flame	Lock-in	Na	No	No	No	Scattering correction
I62	ADL	Flame	Lock-in	Na	No	No	No	

[a]NDL = Nitrogen laser-pumped dye laser; FDL = flashlamp-pumped laser; ADL = argon ion laser-pumped dye laser; Exc-DL = excimer laser-pumped dye laser.

3.2.1. *Limits of Detection with LEAFS*

Table 2.12 collects the best detection limits, in concentration units (ng/mL) so far achieved by LEAFS in either flame or plasma atomizers, together with the linear dynamic ranges obtained and the best combination for the excitation and fluorescence lines. In Table 2.13, these limits are compared with limits of detection by several other atomic methods: Atomic fluorescence flame spectrometry with conventional line sources (AFS-line); atomic fluorescence flame spectrometry with conventional continuum source (AFS-continuum); atomic absorption flame spectrometry (AAS); atomic emission spectrometry with inductively coupled plasma (ICPAES); and laser-enhanced ionization spectrometry in flames (LEIS). In Table 2.14, the best limits of detection in absolute limits (in picograms) for LEAFS with a graphite filament electrothermal atomizer are compared with EAAAS (AAS with an electrothermal atomizer), which has been the "star" of analytical methods for absolute elemental detection limits.

Although current concentration and absolute detection limits by LEAFS have not yet reached those *predicted* (F33, F57), they are nevertheless highly competitive with the best values achieved by other atomic (elemental) methods. The concentration limits of detection in LEAFS approach the values calculated, assuming background (e.g., flame) emission shot noise. If the background can be reduced (as in electrothermal atomizers), then it should be possible to lower the detection limits by $\sim 10^5\times$, assuming the ultimate limiting noise level, that is, detector shot noise, can be reached. Experimentally, with carbon rod atomizers, $\sim 10^3$ atoms of lead per cubic centimeter have indeed been detected (148, 156).

3.2.2. *Analytical Calibration Curves*

In Table 2.12, the linear dynamic ranges of LEAFS (flame) are listed along with the limits of detection. The linear dynamic ranges in LEAFS (ICP) are similar. As an example, Fig. 2.5 shows two typical analytical calibration curves for Sn and Ni.

3.2.3. *Precision*

The precision (percent relative standard deviation) in LEAFS is generally slightly poorer than that achieved by AAS, ICPAES, and conventional source AFS, mainly because of the pulse-to-pulse stability of pulsed dye lasers assuming no optical saturation. The precision is limited to ~3–5% for a 1-s integration time. In Fig. 2.6, a typical precision curve for Fe is given (138).

Table 2.12. Concentration Detection Limits (Aqueous Solution) Obtained by Laser-excited Atomic Fluorescence Spectrometry

Element	$\lambda_{ex}/\lambda_{fl}$[a]	Laser-Excited AFS[c-f]		
		Type of AF[b]	LOD(ng/mL)	LDR
Ag	328.1/328.1	RF	4	4.2
Al	394.4/396.1	S-DLF	0.4	—
Au	267.6/242.8	TA-AS-SLF	4	5.5
B	249.6/249.7	S-DLF	4	—
Ba	455.4/614.2(i)	S-DLF	0.7	—
Bi	306.8/306.8	RF	3	5.2
Ca	422.7/422.7	RF	0.01	5.0
Cd	228.8/228.8	RF	8	3.5
Ce	371.6/294.1(i)	TA-AS-SLF	500	—
Co	357.5/347.4	AS-DLF	19	5.0
Cr	359.3/359.3	RF	1	5.5
Cu	324.7/324.7	RF	1	5.0
Dy	364.5/356.3(i)	TA-AS-SLF	300	—
Er	400.8/400.8	RF	500	—
Eu	459.4/462.7	S-DLF	20	—
Fe	296.7/373.5	S-DLF	30	6.0
Ga	403.3/417.2	S-DLF	0.9	5.4
Gd	336.2/376.8(i)	E-S-SLF	800	—
Ho	405.4/410.4	S-DLF	100	—
In	410.4/451.1	S-DLF	0.2	6.2
Ir	266.5/406.9	S-DLF	9	4.5
Li	670.8/670.8	RF	0.5	4.3
Lu	465.8/513.5	S-DLF	3,000	—
Mg	285.2/285.2	RF	0.2	6.0
Mn	279.5/279.5	RF	0.4	5.4
Mo	313.2/317.0	S-SLF	5	—
Na	589.0/589.0	RF	0.1	5.7
Nb	405.9/408.0	E-S-SLF	1,400	—
Nd	463.4/489.7	S-SLF	2,000	—
Ni	311.2/342.0	S-DLF/S-SLF	2	6.0
Os	442.0/426.1	TA-AS-SLF	150,000	—
Pb	383.3/405.8	S-DLF	0.02	—
Pd	324.3/340.4	E-S-SLF	1	6.0
Pr	422.5/430.6(i)	S-DLF	1,000	—
Pt	264.7/270.2	S-DLF	0.7	6.0
Rh	369.2/350.2	TA-AS-SLF	100	—
Ru	287.5/366.3	S-DLF	2	6.0
Sc	391.2/402.4	E-S-SLF	10	—
Si	288.1/251.6	E-AS-SLF	1	—
Sm	367.4/373.9(i)	S-SLF	100	—

Table 2.12. (*Continued*)

Element	$\lambda_{ex}/\lambda_{fl}$[a]	Laser-Excited AFS[c-f]		
		Type of AF[b]	LOD(ng/mL)	LDR
Sn	300.9/317.5	S-DLF	3	—
Sr	460.7/460.7	RF	0.3	5.0
Tb	370.3/350.9	?	500	—
Ti	307.8/316.2(i)	E-S-DLF	1	—
	307.8/316.8(i)	E-TA/S-SLF	1	—
Tl	276.7/352.9	S-DLF	0.8	—
U	409.0/385.9	AS-DLF	20	—
V	268.8/290.8(i)	S-DLF	3	—
Y	508.7/371.0(i)	E-AS-DLF	0.6	—
Yb	398.8/346.4	TA-AS-SLF	10	—
Zr	310.6/256.8(i)	E-AS-DLF	3	—
	310.6/257.1(i)	E-AS-SLF	3	—

[a] $\lambda_{ex}/\lambda_{fl}$ = excitation and fluorescence wavelengths, in nm. (i) means ionic fluorescence.
[b] RF = resonance fluorescence; DLF = direct line fluorescence; SLF = stepwise line fluorescence; S- = Stokes; AS- = anti-Stokes; TA = thermally assisted; E = excited states; LOD = limit of detection; LDR = linear dynamic ranges, number of decades.
[c] S. J. Weeks, H. Haraguchi, and J. D. Winefordner, *Anal. Chem.*, **50**, 360 (1978).
[d] N. Omenetto, N. N. Hatch, L. M. Fraser, and J. D. Winefordner, *Anal. Chem.*, **45**, 195 (1973); N. Omenetto, N. N. Hatch, L. M. Fraser, and J. D. Winefordner, *Spectrochim. Acta*, **28B**, 66 (1973). These values were obtained with one of the first laser experimental fluorescence setups and can be considered, for some elements, of historical interest.
[e] N. Omenetto, H. G. C. Human, P. Cavalli, and G. Rossi, *Spectrochim. Acta*, **39B**, 115 (1984).
[f] S. Kachin, B. W. Smith, and J. D. Winefordner, *Appl. Spectrosc.*, **39**, 587 (1985).

3.2.4. *Spectral Selectivity*

The spectral selectivity of LEAFS (also see Table 2.9 for a comparison with other atomic methods) is the highest of all atomic methods, perhaps *all* methods for analysis of elements. The high spectral selectivity rests with the extreme excitation selectivity based on single-line laser excitation *and* upon emission selectivity (selection of the fluorescence wavelength to observe the AFS signal). In Fig. 2.7, the excitation spectrum of Na is given (Fig. 2.7a), which indicates that a dye laser with a bandwidth (FWHM) of ~0.03 nm allows selection of either of the Na-*D* lines for excitation. In this case, as shown in Fig. 2.7b, the emission monochromator's bandpass was quite large, here 1.6 nm, to allow measurement of the fluorescence from both Na-*D* lines, since mixing collisions in the flame populate both Na-*D* states. Of course, the monochromator bandpass could be reduced to resolve the two lines, thus adding to the selectivity of the method.

Table 2.13. Limits of Detection (Aqueous Solution) Obtained by Laser-excited Atomic Fluorescence Spectrometry and by Several Other Methods (ng/mL)

Element	AFS Line[a]	AFS Continuum[b]	LEAFS (flame)[c]	AAS[d]	ICPAES[e]	LEIS[f]	LEAFS (ICP)[g]
Ag	0.1	1	4	2	0.2 (4)	1	—
Al	100	200	0.6	20	0.4	0.2	0.4
As	100	—	—	400	2	—	—
Au	1,000	150	4[ΔΔ]	4[ΔΔ]	—	—	—
Ba	—	—	8	20	0.01 (0.2)	0.2	0.7
Be	10	15	—	2	— (0.3)	—	—
Bi	10	—	3	30	— (50)	2	—
Ca	20	—	0.8	2	0.0001 (4)	0.1	2
Cd	0.001	6	8	1.5	0.07** (1)	0.1*	—
Ce	—	—	500*	—	0.4 (20)	—	—
Co	5	15	200*	15	0.1** (2)	0.08*	—
Cr	50	1.5	1	3	0.2 (4)	2	—
Cu	1	1.5	1	2	0.04** (2)	0.7*	—
Dy	—	—	300*	—	— (2)	—	—
Er	—	—	500*	—	— (—)	—	—
Eu	—	—	20*	—	— (1)	—	—
Fe	8	10	30	10	0.09(2)	2	50*
Ga	10	—	(0.06)†				
Gd	—	—	0.9	—	0.6(40)	0.7	1
Ge	15,000	—	800*	—	0.5(8)	0.006	—
Hf	—	—	—	—	— (50)		—
Hg	80	—	—	200	— (—)	—	—
Ho	—	—	—	—	— (50)	—	—
In	100	25	100*	—	— (—)	—	—
Li	—	—	0.2	—	— (40)	0.008	300*
Lu	—	—	0.5	1	— (3)	0.001	—
Mg	1	0.1	3000*	—	— (—)	—	—
Mn	6	2	0.2	0.2	0.003 (20)	0.1	—
Mo	500	100	0.4	3	0.02 (0.5)	0.3	—
Na	100,000	—	12	20	0.4 (5)	—	5
Nb	—	—	<0.1	0.5	0.02 (10)	0.05	—
Nd	—	—	1500*	—	0.2 (20)	—	—
Ni	3	25	2000*	10	— (10)	—	—
Os	—	—	0.5[Δ]	—	0.2 (6)	0.08	—
Pb	10	50	150,000*	15	— (200)	—	—
Pd	1,000	100	0.02**	—	1** (20)	0.09*	1
Pr	—	—	1[ΔΔ]	—	2 (40)	—	—
Pt	50,000	700	1000*	—	— (30)	—	—
Rh	3,000	—	0.7[ΔΔ]	—	— (30)	—	—
Ru	—	—	100*	—	— (30)	—	—
Sb	—	—	2[ΔΔ]	—	— (60)	—	—
Sc	—	—	50*	30	— (30)	—	—
Se	40	—	10*	—	— (1)	—	100
Si	600	—	—	250	1*** (20)	—	—
Sm	—	—	—	100	— (10)	—	1
Sn	30	150	100*	—	— (10)	—	—
Sr	30	0.9	3[Δ]	70	3 (6)	3	3
Tb	—	—	0.3	1	0.003 (0.2)	—	0.5
Te	5	—	500*	—	— (—)	—	—
Ti	—	200	—	70	— (20)	—	—
Tl	8	6	2	80	0.03 (1)	0.2	1
Tm	—	—	0.8**	30	— (75)	0.09	7
V	70	30	100*	—	—	—	—
Yb	—	—	30	50	0.06 (2)	—	3
			10*	—	—	—	—

87.11

Table 2.13 (*Continued*)

Element	AFS Line[a]	AFS Continuum[b]	LEAFS (flame)[c]	AAS[d]	ICPAES[e]	LEIS[f]	LEAFS (ICP)[g]
Y	—	—	—	200	0.08	—	0.6
Zn	0.2	15	—	1	0.1 (2)	—	—
Zr	—	—	—	1,000	0.3	—	3

[a] The values come from references within J. D. Winefordner, *J. Chem. Ed.*, **55**, 72 (1978).
[b] The values come from D. J. Johnson, F. W. Plankey, and J. D. Winefordner, *Anal. Chem.*, **46**, 1858 (1974).
[c] Values from S. J. Weeks, H. Haraguchi, and J. D. Winefordner, *Anal. Chem.*, **50**, 360 (1978), except those with * which were taken from references listed in Winefordner, *J. Chem. Ed.*, **55**, 72 (1978). The one with † was taken from M. S. Epstein et al., *Spectrochim. Acta*, **35B**, 233 (1980), that with ** were taken from M. S. Epstein et al., *Appl. Spectrosc.*, **34**, 372 (180), those with [a] was taken from H. G. C. Human, et al., *Spectrochim. Acta*, **39B**, 587 (1985).
[d] All values come from Perkin-Elmer atomic absorption commercial literature on the Model 460.
[e] All values from P. W. J. M. Boumans and F. J. De Boer, *Spectrochim. Acta*, **30B**, 309 (1975), except for those with ** and those in ( ). All values in ( ) come from commercial literature from Jarrell-Ash Division, and Fisher Scientific Co., Waltham, Mass. for their third-generation ICP Plasma Atom Comp. All values with ** come from K. W. Olson, J. W. Haas, and V. A. Fassel, *Anal. Chem.*, **49**, 632 (1977).
[f] Values taken from G. C. C. Turk, et al., *Anal. Chem.*, **51**, 1890 (1979), except * are dual laser-excited values taken from G. C. Turk, J. C. Travis, J. R. Dobbs, and T. C. O'Haver, *Anal. Chem.*, **54**, 643 (1982).
[g] Values taken from N. Omenetto et al., *Spectrochim. Acta*, **39B**, 115 (1984) except from those designated with *, which were taken from M. Epstein et al., *Anal. Chim. Acta*, **113**, 221 (1980).

Table 2.14. Absolute Limits of Detection (Aqueous Solution) by Laser-excited Atomic Fluorescence Spectrometry in Graphite Atomizer and by Electrothermal Atomizer Atomic Absorption Spectrometry (EAAAS)

	LOD (pg)	
Element	Laser AFS[a]	EAAS[b]
Ag	0.1	0.4
Co	0.06	3
Cu	0.15	2
Eu	300	2,000
Fe	0.1	5
Ir	6	2,000
Mn	0.2	1
Na	0.6†	50
Pb	0.0015	2
Pt	120	200
Sn	5†	0.6
Tl	0.1*	4

[a] All values from M. A. Bolshov, A. V. Zybin, and I. I. Smirenkina, *Spectrochim. Acta*, **36B**, 1143 (1981) except for those with † which are from P. Wittman, University of Florida, Ph.D. dissertation, 1982, and for those with *, which were taken from H. G. C. Human et al., *Spectrochim. Acta*, **39B**, (1984). It is worth mentioning that similar results were also obtained by J. Tilch et al., Proceedings of "Analytikteffen 1982," Neubrandenburg, DDR, November, 1982.
[b] Data from commercial literature (Perkin-Elmer, HGA-2100).

A good example of the much greater spectral selectivity of LEAFS (in the ICP) compared to ICPAES is given in Fig. 2.8. In the top system, the LEAFS spectrum of Y(II) in an iron matrix (100 μg/mL Y in 5000 μg/mL Fe) is given in the range $\approx$370–372 nm, and in the bottom spectrum, the ICPAES emission spectrum is given. It is quite obvious that in the fluorescence spectrum no problems arise with spectral interferences from Fe, whereas in the lower emission spectrum, Fe emission at 371.030 nm overlaps the 370.925 nm Y(II) line (I54), and one has therefore to search for another (perhaps less sensitive) emission line.

3.3. RF-ICP versus Flame Cells for Fluorescence

The flame has been used as an atom reservoir in most of the previous studies involving laser excitation. However, several publications (I53, I54, I56, I57)

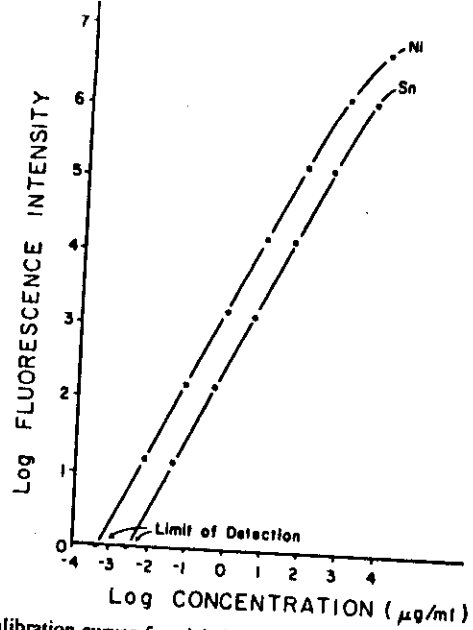

Fig. 2.5. Analytical calibration curves for nickel fluorescence excited at 300.249 nm and measured at approximately 342 nm and tin fluorescence excited at 300.914 nm and measured at 317.505 nm (139).

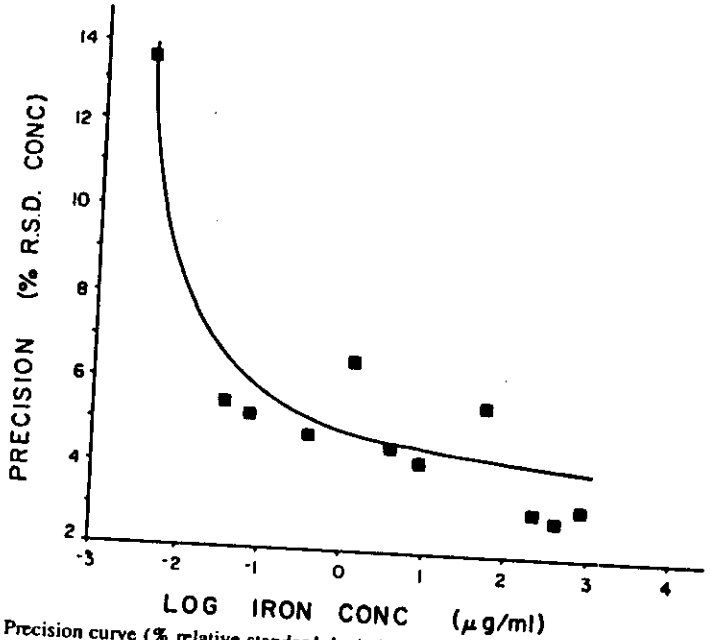

Fig. 2.6. Precision curve (% relative standard deviation vs concentration) for LEAFS measurement of Fe (138). The Chromatix CMX-4 flashlamp dye laser in the single-pass configuration is used (see Fig. 2.3b).

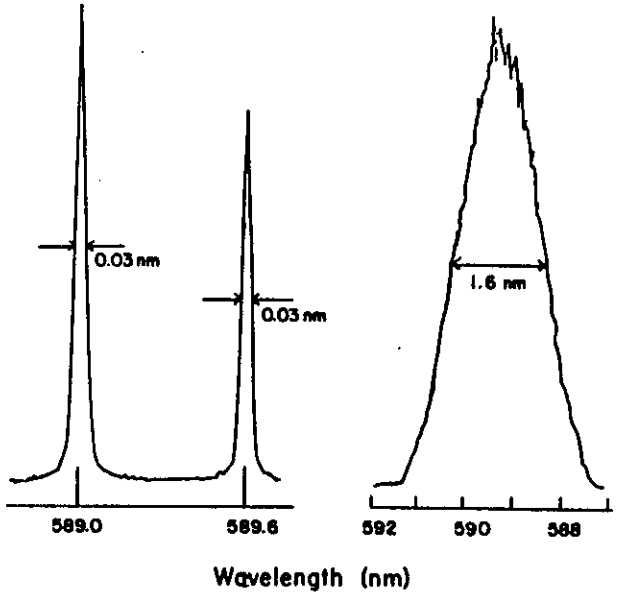

Fig. 2.7. Excitation and fluorescence profile of Na-*D* lines (at 589.0 nm and 589.6 nm) in an air-acetylene flame (126). The monochromator slit width was 0.8 mm in both cases. (a) Profile observed by scanning the dye laser (excitation spectrum); (b) profile observed by scanning the emission monochromator (emission spectrum).

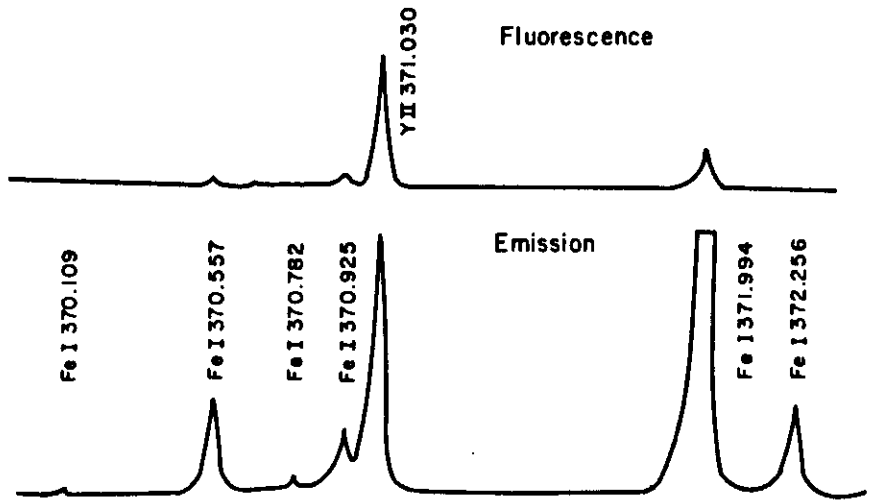

Fig. 2.8. Comparison of emission and fluorescence spectra of yttrium in an iron matrix. Conditions: 100 μg/mL Y in 5000 μg/mL Fe; RF power = 1 kW; 15 mm observation height above lead coil using conventional short torch; emission slit width = 0.02 mm (0.04 nm bandpass) and fluorescence slit width = 1 mm (2 nm bandpass) (154).

have recently described the use of a radio-frequency Ar inductively coupled plasma as an atom–ion reservoir for laser-excited fluorescence. The following advantages of an ICP over a flame have been stressed: (i) both ion and atom lines can be excited; (ii) excitation of atoms and ions from levels up to ≈ 2 eV above the ground state can be efficiently done; and (iii) the ICP is a rather ideal atom–ion reservoir for several elements because of its high quantum efficiency. Indeed, Uchida et al. (I53, I54) have found that the quantum efficiencies of atoms with rather simple energy level diagrams, as Na, Li, and so on, approach unity low in the plasma, decreasing rather slowly with the increase in the height above the coil. Analytical studies with a pulsed N_2 dye laser ICP system (I53, I54) have so far been disappointing. However, the detection limits obtained with an excimer pumped dye laser (I56, I57) and a conventional ICP emission setup, were found to be superior to "standard" tabulated emission values for several of the elements investigated.

3.4. In Situ Elemental Analysis

Measures and Kwong (I34, I35) have reported on a technique based on laser ablation and selectively excited fluorescence (TAB LASER) for micro-ultratrace determination of in situ elements in solid samples. A block diagram of the instrumental approach is shown in Fig. 2.9. The authors were able to determine Cr in samples of NBS standard reference steel, doped skim milk, and doped flour. In their approach, a single pulse from an ablation laser (e.g., Q-switched ruby laser) strikes the sample target producing a plume that expands rapidly into a low-pressure region (10^{-3}–10^{-4} torr). After an appropriate delay to minimize Mie scatter from particulate debris and plasma background emission, the outward-streaming highly recombined plume of material is interrogated by a brief pulse (6 ns) of laser radiation that is tuned to one of the strong transitions of the analyte. The resulting saturated resonance fluorescence was directly related to the concentration of the trace element within the target.

3.5. Analytical Applications

Few applications of LEAFS to real analyses have been carried out. Several are listed in Table 2.15.

3.6. Diagnostics of Plasmas and Flames

The potentiality of LEAFS to the measurement of physical parameters in flames and plasmas with spatial ($\gtrsim 1$ mm^3), and temporal ($\gtrsim 1$ μs) resolution is apparent

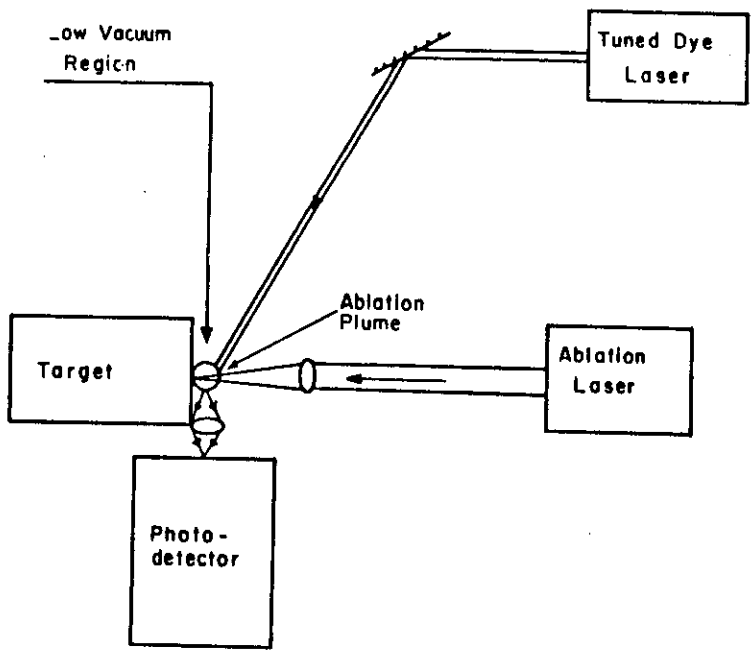

Fig. 2.9. Trace (element) analyzer based on laser ablation and selectivity excited radiation (redrawn from I34).

from the previous discussion. No attempt will be made to give a detailed evaluation of the use of LEAFS for average (multiple pulses) and single-pulse temperature, absolute concentration, rise velocity, and quantum efficiency measurements. The reader is referred to several excellent discussions of these parameters in the fundamental references (F4, F5, F9, F20, F21, F26, F28, F32, F33, F37, F40–42, F44–46, F50, F54, and other references in various journals, but especially *Appl. Optics*). The laser characteristics of vital importance for such studies include: high peak spectral irradiance (optical saturation possible); short pulse width (single pulse measurement possible); collimation and small beam size (spatial resolution possible).

4. EPILOGUE

The great excitement evident in the early workers on LEAFS is still present. However, the researchers of LEAFS have become more realistic in recent years on where LEAFS will find analytical usefulness (refer to Tables 2.1 and 2.2). In Table 2.16, a summary of the present status of LEAFS for analytical use is given.

Table 2.15. Determination of Various Elements in Different Materials by Laser-excited Atomic Fluorescence Spectrometry

Sample	Element	LEAFS Analysis	Certified Value	Reference
Trace element in waters (SRM-1643)	Fe	78 ng/g	75 ± 1 ng/g	138
Unalloyed copper (SRM-394)	Ni	50 ± 2 ng/g	44 ± 1 ng/g	139
	Fe	145 ± 6 μg/g	147 ± 8 μg/g	138
Unalloyed copper (SRM-396)	Sn	66 ± 3 μg/g	65 ± 5 μg/g	139
	Sn	0.7 ± 0.2 μg/g	0.8 ± 0.3 μg/g	138
Fly ash (SRM-1633)	Ni	4.1 ± 0.1 μg/g	4.2 ± 0.1 μg/g	139
	Fe	6.2 ± 0.2 %	6.2 ± 0.3 %	
Blood	Ni	99 ± 3 μg/g	98 ± 3 μg/g	138
	Pb	8–40 μg/100 mL	—	139
Soil extracts	Fe, Co, Cu	10^{-9}–10^{-4} %	—	158
				149

Table 2.16. Where Will Laser-excited Atomic Fluorescence Spectrometry Find Analytical Usefulness?

1. Specialized analyses where improved sensitivity, detection power, and spectral selectivity needed.
2. Optimization studies where combustion (plasma) diagnostics needed (temperature profiles, species profiles, deexcitation rate constants).
3. Spatial profile studies where sample is ablated by a separate means and plume is then excited.
4. Remote-sensing analysis, where the sample (solid, liquid, gas) can be directly addressed with a laser beam.
5. Semiquantitative absolute analysis, where calibration standards are not available.

REFERENCES

Reviews (R)

R1. N. Omenetto, L. M. Fraser, and J. D. Winefordner, *Appl. Spectrosc. Rev.*, **7**, 147 (1973).
R2. R. Browner, *Analyst*, **99**, 617 (1974).
R3. T. S. West, *Analyst*, **99**, 886 (1974).
R4. J. D. Winefordner, *Chem. Tech.*, **2**, 123 (1975).
R5. V. A. Razumov, *Zh. Anal. Khim.*, **32**, 596 (1977).
R6. K. Schofield, *J. Quant. Spectrosc. Radiat. Transfer*, **17**, 13 (1977).
R7. N. Omenetto and J. D. Winefordner, Chapter 4 in *Analytical Laser Spectroscopy*, N. Omenetto, Ed., Wiley, New York, 1979.
R8. J. D. Winefordner, *J. Chem. Ed.*, **55**, 72 (1978).
R9. J. D. Winefordner, in *New Applications of Lasers to Chemistry*, G. M. Hieftje, Ed., ACS Symposium Series No. 85, Washington, D.C., 1978.
R10. K. Sakurai, *Gendai Kagaku*, **92**, 29 (1978).
R11. C. G. Morgan. *Chem. Soc. Rev.*, **8**, 367 (1979).
R12. V. A. Razumov and A. M. Zvyagintsev, *Zh. Prikl. Spektrosk.*, **31**, 381 (1979).
R13. R. A. Keller and J. C. Travis, Chapter 7 in *Analytical Laser Spectroscopy*, N. Omenetto, Ed., Wiley, New York, 1979.
R14. N. Omenetto and J. D. Winefordner, *Prog. Anal. At. Spectrosc.*, **2**, 1 (1979).
R15. T-T, Lin, *Fen. Hsi. Hua. Hsueh.*, **8**, 567 (1980).
R16. S. J. Weeks and J. D. Winefordner, in *Lasers in Chemical Analysis*, G. M. Hieftje, J. C. Travis, and F. E. Lytle, Eds., Humana Press, Clifton, N.J., 1981.
R17. N. Omenetto and J. D. Winefordner, *CRC Crit. Rev. Anal. Chem.*, **13**, 59 (1981).
R18. J. D. Winefordner, in *Recent Advances in Analytical Chemistry*, K. Fuwa, Ed., Pergamon Press, Oxford, 1982.
R19. N. A. Narasimham, *Pure Appl. Chem.*, **54**, 841 (1982).

Fundamental Studies (F)

F1. L. Allen and J. H. Eberly, *Optical Resonances and Two Level Atoms*, Wiley, New York, 1975.

F2. R. H. Pantell and H. E. Puthoff, *Fundamentals of Quantum Electronics*, Wiley, New York, 1969.
F3. A. Yariv, *Introduction to Optical Electronics*, Holt, Rinehart, and Winston, New York, 1971.
F4. C. Th. J. Alkemade, Tj. Hollander, W. Snelleman, and P. J. Th. Zeegers, *Metal Vapours in Flames*, Pergamon, Oxford, 1982.
F5. D. R. Crosley, *Laser Probes for Combustion Chemistry*, ACS Symposium Series 134, Washington, D.C. 1979.
F6. A. Corney, *Atomic and Laser Spectroscopy*, Clarendon Press, Oxford, 1977.
F7. N. Omenetto, Ed., *Analytical Laser Spectroscopy*, Wiley, New York, 1979.
F8. J. Steinfeld, Ed., *Laser and Coherence Spectroscopy*, Plenum, New York, 1978.
F9. N. Omenetto and J. D. Winefordner, Chapter 4 in *Analytical Laser Spectroscopy*, N. Omenetto, Ed., Wiley, New York, 1979.
F10. R. M. Measures, *J. Appl. Phys.*, **39**, 5232 (1968).
F11. A. B. Rodrigo and R. M. Measures, *IEEE J. Quantum Electronics*, **QE-9**, 972 (1973).
F12. E. H. Piepmeier, *Spectrochim. Acta.*, **27B**, 431 (1972).
F13. E. H. Piepmeier, *Spectrochim. Acta.*, **27B**, 445 (1972).
F14. N. Omenetto and J. D. Winefordner, *Appl. Spectrosc.*, **26**, 555 (1972).
F15. N. Omenetto, P. Benetti, L. P. Hart, J. D. Winefordner, and C. Th. J. Alkemade, *Spectrochim. Acta*, **28B**, 289 (1973).
F16. N. Omenetto, L. P. Hart, P. Benetti, and J. D. Winefordner, *Spectrochim. Acta*, **28B**, 301 (1973).
F17. B. L. Sharp and A. Goldwasser, *Spectrochim. Acta*, **31B**, 431 (1976).
F18. J. Kuhl, S. Neumann, and M. Kriese, *Z. Naturforsch*, **28A**, 273 (1973).
F19. C. Th. J. Alkemade, Talk at 20th Colloquim Spectroscopicum Internationale, Prague, 1977.
F20. J. W. Daily, *Appl. Optics*, **16**, 2322 (1977).
F21. J. W. Daily, *Appl. Optics*, **16**, 568 (1977).
F22. B. Smith, J. D. Winefordner, and N. Omenetto, *J. Appl. Phys.*, **48**, 2676 (1977).
F23. M. A. Bolshov, A. V. Zybin, V. G. Koloshnikov, and K. N. Koshelev, *Spectrochim. Acta*, **32B**, 279 (1977).
F24. C. A. Van Dijk, *Optics Commun.*, **22**, 343 (1977).
F25. G. D. Boutilier, J. D. Bradshaw, S. J. Weeks, and J. D. Winefordner, *Appl. Spectrosc.*, **31**, 307 (1977).
F25a. N. Omenetto, G. D. Boutilier, S. J. Weeks, B. W. Smith, and J. D. Winefordner, *Anal. Chem.*, **49**, 1076 (1977).
F26. J. W. Daily, *Appl. Optics*, **16**, 568 (1977).
F27. D. R. DeOlivares and G. M. Hieftje, *Spectrochim. Acta*, **33B**, 79 (1978).
F28. J. W. Daily, *Appl. Optics*, **17**, 225 (1978).
F29. C. A. Van Dijk, P. J. Th. Zeegers, G. Nienhuis, and C. Th. J. Alkemade, *J. Quant. Spectrosc. Radiat. Transfer*, **20**, 55 (1978).
F30. G. D. Boutilier, M. B. Blackburn, J. M. Mermet, S. J. Weeks, H. Haraguchi, J. D. Winefordner, and N. Omenetto, *Appl. Optics*, **17**, 2291 (1978).
F31. J. S. Hosch and E. H. Piepmeier, *Appl. Spectrosc.*, **32**, 444 (1978).
F32. K. G. Muller and M. Stania, *J. Appl. Phys.*, **49**, 5801 (1978).
F33. N. Omenetto and J. D. Winefordner, *Prog. Anal. At. Spectrosc.*, **2**, 1 (1979).

F34. E. H. Piepmeier, Chapter 3 in *Analytical Laser Spectroscopy*, N. Omenetto, Ed., Wiley, New York, 1979.
F35. C. A. Van Dijk, P. J. Th. Zeegers, and C. Th. J. Alkemade, *J. Quant. Spectrosc. Radiat. Transfer*, **21**, 115 (1979).
F36. R. A. Van Calcar, M. J. M. Van de Ven, B. K. Van Uitert, K. J. Bienwenga, Tj. Hollander, and C. Th. J. Alkemade, *J. Quant. Spectrosc. Radiat. Transfer*, **21**, 11 (1979).
F37. J. D. Berg and W. L. Shackleford, *Appl. Optics*, **18**, 2093 (1979).
F38. G. C. Turk, J. L. Travis, J. R. DeVoe, and T. C. O'Haver, *Anal. Chem.*, **51**, 1890 (1979).
F39. J. C. Travis, P. K. Schenck, G. C. Turk, and W. G. Mallard, *Anal. Chem.*, **51**, 1516 (1979).
F40. J. W. Daily, in *Laser Probes for Combustion Chemistry*, D. Crosley, Ed., ACS Symposium Series 134, Washington, D.C., 1979.
F41. J. W. Daily, Paper at 6th Biennial Turbulance Symposium, University of Missouri, Rolla, 1979.
F42. M. B. Blackburn, J. M. Mermet, G. D. Boutilier, and J. D. Winefordner, *Appl. Optics*, **18**, 1804 (1979).
F43. N. Omenetto, M. S. Epstein, J. D. Bradshaw, S. Bayer, J. J. Horvath, and J. D. Winefordner, *J. Quant Spectrosc. Radiat. Transfer*, **22**, 287 (1979).
F44. C. H. Muller, K. Schofield, and M. Steinberg, *J. Chem. Phys.*, **72**, 6620 (1980).
F45. C. Chan and J. W. Daily, *Appl. Optics*, **19**, 1357 (1980).
F46. R. P. Lucht, D. W. Sweeney, and N. M. Laurendeau, *Appl. Optics*, **19**, 3295 (1980).
F47. N. Omenetto, J. Bower, J. Bradshaw, C. A. Van Dijk, and J. D. Winefordner, *J. Quant. Spectrosc. Radiat. Transfer*, **24**, 147 (1980).
F48. C. A. Van Dijk and C. Th. J. Alkemade, *Combust. Flame*, **38**, 37 (1980).
F49. C. A. Van Dijk, N. Omenetto, and J. D. Winefordner, *Appl. Spectrosc.*, **35**, 389 (1981).
F50. D. R. DeOlivares and G. M. Hieftje, *Spectrochim. Acta.*, **36B**, 1059 (1981).
F51. R. M. Measures, P. G. Cardinal, and G. W. Schinn, *J. Appl. Phys.*, **52**, 1269 (1981).
F52. C. Th. J. Alkemade, *Appl. Spectrosc.*, **35**, 1 (1981).
F53. N. Omenetto, *Spectrochim. Acta*, **37B**, 1009 (1982).
F54. B. T. Ahn, G. J. Bastiaans, and F. Albahodily, *Appl. Spectrosc.*, **36**, 106 (1982).
F55. N. Omenetto, C. A. Van Dijk and J. D. Winefordner, *Spectrochim. Acta*, **37B**, 703 (1982).
F56. H. Uchida, M. A. Kosinski, N. Omenetto, and J. D. Winefordner, *Spectrochim. Acta B*, **38B**, 529 (1983).
F57. H. Falk, *Prog. Anal. At. Spectrosc.*, **3**, 181 (1980).
F58. H. Uchida, M. A. Kosinski, N. Omenetto, and J. D. Winefordner, *Spectrochim. Acta*, **39B**, 63 (1984).

Instrumental/Methodology (I)

I1. M. B. Denton and H. V. Malmstadt, *Appl. Phys. Lett.*, **18**, 485 (1971).
I2. L. M. Fraser and J. D. Winefordner, *Anal. Chem.*, **43**, 1693 (1971).

11.53

13. J. Kuhl and G. Marowsky, *Optics Commun.*, **4**, 125 (1971).
14. L. M. Fraser and J. D. Winefordner, *Anal. Chem.*, **44**, 1444 (1972).
15. N. Omenetto, N. N. Hatch, L. M. Fraser, and J. D. Winefordner, *Anal. Chem.*, **45**, 195 (1973).
16. N. Omenetto, N. N. Hatch, L. M. Fraser, and J. D. Winefordner, *Spectrochim. Acta*, **28B**, 65 (1973).
17. J. Kuhl, S. Neamann, and M. Kriese, *Z. Naturforsch.*, **28A**, 273 (1973).
18. J. Kuhl and H. Spitschan, *Optics Commun.*, **7**, 256 (1973).
19. S. Neumann and M. Kriese, *Spectrochim. Acta*, **29B**, 127 (1974).
110. P. W. Pace and J. B. Atkinson, *J. Phys.*, **7E**, 556 (1974).
111. F. C. M. Coolan and H. L. Hagedoorn, *J. Opt. Soc. Am.*, **65**, 952 (1975).
112. W. M. Fairbank, T. W. Hansch, and A. L. Schawlow, *J. Opt. Soc. Am.*, **69**, 199 (1975).
113. B. L. Sharp and A. Goldwasser, *Spectrochim. Acta*, **31B**, 431 (1976).
114. R. B. Green, J. C. Travis, and R. A. Kellen, *Anal. Chem.*, **48**, 1954 (1976).
115. H. L. Brod and E. S. Yeung, *Anal. Chem.*, **48**, 344 (1976).
116. S. Mayo, R. A. Keller, J. C. Travis, and R. B. Green, *J. Appl. Phys.*, **47**, 4012 (1976).
117. A. Elbern, Proc. Int. Symp. on Wall Interaction, Julich, RFG, 1976.
118. M. A. Bolshov, A. V. Zybin, L. A. Zybina, V. G. Koloshnikov, and I. A. Majorov, *Spectrochim. Acta.*, **31B**, 493 (1976).
119. J. A. Gelbwachs, C. F. Klein, and J. E. Wessel, *Appl. Phys. Lett.*, **30**, 489 (1977).
120. J. A. Perry, M. F. Bryant, and H. V. Malmstadt, *Anal. Chem.*, **49**, 1702 (1977).
121. B. Smith, J. D. Winefordner, N. Omenetto, *J. Appl. Phys.*, **48**, 2676 (1977).
122. B. W. Smith, M. B. Blackburn and J. D. Winefordner, *Canad. J. Spectrosc.*, **22**, 57 (1977).
122a. N. Omenetto, *Anal. Chem.*, **48**, 75A (1976).
123. M. A. Bolshov, A. V. Zybin, V. G. Koloshnokov, and K. N. Koshelev, *Spectrochim. Acta*, **32B**, 279 (1977).
124. M. Maeda, M. Matsumoto, and M. Yashushi, *Oyo Butsuri*, **46**, 1184 (1977).
125. L. Patemack, P. A. Baronavski, and J. R. McDonald, *J. Chem. Phys.*, **69**, 4830 (1978).
126. S. J. Weeks, H. Haraguchi, and J. D. Winefordner, *Anal. Chem.*, **50**, 360 (1978).
127. J. P. Hohimer and P. J. Hargis, *Anal. Chim. Acta*, **97**, 43 (1978).
128. D. A. Goff and E. S. Yeung, *Anal. Chem.*, **50**, 625 (1978).
129. A. S. Gonchakov, N. B. Zorov, and Y. Y. Kuzakov, *J. Anal. Chem. (USSR)*, **34**, 2057 (1979).
130. A. S. Gonchakov, N. B. Zorov, Y. Y. Kuzakov, and O. I. Matveev, *Anal. Lett.*, **12**, 1037 (1979).
131. A. S. Gonchakov, N. B. Zorov, Y. Y. Kuzakov, and O. I. Matveev, *J. Anal. Chem. (USSR)*, **34**, 2312 (1979).
132. J. P. Hohimer and P. J. Hargis, *Anal. Chem.*, **51**, 430 (1979).
133. B. D. Pollard, M. B. Blackburn, S. Nikdel, A. Massoumi, and J. D. Winefordner, *Appl. Spectrosc.*, **33**, 5 (1979).
134. R. M. Measures and H. S. Kwong, *Appl. Optics*, **18**, 281 (1979).
135. H. S. Kwong and R. M. Measures, *Anal. Chem.*, **51**, 428 (1979).

136. V. I. Balykin, V. A. Letkohov, and V. I. Mishin, *Zh. Eksp. Teor. Fiz.*, **77**, 2221 (1979).
137. E. Miron, R. David, G. Erez, S. Lavi, and L. A. Levin, *J. Opt. Soc. Am.*, **69**, 256 (1979).
138. M. S. Epstein, S. Bayer, J. Bradshaw, E. Voigtman, and J. D. Winefordner, *Spectrochim. Acta*, **35B**, 233 (1980).
139. M. S. Epstein, J. Bradshaw, S. Bayer, J. Bower, E. Voitman, and J. D. Winefordner, *Appl. Spectrosc.*, **34**, 372 (1980).
140. M. S. Epstein, S. Nikel, J. D. Bradshaw, M. A. Kosinski, J. N. Bower, and J. D. Winefordner, *Anal. Chim. Acta*, **113**, 221 (1980).
141. C. L. Pan, J. V. Prodan, W. M. Fairbanks, and C. Y. She, *Optics Lett.*, **5**, 459 (1980).
142. D. J. Ehrlich, R. M. Osgood, G. C. Turk, and J. C. Travis, *Anal. Chem.*, **52**, 1354 (1980).
143. R. P. Fraeholz and J. A. Gelbwachs, *Appl. Optics*, **19**, 2735 (1980).
144. M. Lino, H. Yano, Y. Takubo, and M. Shimzau, *J. Appl. Phys.*, **52**, 6025 (1981).
145. A. W. Miziolek and R. J. Willis, *Optics Lett.*, **6**, 528 (1981).
146. A. W. Miziolek, *Anal. Chem.*, **53**, 118 (1981).
147. J. J. Horvath, J. D. Bradshaw, J. N. Bower, M. S. Epstein, and J. D. Winefordner, *Anal. Chem.*, **53**, 6 (1981).
148. M. A. Bolshov, A. V. Zybin, V. G. Koloshnikov, *Spectrochim. Acta*, **36B**, 345 (1981).
149. M. A. Bolshov, A. V. Zybin and I. I. Smirenkina, *Spectrochim. Acta*, **36B**, 1143 (1981).
150. M. Heaven, T. A. Miller, R. R. Freeman, J. C. White, and J. Bokor, *Chem. Phys. Lett.*, **86**, 458 (1982).
151. O. I. Matveev, N. B. Zorov, and Y. Y. Kuzyakov, *Vestn. Mosk. Univ. Ser. Z. Khim.*, **19**, 537 (1982).
152. M. O. Rodgers, J. D. Bradshaw, K. Lin, and D. D. Davis, *Optics Lett.*, **7**, 359 (1982).
153. H. Uchica, M. A. Kosinski, and J. D. Winefordner, *Spectrochim. Acta.*, **38B**, 5 (1983).
154. M. A. Kosinski, H. Uchida, and J. D. Winefordner, *Talanta*, **30**, 339 (1983).
155. N. Omeretto and H. G. C. Human, *Spectrochim. Acta*, **39B**, 1333 (1984).
156. H. G. C. Human, N. Omenetto, P. Cavalli, and G. Rossi, *Spectrochim. Acta*, **39B**, 1345 (1984).
157. N. Omenetto, H. G. C. Human, P. Cavalli, and G. Rossi, *Spectrochim. Acta*, **39B**, 115 (1984).
158. N. Omeretto, H. G. C. Human, P. Cavalli, and G. Rossi, *Analyst*, (1984).
159. R. P. Fraeholz and J. A. Gelbwachs, *Spectrochim. Acta*, **39B**, 807 (1984).
160. J. Tilch, H. J. Paetzold, H. Falk, and K. P. Schmidt, "Analytiktriffen 1982," Atomspektroskopie, Neubrandenburg, DDR, November 1982, Abstract N.DV55.
161. N. Omenetto, L. P. Hart, and J. D. Winefordner, *Appl. Spectrosc.*, **38**, 619 (1984).
162. L. P. Hart, C. Th. J. Alkemade, N. Omenetto, and J. D. Winefordner, *Appl. Spectrosc.*, **39**, 677 (1985).

Spectrochimica Acta, Vol. 39B, Nos 9–11, pp. 1333–1343, 1984
Printed in Great Britain

0584-8547/84 $03.00 + .00
Pergamon Press Ltd

Laser excited analytical atomic and ionic fluorescence in flames, furnaces and inductively coupled plasmas—I. General considerations*

N. Omenetto and H. G. C. Human†
Joint Research Centre, Chemistry Division, 21020 Ispra (Varese), Italy

(*Received* 31 *January* 1983)

Abstract—Several important parameters for the analytical use of laser excited fluorescence spectrometry in flames, graphite furnaces and inductively coupled plasmas are discussed in some detail. These parameters include the laser characteristics such as peak power, pulse duration, spectral bandwidth and repetition rate, the choice of the excitation line, the optical arrangement and the detection system, this last one centred on the widespread use of the boxcar averager. It is shown that, if the ultimate sensitivity is the goal to be achieved, then the choice must be the electrothermal atomization. However, even for flames and inductively coupled plasmas, excellent results are possible provided that: (i) the laser system allows complete spectral coverage in the ultraviolet; (ii) saturation of the fluorescence signal can be approached over a large sample volume; and (iii) the gated detection parameters and the laser repetition frequency are optimized with respect to each other so as to reach the maximum signal-to-noise ratio.

1. Introduction

Laser induced fluorescene has gained a firm reputation as one of the most attractive tools for studying the complicated dynamics of combustion processes [1–3]. In fact, like all "scattering" methods, e.g. Raman techniques, it is intrinsically characterized by high spatial resolution, thus providing local data without the necessity of sometimes inaccurate Abel inversion procedures. In addition, with pulsed laser excitation, temporal resolution is also possible.

From an analytical point of view, the technique of laser induced fluorescence has been applied to atomizers such as atmospheric pressure flames [4–17], graphite furnaces [18–23],

*Dedicated to Prof. K. Laqua on the occasion of his 65th birthday.
†On leave from CSIR, National Institute for Materials Research, Pretoria, South Africa.

[1] D. R. Crosley, Ed. Laser probes for combustion chemistry, *ACS Symposium Series* **134**. American Chemical Society, Washington (1980).
[2] N. Omenetto and J. D. Winefordner, *Prog. Anal. Atom. Spectrosc.* **2** (1/2) (1979).
[3] C. Th. J. Alkemade, T. Hollander, W. Snelleman and P. J. Th. Zeegers, *Metal Vapours in Flames*. Pergamon Press, Oxford (1982).
[4] M. B. Denton and H. V. Malmstadt, *Appl. Phys. Lett.* **18**, 485 (1971).
[5] L. M. Fraser and J. D. Winefordner, *Anal. Chem.* **43**, 1693 (1971).
[6] L. M. Fraser and J. D. Winefordner, *Anal. Chem.* **44**, 1444 (1972).
[7] N. Omenetto, N. N. Hatch, L. M. Fraser and J. D. Winefordner, *Anal. Chem.* **45**, 195 (1973).
[8] N. Omenetto, N. N. Hatch, L. M. Fraser and J. D. Winefordner, *Spectrochim. Acta* **28B**, 65 (1973).
[9] R. B. Green, J. C. Travis and R. A. Keller, *Anal. Chem.* **48**, 1954 (1976).
[10] J. Kuhl, S. Neumann and M. Kriese, *Z. Naturforsch.* **28A**, 273 (1973).
[11] J. Kuhl and H. Spitschan, *Opt. Comm.* **7**, 256 (1973).
[12] S. J. Weeks, H. Haraguchi and J. D. Winefordner, *Anal. Chem.* **50**, 360 (1978).
[13] J. A. Gelbwachs, C. F. Klein and J. E. Wessel, *Appl. Phys. Lett.* **30**, 489 (1977).
[14] B. W. Smith, M. B. Blackburn and J. D. Winefordner, *Can. J. Spectrosc.* **22**, 57 (1977).
[15] J. J. Horvath, J. D. Bradshaw, J. N. Bower, M. S. Epstein and J. D. Winefordner, *Anal. Chem.* **53**, 6 (1981).
[16] M. S. Epstein, J. Bradshaw, S. Bayer, J. Bower, E. Voigtman and J. D. Winefordner, *Appl. Spectrosc.* **34**, 372 (1980).
[17] M. S. Epstein, S. Bayer, J. Bradshaw, E. Voigtman and J. D. Winefordner, *Spectrochim. Acta* **35B**, 233 (1980).
[18] S. Neumann and M. Kriese, *Spectrochim. Acta* **29B**, 127 (1974).
[19] J. P. Hohimer and P. J. Hargis, Jr, *Appl. Phys. Lett.* **30**, 344 (1977).
[20] A. W. Miziolek and R. J. Willis, *Opt. Lett.* **6**, 528 (1981).
[21] M. A. Bolshov, A. V. Zybin, V. G. Koloshnikov and M. V. Vasnetsov, *Spectrochim. Acta* **36B**, 345 (1981).
[22] M. A. Bolshov, A. V. Zybin and I. I. Smirenkina, *Spectrochim. Acta* **36B**, 1143 (1981).
[23] J. Tilch, H. J. Paetzold, H. Falk and K. P. Schmidt, *Analytiktreffen* 1982, *Atmospektroskopie*, Neubrandenburg (DDR), 8–12 November 1982, Abstract N. DV 55.

inductively coupled plasmas [24–26] and other types of atom cells [27–31]. In flame and plasma work, some early results as well as some of the recent ones are of rather discontinuous quality, the detection limits being in several cases inferior to those given with the same or similar experimental facilities by either atomic emission or atomic absorption. As a result, one is led to reach the disappointing conclusion that, in practice, the technique of laser induced fluorescence does not represent the significant improvement over the other analytical techniques as it was theoretically predicted and repeatedly emphasized in the literature. On the other hand, the results published by Bolshov *et al.* [22] and by Tilch *et al.* [23] for electrothermal atomization and pulsed laser excitation represent the best detection limits obtained so far for the elements investigated. Furthermore, recent experiments carried out in the authors' laboratory [32], while confirming the detection limits published for graphite atomizers, have shown that the combination of pulsed laser excitation and the inductively coupled plasma as atomizer/ionizer allows very low detection limits to be reached for all the refractory elements investigated. In addition, the sensitivity in the separated air–acetylene flame is more than adequate for solving several analytical problems, such as the direct determination of lead in whole blood, which up to now is almost entirely carried out by graphite furnace atomic absorption [33].

The experimental details of our laser set-up as well as an extensive characterization of the fluorescence process for several elements atomized/ionized in a commercial argon inductively coupled plasma will be described in the second part of this work. This first paper is intended to evaluate in some details and in an unified manner all the theoretical and experimental parameters of importance in a laser fluorescence set-up. The discussion is centered on a pulsed laser system, but most of it applies equally well to continuous wave laser excitation. Due to the extensive literature on the subject, some parameters have already been discussed elsewhere. However, the treatment is spread in several publications and, more important, the role played by different parameters has been, in the authors' opinion, either overemphasized or overlooked.

Four main topics will be treated, namely: (i) the laser as well as the atom characteristics (power, pulse duration and bandwidth for the laser and absorption oscillator strength and wavelength of the transition for the atom); (ii) the optical arrangement; (iii) the atomization system and finally (iv) the detection system.

The laser is assumed to interact with all absorbing atoms. This is justified if the spectral bandwidth of the laser is much larger than the atomic absorption profile (continuum source case) or, in the case of monochromatic excitation, if the velocity changing collisions in the atomizer are so frequent that the original monokinetic sets of atoms are forced to absorb everywhere within the absorption profile. This is tantamount to saying that inhomogeneous broadening (due to the Doppler effect) does not need to be considered. In addition, coherence effects [2, 3, 34] are neglected and the atomic vapour is optically thin so that filtering (self-absorption, pre- and postfilter) effects can safely be disregarded.

2. The Primary Excitation Step

2.1. *Attainment of saturation*

It is well known that the fluorescence signal does not respond linearly to very high values of the excitation source irradiance, reaching a plateau as a consequence of the saturation of the

[24] M. S. Epstein, S. Nikdel, J. D. Bradshaw, M. A. Kosinski, J. N. Bower and J. D. Winefordner, *Anal. Chim. Acta* **113**, 221 (1980).
[25] H. Uchida, M. A. Kosinski and J. D. Winefordner, *Spectrochim. Acta* **38B**, 5, 1983.
[26] N. Omenetto, H. G. C. Human, P. Cavalli and G. Rossi, *Spectrochim. Acta* **39B**, 115 (1984).
[27] W. M. Fairbank, Jr, T. W. Haensch and A. L. Schawlow, *J. Opt. Soc. Am.* **65**, 199 (1975).
[28] D. A. Jennings and R. A. Keller, *J. Am. Chem. Soc.* **94**, 9249 (1972).
[29] H. L. Brod and E. S. Yeung, *Anal. Chem.* **48**, 344 (1976).
[30] J. Kuhl and G. Marowsky, *Opt. Comm.* **4**, 125 (1971).
[31] E. Miron, R. David, G. Erez, S. Lavi, and L. A. Levin, *Appl. Phys. Lett.* **35**, 737 (1979).
[32] H. G. C. Human, N. Omenetto, P. Cavalli and G. Rossi, *Spectrochim. Acta* **39B**, 1345 (1984).
[33] N. Omenetto, H. G. C. Human, P. Cavalli and G. Rossi, *Analyst* (in press).
[34] J. W. Daily, *Appl. Opt.* **16**, 2322 (1977).

transition [2, 3, 35, 36]. Under these conditions, the fluorescence radiance will be maximal and independent of the laser irradiance. Saturation will be approached when the radiative transition rate, which is given by the product of the Einstein coefficient of induced absorption and the spectral energy density of the laser source, will become comparable to the collisional quenching rate of the excited level.

By using the classical relationships between the Einstein coefficients and the definition of spectral irradiance, we obtain for the radiative excitation rate, R_{lu} (s^{-1}), from the lower level, l, to the upper level, u, of a transition, the following expression

$$R_{lu} = \frac{g_u}{g_l} A_{ul} \left(\frac{\lambda_{ul}^5}{8\pi hc^2} \right) E_\lambda(\lambda_{ul}) \tag{1}$$

where

g_u, g_l = statistical weights of upper and lower levels;
A_{ul} = Einstein coefficient of spontaneous emission (s^{-1});
= $(g_l f_{lu}/1.5\lambda_{ul}^2 g_u)$, where f_{lu} is the absorption oscillator strength of the transition $l \rightarrow u$;
λ_{ul} = wavelength of the absorbing transition at the line centre (cm);
h = Planck constant (Js);
c = velocity of light ($cm\,s^{-1}$);
$E_\lambda(\lambda_{ul})$ = spectral irradiance of the laser source ($J\,s^{-1}\,cm^{-2}\,cm^{-1}$);
= $(Q/\Delta t_l S_l \delta\lambda_l)$, where Q (J) is the energy of the laser pulse of duration Δt_l(s), S_l is the laser cross-section at the atomizer (cm^2) and $\delta\lambda_l$ is the laser spectral bandwidth (cm);
$\frac{Q}{\Delta t_l} = \Phi_l$ = laser power or laser flux (W).

By substituting the values for the fundamental constants, the rate expression becomes

$$R_{lu} = 6.7 \times 10^{10} \left(\frac{g_u}{g_l} \right) A_{ul} \lambda_{ul}^5 \frac{\Phi_l}{S_l \delta\lambda_l}. \tag{1a}$$

It is then clear that the absorption rate increases with the fifth power of the wavelength and proportionally to the Einstein coefficient of spontaneous emission. As a consequence, as it was repeatedly pointed out [2], saturation will be more difficult to achieve for weak transitions and/or for ultraviolet transitions.

Table 1 collects the values of the radiative absorption rates per unit laser spectral irradiance for several elements together with the values of the absorption oscillator strength and the spontaneous emission probabilities of some strong transitions. As one can see, these values span from 1.4×10^{-2} for rubidium at 780.023 nm to 5.5×10^{-5} for nickel at 232.003 nm. This means that a laser spectral irradiance of approximately $10^{10}\,W\,cm^{-2}\,cm^{-1}$ will be sufficient to approach saturation for the rubidium atomic transition while this value should be increased by more than three orders of magnitude for the ultraviolet nickel resonance line.

One should then seek for the maximum attainable spectral irradiance and therefore laser power has to be maximized rather than the pulse energy. This in turn means that the duration of laser pulse plays a very important role. Short laser pulses might be more difficult to handle for efficient signal detection (see later) but help in approaching saturation conditions. In addition, whenever an atomic system has a metastable level that can accumulate atoms, then the number of photons emitted by the atom during the interaction time with the laser beam decreases drastically, thus making longer excitation times ineffective [22]. The same consideration holds for the well-demonstrated side effects such as ion formation [37] and enhanced chemical reactions [38]. In order to extract useful signal from all the atoms, the excitation pulse must be shorter than the reaction time of these processes. For diagnostic

[35] E. H. Piepmeier, *Spectrochim. Acta* 27B, 431 (1972).
[36] E. H. Piepmeier, *Spectrochim. Acta* 27B, 445 (1972).
[37] J. C. Travis, G. C. Turk and R. B. Green, *Anal. Chem.* 54, 1006A (1982).
[38] C. H. Muller, K. Schofield and M. Steinberg, *J. Chem. Phys.* 72, 6620 (1980).

Table 1. Radiative absorption rates per unit laser spectral irradiance for several strong atomic and ionic transitions*

Element	Transition ($l \rightarrow u$)	Wavelength (nm)	$g_l f_{lu}$	A_{ul} ($\times 10^{-8}$)(s^{-1})	$R_{lu}/E_\lambda(\lambda_{ul})$ ($s^{-1}\,W^{-1}\,cm^2\,cm$)
Ag	$^2S_{1/2} \rightarrow {}^2P_{3/2}$	328.068	0.9	1.4	7.10×10^{-4}
Al	$^2P_{1/2} \rightarrow {}^2S_{1/2}$	394.403	0.25	0.53	3.43×10^{-4}
Au	$^2S_{1/2} \rightarrow {}^2P_{3/2}$	242.795	0.6	1.7	1.92×10^{-4}
Ba	$^1S_0 \rightarrow {}^1P_1$	553.548	1.6	0.12	1.24×10^{-3}
Ba*	$^2S_{1/2} \rightarrow {}^2P_{3/2}$	455.403	1.75	1.41	3.70×10^{-3}
Be	$^1S_0 \rightarrow {}^1P_1$	234.861	1.2	4.8	6.94×10^{-4}
Bi	$^4S_{3/2} \rightarrow {}^4P_{1/2}$	306.772	0.4	1.42	1.29×10^{-4}
Ca	$^1S_0 \rightarrow {}^1P_1$	422.673	1.65	2.05	5.6×10^{-3}
Ca*	$^2S_{1/2} \rightarrow {}^2P_{3/2}$	393.367	1.3	1.4	1.77×10^{-3}
Cd	$^1S_0 \rightarrow {}^1P_1$	228.802	1.2	5.1	6.46×10^{-4}
Cr	$^7S_3 \rightarrow {}^7P_4$	357.869	2.4	1.4	7.0×10^{-4}
Cs	$^2S_{1/2} \rightarrow {}^2P_{3/2}$	852.110	1.52	0.35	2.11×10^{-2}
Cu	$^2S_{1/2} \rightarrow {}^2P_{3/2}$	324.754	0.86	1.36	6.6×10^{-4}
Fe	$^5D_4 \rightarrow {}^5F_5$	248.327	3.5	3.44	2.65×10^{-4}
Ga	$^2P_{1/2} \rightarrow {}^2D_{3/2}$	287.424	0.4	0.81	2.13×10^{-4}
Ga	$^2P_{1/2} \rightarrow {}^2S_{1/2}$	403.298	0.2	0.41	3.0×10^{-4}
Hg	$^1S_0 \rightarrow {}^3P_1$	253.652	0.34	1.2	2.48×10^{-4}
In	$^2P_{1/2} \rightarrow {}^2D_{3/2}$	303.936	0.6	1.1	3.9×10^{-4}
In	$^2P_{1/2} \rightarrow {}^2S_{1/2}$	410.176	0.25	0.5	3.85×10^{-4}
K	$^2S_{1/2} \rightarrow {}^2P_{3/2}$	766.491	1.4	0.397	1.4×10^{-2}
K	$^2S_{1/2} \rightarrow {}^2P_{1/2}$	769.898	0.68	0.382	6.9×10^{-3}
Mg	$^1S_0 \rightarrow {}^1P_1$	285.213	1.65	4.51	1.71×10^{-3}
Mn	$^6S_{5/2} \rightarrow {}^6P_{7/2}$	279.482	3.5	3.73	5.7×10^{-4}
Mn	$^6S_{5/2} \rightarrow {}^6P_{5/2}$	403.076	0.35	0.18	1.75×10^{-4}
Na	$^2S_{1/2} \rightarrow {}^2P_{3/2}$	588.995	1.3	0.624	5.94×10^{-3}
Na	$^2S_{1/2} \rightarrow {}^2P_{1/2}$	589.592	0.66	0.633	3.0×10^{-3}
Ni	$^3F_4 \rightarrow {}^3G_5$	232.003	0.9	1.01	5.5×10^{-5}
Pb	$^3P_0 \rightarrow {}^3P_1$	283.306	0.2	0.55	2×10^{-4}
Rb	$^2S_{1/2} \rightarrow {}^2P_{3/2}$	780.023	1.35	0.37	1.43×10^{-2}
Rb	$^2S_{1/2} \rightarrow {}^2P_{1/2}$	794.760	0.65	0.34	7.3×10^{-3}
Sc	$^2D_{3/2} \rightarrow {}^2F_{5/2}$	390.749	2.7	1.96	3.3×10^{-3}
Sn	$^3P_0 \rightarrow {}^3D_1$	224.605	0.4	1.74	1.99×10^{-4}
Sr	$^1S_0 \rightarrow {}^1P_1$	460.733	1.8	1.88	7.93×10^{-3}
Sr*	$^2S_{1/2} \rightarrow {}^2P_{3/2}$	407.771	1.5	1.5	2.3×10^{-3}
Sr*	$^2S_{1/2} \rightarrow {}^2P_{1/2}$	421.552	0.7	1.31	1.2×10^{-3}
Ti	$^3F_3 \rightarrow {}^3G_4$	364.268	1.8	1	5.5×10^{-4}
Tl	$^2P_{1/2} \rightarrow {}^2D_{3/2}$	276.787	0.7	1.52	3.3×10^{-4}
Tl	$^2P_{1/2} \rightarrow {}^2S_{1/2}$	377.572	0.3	0.7	3.6×10^{-4}
Tl	$^2P_{3/2} \rightarrow {}^2S_{1/2}$	535.046	0.5	0.58	8.5×10^{-4}
V	$^4F_{3/2} \rightarrow {}^4G_{5/2}$	318.398	2.1	2.3	7.60×10^{-4}
Zn	$^1S_0 \rightarrow {}^1P_1$	213.856	1.35	6.55	5.92×10^{-4}
Zr	$^3F_4 \rightarrow {}^3G_5$	360.119	2	0.93	4.6×10^{-4}

*The values of the oscillator strengths have been taken from Alkemade *et al.* [3], and the values of the spontaneous emission probabilities have been calculated accordingly.

purposes, i.e. when laser induced fluorescence is applied to combustors to gather information such as number densities or temperature, the knowledge of the temporal evolution of the excited state population is of essential relevance [2].

For the same laser power, one can of course increase the excitation spectral irradiance by decreasing the cross-section and/or the bandwidth. The role of the cross-section will be discussed later. For the bandwidth, it can be decreased by inserting an etalon in the laser cavity so that, at the expense of some peak power, the spectral irradiance can increase by orders of magnitude [39]. If saturation is already achieved without the narrowing element in the cavity, then the fluorescence signal will not increase by reducing the bandwidth. However, the spectral resolution will be much better and, more important, the scattering signal and its

[39] J. Kuhl, G. Marowsky, P. Kunstmann and W. Schmidt, *Z. Naturforsch.* 27A, 601 (1972).

associated noise will decrease. Therefore, it is always advisable to work at a reduced excitation bandwidth.

It is worth noting, however, that these considerations cannot be taken for granted when the bandwidth becomes smaller than the absorption profile, i.e. when the assumption of a continuum excitation source ceases to be valid.

2.2. *Choice of the excitation line*

In one of the first papers on the characterization of the fluorescence of some transition elements in the nitrous oxide acetylene flame, the lack of attaining of better detection limits was attributed to the fact that the most useful *absorption* transitions could not be reached by the laser [8]. Indeed, when one considers the atomic absorption resonance lines possessing the highest value of the oscillator strength, one realizes that about 60 °/₀ of the elements have their first resonance lines below 350 nm [40].

When comparing two different absorption lines, starting from two lower levels, l and l', and reaching two upper levels, u and u', with $\lambda_{u'l'} < \lambda_{ul}$, we obtain for the ratio of the radiative rates the following expression

$$\frac{R_{lu}}{R_{l'u'}} = \left(\frac{g_u g_{l'}}{g_{u'} g_l}\right)\left(\frac{A_{ul}}{A_{u'l'}}\right)\left(\frac{\lambda_{ul}^5}{\lambda_{u'l'}^5}\right)\left\{\frac{E_\lambda(\lambda_{ul})}{E_\lambda(\lambda_{u'l'})}\right\} \tag{2}$$

or, by using the relationship between A_{ul} and f_{lu},

$$\frac{R_{lu}}{R_{l'u'}} = \left(\frac{f_{lu}}{f_{l'u'}}\right)\left(\frac{\lambda_{ul}^2}{\lambda_{u'l'}^2}\right)\left\{\frac{E_\lambda(\lambda_{ul})}{E_\lambda(\lambda_{u'l'})}\right\}. \tag{2a}$$

However, it is not the rate itself but the number of absorbing transitions, R'_{lu}, that needs to be considered when comparing different absorption lines. This number is given by $R_{lu} n_l$, i.e. by the product of the rate as given above and the number density (cm^{-3}) of the lower level. Thus, Eqn (2a) holds if the lower levels of the transition are the same ($l = l'$). When $l \neq l'$ (with $l' < l$), the ratio of the number of absorption transitions becomes

$$\frac{R'_{lu}}{R'_{l'u'}} = \left(\frac{f_{lu}}{f_{l'u'}}\right)\left(\frac{\lambda_{ul}^2}{\lambda_{u'l'}^2}\right)\left\{\frac{E_\lambda(\lambda_{ul})}{E_\lambda(\lambda_{u'l'})}\right\}\left\{\frac{g_l}{g_{l'}}\exp\left(-\frac{\Delta E_{ll'}}{kT}\right)\right\} \tag{3}$$

where $\Delta E_{ll'}$ is the energy difference between levels l and l', k the Boltzmann constant and T the temperature.

Several considerations can be made by inspecting Eqns (2) and (3).

(i) If one takes into account excitation transitions above and below 360 nm (which can be set as the lowest wavelength limit that can be reached directly with dye lasers without the need of frequency doubling), the laser spectral irradiance ratio in the right hand side of Eqn (2a) can vary between 10 and 100. This assumes a 10 °/₀ efficiency for frequency doubling crystals between 260 and 300 nm and 1 °/₀ efficiency between 217 and 260 nm. Because the second factor in parenthesis can reach a value of ~ 30 (for $\lambda_{u'l'} \sim 200$ nm and $\lambda_{ul} \sim 600$ nm), then Eqn (2a) shows that a transition in the visible characterized by an absorption oscillator strength that is thousands times lower than those for u.v. transitions can still result in the same radiative absorption rate. If the lower level of the transition is the same, this consideration will also apply to the number of absorbing transitions. For example, in the case of the two resonance lines of manganese at 279.482 and 403.076 nm, sharing the same lower level ($^6S_{5/2}$) and characterized by a tenfold difference in the f-values in favour of the u.v. line [3], one calculates that, because of the wavelength ratio and of the greater laser spectral irradiance at 400 nm (~ 4 ×), the ratio of the number of absorbing transitions is almost unity (0.82). In this case, however, since the upper levels for the transitions are different, quenching effects might also be different.

(ii) When the lower levels are different, the radiative rate can be much higher for the transition at the longer wavelength but the Boltzmann factor in the population density makes the number of transitions more favourable for the ultraviolet excitation line. For example, in the case of thallium, if one compares the radiative rate at 535.046 nm ($^2P_{3/2} \rightarrow {}^2S_{1/2}$),

[40] W. J. Price, *Spectrochemical Analysis by Atomic Absorption Spectrometry*. Heyden, London (1979).

obtained with a laser power of 400 kW, with that at 276.787 nm ($^2P_{1/2} \rightarrow {}^2D_{3/2}$), with a laser flux of 25 kW, it can be seen that the rate for the u.v. transition is ~ 40 times lower, despite its larger value of the oscillator strength. In a system at 2500 K, however, the $^2P_{3/2}$ level is scarcely populated since its energy difference with the ground state ($^2P_{1/2}$) is almost 1 eV. As a result, the number of absorbing transitions, as given by Eqn (3), is 2.45 times higher for the 276.787 nm line. In general, the low population of the absorbing level plays more than the low f-value.

One should stress here that the above discussion refers to the *signal alone* and not to the signal-to-noise ratio, which is ultimately the most important quantity to be considered. At longer wavelengths, the background emission from flames, furnaces and inductively coupled plasmas and its associated noise increase considerably. For example, it has been reported that the plasma background emission spectral radiance increases by a factor of 54 from 200 to 400 nm [41]. It is therefore mandatory to give careful consideration to all the parameters entering Eqns (1)–(3) in order to find the best possible combination.

3. The Excitation and Detection Optics

Several ways of improving excitation and collection efficiencies by means of properly positioned mirrors have been described in the literature and are discussed in Refs [2] and [3]. In addition, light traps and baffles or suitable restricting apertures have a major role in preventing laser light reflected and scattered from the environment from entering the monochromator and reaching the detector.

In reviewing the analytical applications of laser absorption and emission spectroscopy, Harris and Lytle have stated that "no consensus exists as to whether the laser beam should simply traverse the atom reservoir, be focused into it or be expanded and collimated through it" [42]. In order to put these alternatives in the right perspective for analytical work, we have felt it useful to present here a simple derivation, adapted from Wright [43], aimed at defining the *sample* volume from which the signal is observed in terms of the geometrical parameters of the laser and of the fluorescence monochromator.

We define the following quantities, whose significance will become clear from their mutual relationships given below:

d_l = laser diameter (cm)
L_l = laser length (cm)
$\Delta\lambda_s$ = spectral bandwidth of the fluorescence spectrometer (cm)
R_d = reciprocal linear dispersion of the spectrometer (nm cm^{-1})
h_s = spectrometer slit height (cm)
W_s = spectrometer slit width (cm)
M = magnification of the collection system
F = F-number of the spectrometer
n_T = total number density of atoms in the atomizer (cm^{-3})
V_c = sample volume (cm^3)
A_l = longitudinal cross-sectional area of laser beam traversing the atomizer ($= d_l L_l$) (cm^2)
A_s = spectrometer slit area (cm^2)
Ω_F = fluorescence collection solid angle (sr)
Ω_s = spectrometer solid angle (sr)

Let now the optical system used to collect the radiation be such that the *length* of the laser image in the atomizer fills the spectrometer slit with a solid angle Ω_F. This can be achieved for example by rotating the monochromator, if possible, or by rotating the laser image with two mirrors or with a Dove prism. The above-defined quantities are then related by the following

[41] D. H. Tracy and S. A. Myers, *Spectrochim. Acta* 37B 1055 (1982).
[42] T. D. Harris and F. E. Lytle, Analytical applications of laser absorption and emission spectroscopy, in *Ultrasensitive Laser Spectroscopy*, Ed. D. S. Kliger, Chap. 7. Academic Press, New York (1983).
[43] M. L. Wright, Environmental Protection Agency, Report N° EPA-R2-73-219 (1973).

expressions

$$A_1\Omega_1 = A_s \cdot \Omega_s$$

$$(d_1 L_1)\cdot\Omega_1 = \left(\frac{\Delta\lambda_s h_s}{R_d}\right)\left(\frac{\pi}{4F^2}\right) \tag{4}$$

$$\Delta\lambda_s = R_d W_s \tag{5}$$

$$M = \frac{\Delta\lambda_s}{R_d d_1} = \frac{h_s}{L_1} \tag{6}$$

$$L_1 = \frac{h_s R_d d_1}{\Delta\lambda_s}. \tag{7}$$

The sample volume is then given by

$$V_c = \frac{\pi d_1^2 L_1}{4} = \frac{\pi d_1^3 h_s R_d}{4\Delta\lambda_s} \tag{8}$$

and the total number of atoms in the sample volume by

$$N = n_T V_c = n_T \frac{\pi d_1^3 h_s R_d}{4\Delta\lambda_s}. \tag{9}$$

If the laser image in the atomizer is not rotated to fill the slit height, then the expression for M and L_1 modifies as follows

$$M' = \frac{\Delta\lambda_s}{R_d L_1'} = \frac{h_s}{d_1}. \tag{10}$$

$$L_1' = \frac{d_1 \Delta\lambda_s}{h_s R_d} \tag{11}$$

and the total number of atoms in the sample volume becomes

$$N' = n_T V_c = n_T \frac{\pi d_1^3 \Delta\lambda_s}{4 h_s R_d}. \tag{12}$$

From the above relationships, we can derive the following conclusions:

(i) As stated before, one can increase the spectral irradiance of the excitation source by decreasing the laser diameter at the atomizer, i.e. by tightly focussing the beam with a condensing lens.

However, it is clear that if, in order to achieve saturation, one has to decrease the beam diameter by, say, a factor of 5 so as to increase the spectral irradiance by a factor of 25, the total number of atoms in the sample volume will decrease 125 times, reducing dramatically the signal level. If the laser power is high, then the best solution will be to expand the beam in the atomizer until the solid angle requirements set by the above equations are fulfilled, while *still* maintaining saturated conditions within the entire sample volume. When the focussing of the laser is mandatory to reach high irradiances, then multipass optics [17] will certainly help.

(ii) If the laser beam through the atomizer and the spectrometer slit are perpendicular to each other, it can be shown by ratioing Eqns (9) and (12) that there will be a loss in the total number of fluorescing atoms given by the ratio $(h_s/w_s)^2$. Such loss for typical values of h_s = 10 mm and w_s = 1 mm already reaches two orders of magnitude.

It is worth stressing here again that these considerations hold only when there are no other source induced signals and noises, such as for example scattering or molecular fluorescence.

Two more remarks seem to be in order. Firstly, the source mirror usually placed in front of the laser to double the excitation solid angle is unnecessary if saturation is approached. Secondly, a mirror placed behind the atomizer in the direction of the monochromator will always be useful when properly matched to the spectrometer solid angle. However, in this case, the measured atomizer background emission and its noise will also increase and one has

to try out experimentally whether its use can improve the signal-to-noise ratio for that particular atomizer and spectral transition. It can be anticipated that such a mirror will be useful for electrothermal atomization of elements of low volatility, where efficient screening of the graphite emission can easily be realized.

4. The Atomizer

A discussion of the figures of merit of the various atomizers that have been tested and are currently used in atomic spectrometry is certainly out of order here. So, only a few considerations will be given.

It can be generally stated that the atomizer is the weakest part of the atomic absorption, fluorescence and emission techniques, possibly with some exception for the inductively coupled plasma in emission work. In this respect, the use of lasers as primary sources of excitation cannot change the situation. On the contrary, if a change exists, it goes in the wrong direction. For example, in laser excited atomic fluorescence with flames, the scattering problems are worsened and one should be aware of the possible interference from molecular fluorescence of flame native species. In addition, in most measurements using boxcar detection (see later) quenching effects are *not* avoided even under saturation conditions [44, 45].

Since flame atomization does not permit the realization of all the advantages of laser excitation, Bolshov *et al.* [22] were led to the conclusion that "laser excitation with flame atomization is unreasonable". However, our experience with the separated air–acetylene flame [33], as well as some of the results published in the literature [12, 17], seem to mitigate such a statement and to show that one can still benefit from the simplicity and rapidity of flame analysis.

It is our opinion that one should not abandon the flame work with laser fluorescence provided that

(i) the peak power of the dye laser output, tunable from the low ultraviolet to the visible, should be capable of approaching saturation of the primary absorption wavelength of the element investigated (see Table 1) after being expanded to approximately 10 mm diameter in the flame; and

(ii) the measuring system should be provided with a variable gate to be properly optimized with regard to the laser pulse duration and the photomultiplier pulse (see later).

It is clear, however, that the flame is rather limited in the number of elements that can be determined. Then, if the laser meets the same requirements put forward for flame work, it is our feeling that the inductively coupled argon plasma is the right alternative to the flame for the following reasons:

(i) it is an ion as well as an atom reservoir;
(ii) it has a high quantum efficiency for several elements;
(iii) it is useful for refractory elements;
(iv) one can efficiently use transitions starting from excited atomic and ionic levels, since they are significantly populated at the plasma temperature; and
(v) the fluorescence optical arrangement can be the same as that used for emission work.

The utility and versatility of the argon inductively coupled plasma for laser fluorescence has in fact been demonstrated recently in our laboratory [26, 32].

If one wants to reach the ultimate sensitivity in analytical laser fluorescence work, however, there is no other choice but to use electrothermal atomizers. As demonstrated by Bolshov *et al.* [22] and by Tilch *et al.* [23], apart from the fact that scattering can be reduced to a minimum and solid sampling might be a reality, one takes advantage of the much less sample dilution in comparison with flames and plasmas. Here, care must be given to the operation of the boxcar and to the repetition frequency of the laser, because of the transient nature of the signal.

If scattering is eliminated (either because of the use of non-resonance transitions or

[44] C. A. van Duk, N. Omenetto and J. D. Winefordner, *Appl. Spectrosc.* 35, 389 (1981).
[45] N. Omenetto, C. A. van Duk and J. D. Winefordner, *Spectrochim. Acta* 37B, 703 (1982).

because of the optimal operation of the atomizer) and the background emission from the incandescent graphite can be properly screened, laser excited saturated fluorescence with suitably arranged optics and detection, will be the most sensitive of all spectroscopic techniques. Indeed, it will rival laser ionization methods [37, 46] in approaching single atom detection.

Of course, one should not overlook the pitfalls of electrothermal atomization in analytical work with real samples. For example, even if the detection limit for lead is at least 3 orders of magnitude better for graphite furnace atomization than for flame atomization, the direct determination of lead in blood by reference to aqueous solutions is not possible with the graphite furnace because of matrix interference.

Furthermore, the atomization of refractory elements will require a careful design of the cell and the excitation/emission geometry.

Despite these limitations, furnace atomization should always be preferred to flame and/or plasma atomization when sensitivity is the goal to be achieved.

5. The Detection System

The requirements of the detection system are clearly different according to the desired information. For saturation studies aimed at evaluating the atom (ion) number density and the temperature of the flame (plasma), fast electronics are needed in order to obtain a faithful reproduction of the fluorescence waveform. On the other hand, for analytical work, the entire pulse is usually of interest and consequently the requirements of high temporal performances of the detection can be relaxed.

The most widely used data processing system is a photomultiplier tube wired for fast response and a box-car integrator where a variable gate can be operated by a suitable reference signal so as to collect information only during the laser firing, therefore avoiding the processing of the background signal (which is not related to the laser) for most of the time. Indeed, with pulse widths in the nanosecond range, the duty factor (given by the product of the pulse duration and the repetition rate) can be as small as 10^{-7}.

The boxcar is usually operated in the "weighted average" mode, i.e. the signal reaches 63% of its final output level (for a given number of pulses averaged) in one "observed time constant". This parameter is given by the time constant of the gate divided by the product of the gate width and the repetition frequency [47]. The steady state signal level is usually reached after about 5 observed time constants.

The signal-to-noise ratio improvement obtained by averaging several pulses over that of a single pulse is approximately given by the square root of the number of pulses averaged [47, 48]. It is essential to recall here that the number of pulses averaged by the boxcar is given by the ratio between the time constant of the gate and the gate duration, and that this holds *irrespective* of the laser repetition rate [48]. Therefore, if one seeks to improve the signal-to-noise ratio, more pulses need to be averaged and this can only be achieved by increasing the time constant of the gate and/or by decreasing the gate width. The effect of increasing the repetition frequency of the laser is that of reducing the measuring time necessary to reach steady state of the signal level.

For a given duration of the fluorescence pulse, the gate width should be adjusted so as to obtain the maximum signal. When working in the exponential averaging mode, in no case should one set a gate width larger than the fluorescence pulse since a loss in the signal level will forcedly result. On the other hand, the use of a gate width smaller than the fluorescence pulse will result in a marginal signal loss, and will provide the advantage of increasing the number of pulses averaged for the same time constant of the gate.

For the model 162–165 boxcar integrator (P.A.R.-EG & G) if the laser is operated at 10 Hz and a 50-ns gate width is combined with 10 μs time constant, the number of pulses averaged

[46] G. I. Bekov and V. S. Letokhov, *Appl. Phys.* **B30**, 161 (1983).
[47] Princeton Applied Research Corporation, Princeton, N. J., USA, Boxcar Averager, Model 165 Instruction Manual.
[48] S. Cova and A. Longoni, An introduction to signals, noise and measurements, in *Analytical Laser Spectroscopy*, Ed. N. Omenetto, Chap. 7, Wiley, New York (1979).

II.64

necessary to reach 63% of the steady state signal level in one observed time constant is approximately 13 [47]. Then the "apparent time constant", which is given by the product of the number of pulses averaged and the gate width, is 0.65 μs and the resulting "observed time constant" is 1.3 s. Steady state will thus be achieved after 6.5 s which corresponds to 65 pulses averaged and to a total measuring time of 13 s. By increasing the repetition rate to 100 Hz, the observed time constant decreases by a factor of 10, reducing the measurement time needed to achieve steady state correspondingly. One should therefore compromise between the maximum allowable repetition rate of the laser and the time constant of the gate, especially in the measurement of fast transients such as those encountered with electrothermal atomizers.

A pre-integration of the fluorescence pulse can be useful from the practical operational standpoint rather than from an anticipated improvement in the signal-to-noise ratio. In fact, by dealing with longer pulses and correspondingly larger gate widths, undesirable effects such as time jittering in the opening of the gate at a fixed time after a triggering has occurred, can be relaxed. Also, the total measuring time decreases.

Finally, it is worth speculating on the fact that in analytical laser excited fluorescence in flames and plasmas one has usually to deal with signals characterized by a remarkable amount of noise, despite the fact that saturation is approached, i.e. laser fluctuations should not affect the fluorescence signal, and that the peak of the signal pulse as measured on the oscilloscope, is of the order of 0.5–1 V.

Such noise may be explained as follows.

(i) With high gain photomultipliers (10^7 or higher), the single photoelectron response observed on a fast oscilloscope (terminated on 50 Ω) is a pulse having a width of some nanoseconds and tens of millivolt as peak height. For example, in the case of an EMI end-on tube (6256 S), operated at −1200 V, we have observed a single photon pulse of ~25 mV and ~30 ns FWHM. It is therefore clear that *large* signal levels (0.5–1 V peak) are in fact generated by a *rather low* number of photoelectrons (20–40) and will have a very high shot noise associated with it. For example, a 250-mV fluorescence pulse, i.e. 10 photoelectrons with 32% shot noise associated, fed into a boxcar integrator operating in the exponential averaging mode and whose time constant and gate width have been arranged so as to average a total number of 100 pulses, i.e. reducing the relative shot noise contribution to 3.2%, would be characterized by approximately 16% peak to peak fluctuations (~5 times the root mean square value) due to shot noise. When this is the case, there will be no much usefulness in ratioing the fluorescence and the laser signals as conventionally done to eliminate the fluctuations of the source.

(ii) When the duration of the laser pulse is comparable with the lifetime of the excited level, the *integrated* signal, even under saturation conditions, will still depend on the decay constant and therefore on the composition of the pertuber bath with the consequence that fluctuations in this composition will be reflected in signal fluctuations [44, 45].

(iii) The spectral bandwidth of the dye laser at the magnesium line (285.213 nm) was found to be 0.012 nm without an etalon in the cavity [32]. The wavelength difference of longitudinal laser resonator modes, for a cavity length of approximately 20 cm is about 3×10^{-4} nm. If the atomic absorption line width is ~0.003 nm, this will correspond roughly to 10 mode spacings out of a total of 40. The strength of each mode will vary from shot to shot and thus produce variations in the laser irradiance over the absorption profile. This matter needs careful consideration and is certainly worth of further experimental investigation.

6. Conclusions

From a broad coverage of the analytical results published so far in the literature, we have attempted in this paper to evaluate what is felt to be the most important parameters to be optimized in order to benefit from the application of the technique of laser excited fluorescence to the analysis of the majority of elements present at trace levels in a large variety of samples.

From the discussion of the laser parameters and the optical arrangement it can be concluded that nowadays the choice of a versatile analytical laser set-up must be directed towards either an excimer-pumped dye laser or, even better, towards a Neodymium YAG-

pumped-dye laser. These systems offer continuous tunability down to the far ultra-violet, since the peak power of the dye in the fundamental wavelength is large enough to efficiently generate frequency up-conversion down to 217 nm in non linear crystals such as KDP or ADP and even below 200 nm by the technique of Raman shifting.

The high laser power can be efficiently used to saturate a large sample volume in the atomizer, this being the key for sensitivity in background noise limited systems. The spectral bandwidth of the laser can easily be narrowed down to approximately the absorption width of the atoms. Such an excitation bandwidth, together with its tunability over that large range of wavelengths, gives to the laser excited fluorescence technique its character of unique spectral selectivity.

Low pressure sputtering chambers as well as glow discharges are certainly good candidates as atomization cells in laser excited fluorescence and research efforts aimed at providing analytical results on solid samples are warranted and justified.

Atmospheric pressure flames and inductively coupled plasmas can be successfully used as atomizers and are both capable of providing detection limits that for many elements are sufficient to allow their direct determination in the sample solution without any prior chemical treatment. In this respect, because of its greater versatility, the inductively coupled plasma has to be preferred.

However, electrothermal atomization provides unprecedented sensitivities for all the elements so far investigated, showing that this must be the only method of choice in all those cases where the available sample size is limited and the elements to be determined are below the limit of determination of the other spectrometric methods.

Acknowledgements—H. G. C. HUMAN would like to thank the Joint Research Center authorities and in particular the Education Training Service of Ispra for the grant of a visiting scientist fellowship.

From: ANALYTICAL LASER SPECTROSCOPY
Edited by G. Kirkbright and
M. Sargent
(Chemical Publishing Corporation, 1985)

ANALYTICAL AND DIAGNOSTIC APPLICATIONS OF LASER INDUCED FLUORESCENCE IN FLAMES AND PLASMAS

N. Omenetto

Joint Research Center
Chemistry Division
Ispra (Varese), Italy

1. INTRODUCTION

The use of tunable lasers has had a significant, if not unique, impact in atomic and molecular fluorescence spectroscopy because of the analytical potential of this source and of the possibility of non-intrusive optical probing of several physical parameters of fundamental interest in laboratory flames and industrial devices for a better understanding of their combustion kinetics.

The lecture is divided in two parts. Firstly, the analytical features of laser excited atomic fluorescence in atmospheric pressure flames and/or other atom reservoirs will be discussed with particular emphasis on analytical figures of merit such as limits of detection, freedom from interferences and range of applicability. Secondly, several methods based on the measurement of selected fluorescence transitions in the saturation regime will be shown to be potentially useful for obtaining spatially and temporally resolved information on parameters such as the flame temperature, the total number densities of species and the quantum efficiency of the transition.

2. ANALYTICAL CONSIDERATIONS[1-6]

The most attractive characteristic of the dye lasers in view of their application to analytical atomic fluroescence spectroscopy were certainly the tunability with respect to wavelength and the power available within the spectral absorption bandwidth. This source was therefore considered to be ideal (although costly) replacement of the conventional excitation sources used in fluorescence work, which were operated in both pulsed (xenon lamps, hollow cathode lamps) and

continuous wave conditions (electrodeless discharge lamps, Eimac Xenon arcs). In addition, the attainment of optical saturation of the fluorescence signal resulted in a number of peculiar theoretical features that are now critically discussed in the following considerations.

2.1. Independence of the Fluorescence Signal upon Source Fluctuations and Atomizer Quantum Efficiency

This outcome can be theoretically seen from the general relationship[7] between the ratio of the atomic populations (see Figure 1a) derived with the assumption of steady state conditions and when the excitation intensity grows very high, i.e.

$$\frac{n_2 g_1}{n_1 g_2} = \frac{6.6 \times 10^3 \lambda_{12}^5 Y_{21} E_{\lambda 12}}{1 + 6.6 \times 10^3 \lambda_{12}^5 Y_{21} E_{\lambda 12}} \qquad (1)$$

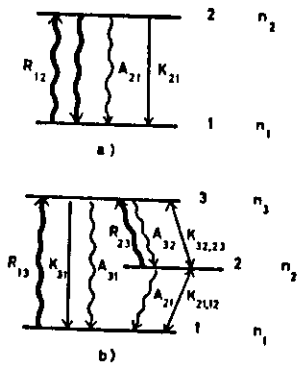

Fig. 1. Simplified energy scheme for a 2-level (1a) and a 3-level (1b) atomic system. n_1, n_2, and n_3 are the population densities (cm^{-3}) of the levels whose statistical weights are g_1, g_2 and g_3. The radiative rate coefficients (sec^{-1}) are indicated as R_{13} for the laser excitation and as A_{21}, A_{31} and A_{32} for the fluorescence. The collisional rate coefficients, both quenching and mixing, (sec^{-1}) are indicated as k_{12}, k_{21}, k_{31}, k_{32} and k_{23}. $n_T = n_1 + n_2$ or $n_T = n_1 + n_2 + n_3$ represents the total number density (cm^{-3}).

In this Equation, the following quantities are defined:

$E_{\lambda 12} \equiv \frac{\Phi_\ell}{\delta\lambda_\ell S_\ell}$ = spectral irradiance of the laser, considered as a continuum source with respect to the atomic absorption profile. Here Φ_ℓ(W) is the laser power, $\delta\lambda_\ell$ (cm) is the laser spectral bandwidth and S_ℓ (cm^2) is the laser cross section;

$Y_{21} = \left(\frac{A_{21}}{A_{21} + k_{21}}\right)$ = quantum efficiency of the transition;

A_{21}, k_{21} = Einstein coefficient of spontaneous emission and collisional quenching coefficient, sec^{-1}, respectively.

Therefore, one can see that the population of the excited level depends upon the product of the laser irradiance and the quantum efficiency. If this product grows much higher than unity, then $n_2 g_1 = n_1 g_2$ and if the statistical weights are the same, $n_2 = (n_T/2)$ when n_T is the total number of atoms in the (closed) two level system considered. As a consequence, the fluorescence signal (proportional to n_2) reaches a plateau and becomes independent on the laser irradiance.

In order to reach saturation, the laser induced radiative rate, R_{12}, must be greater than the quenching rate, k_{21}. Classical considerations[1,5] result in the following relationships

$$R_{12} = \frac{g_2}{g_1} A_{21} \left(\frac{\lambda_{12}^5}{8\pi hc^2}\right) E_{\lambda 12} \qquad (2)$$

and

$$k_{21} = \sum_j n_j \sigma_j \bar{v}_j \qquad (3)$$

where n_j is the density of the quenching species, σ_j the cross section for the quenching process and $\bar{v}_j$ the mean relative velocity of the collision partners. Typical values for flames at atmospheric pressure are $n_j \approx 10^{18}\ cm^{-3}$, $v_j \approx 10^5$ cm sec^{-1} and $\sigma_j \approx 10^{-15}\ cm^2$, which give $k_{21} \approx 10^8\ sec^{-1}$. Therefore, one can calculate that the excitation rate resulting from the use of a Xenon arc ($\sim 10^4$ W cm^{-2} nm^{-1}) at $\lambda_{12} = 400$ nm and for a strong transition ($A_{21} \sim 10^8\ sec^{-1}$) is approximately $10^4\ s^{-1}$ while that of a pulsed laser having 10 kW cm^{-2} over a bandwidth of 0.03 nm is approximately $10^9\ sec^{-1}$. However, it is worth pointing out here that R_{21} varies with wavelength: for the same laser power and spectral bandwidth, R_{12} turns out to be

5.4×10^8 sec^{-1} at 300 nm and 7×10^7 sec^{-1} at 200 nm. Therefore, much higher laser powers are needed to saturate optical transitions down in the ultraviolet.

On the other hand, some further considerations are necessary and should not be overlooked. The foregoing theoretical predictions on the independence of the fluorescence signal upon the fluctuations of the laser source and the quantum efficiency of the atomizer hold for the rather unrealistic approximation of a unit step excitation pulse for the laser irradiance (i.e. $E_\lambda = 0$ for $t < 0$ and E_λ° for $t > 0$ and for a measuring system that would faithfully reproduce the temporal behavior of n_2 (t). When boxcar integrators are used (which is quite common in pulsed[8] that, even for a rectangular laser pulse of duration Δt_g, the signal will depend again upon the source fluctuations and the quantum efficiency whenever the gate width of the measuring device is larger than the width of the fluorescence pulse. Indeed (see Figure 2) one can easily derive for the excited state population the following expression[8]

$$\int_0^\infty n_2(t)dt = \int_0^{\Delta t_g} n_2(t)dt + \int_{\Delta t_g}^\infty n_2(t)dt = \tag{4}$$

$$= \left[\frac{E_\lambda^\circ n_\tau}{gE_\lambda^\circ + A}\right]\left\{\Delta t_g + \left[1 - e^{-(gE_\lambda^\circ + A)\Delta t_g}\right]\left[\frac{1}{A} - \frac{1}{gE_\lambda^\circ + A}\right]\right.$$

where

$$A \equiv A_{21} + k_{21} \text{ and } g \equiv \left(1 + \frac{g_1}{g_2}\right).$$

From this expression, one can see that even in the saturation limit (i.e. when E_λ° grows to infinity) n_2 (t), and therefore the fluorescence signal, is given by

$$(n_2)_{E_\lambda^\circ \to \infty} = \left[\frac{n_\tau}{1 + \frac{g_1}{g_2}}\right]\left[\Delta t_g + \frac{1}{A_{21} + k_{21}}\right] \tag{5}$$

and thus is still dependent upon the quantum efficiency of the transition via the second term in parenthesis. It would then be advisable to provide the possibility of changing the measuring gate width, ideally along the entire fluorescence waveform, provided that the signal-to-ncise ratio is still acceptable.

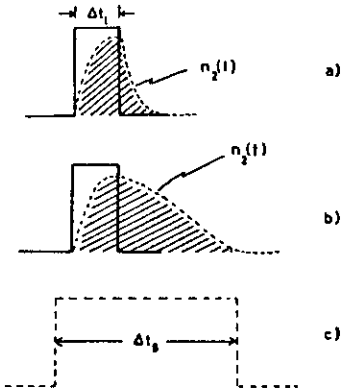

Fig. 2. Schematic representation of the measurement performed by a boxcar integrator whose gate width, Δt_g, is larger than the fluorescence pulse, proportional to n_2(t), excited by a rectangular laser pulse of duration Δt_l. a) high quenching flame; b) low quenching flame; c) gate width. It can be noticed that, assuming saturation, the time response of the signal within the laser pulse is the same, irrespective of quenching.

2.2. Improved Linear Dynamic Range of the Analytical Calibration Curves

It is well known[1] that the fluorescence curves of growth are characterized at high concentrations by a zero slope (in case of a continuum excitation source) or a negative slope (in case of a line excitation source). This behavior is essentially due to the self-absorption factor (radiation trapping) which decreases the fluorescence radiation on its way towards the detection system. It should be stressed here that the atomizer is assumed to be completely illuminated by the source while the entire fluorescence volume is seen by the detector: in this case, geometrical artifacts such as prefilter and postfilter effects do not enter into consideration. When saturation is reached the absorption coefficient, which is proportional to the difference between the atomic populations of the levels, approaches zero. As a consequence, the medium becomes transparent and no self-absorption can occur. The improved linearity of the analytical curves has been shown experimentally[9]. However, one should realize that if the laser beam is focussed at the center of the atomizer, the presence of self-reversal, which will affect the shape of the calibration curves, must be considered.

2.3. Signal-to-Noise Improvement for Background Noise Limited Systems

Because of the gated operation of the detection system, the background is only measured during the opening of the gate at a frequency dictated by the repetition rate of the laser. In this case, the low duty cycle characteristic of the most pulsed lasers used for analytical applications should result in a significant improvement in the signal-to-noise ratio as compared to a cw operated source and a cw detection system, but only if the average spectral irradiance of the pulse source equals that of the cw source. Moreover, the theoretical improvement is predicted by assuming that, during the pulse, the fluorescence follows linearly the source power Because of saturation, the increase in the fluorescence is (much) less and then the comparison will always be in favor of the cw system. On the other hand, the wavelength coverage (fundamental and frequency doubled) provided by pulsed lasers is still larger than that achieved with cw lasers.

Extensive considerations related to this topic can be found in the literature[1,3,5,10].

2.4. Analytical Sensitivity and Detection Limits

If the theoretical considerations made previously (Paragraph 2.1) hold, the maximum fluorescence signal will be measured when saturation is achieved, since for equal statistical weights, the population of both levels will be halved. Extensive theoretical calculations have been made aimed at giving order of magnitude estimates of the minimum detectable concentration of an atomic species in conventional analytical atomizers[2,5,11]. The calculations are based on signal-to-noise ratio considerations and the detection limits are referred to that concentrations level (usually in aqueous solution) which would give a signal to root-mean-square noise ratio of 3. As clearly pointed out by Alkemade[2] one should distinguish between "extrinsic" and "intrinsic" limit of detection, the difference being given by the fact that in the last case the main limiting noise is not due to the background or to the detector but to the inherent statistical fluctuation in the number of atoms present in the volume probed by the laser. Indeed, it has been reported in the literature[2,5,11] that such number can be extremely small so that single atom detection seems to be within the reach of the fluorescence technique. The reader is warned, however, that this spectacular sensitivity has been achieved in low pressure vapor cells and/or specially designed quartz containers where the atoms are surrounded by an inert atmosphere. In conventional atomizers at atmospheric pressure, the sensitivity is expected to be much poorer. In addition, the low number of atoms in the probe volume usually means that many more atoms ($\sim 10^3$x) are needed in the atomizer volume, which is finally what matters for analytical purposes.

It is worth remembering that the calculated limit of detection is given, in number of atoms per unit volume, and therefore needs to be related to the concentration (usually in /μg/mL or ppm) of the element in the solution aspirated into the flame or plasma or introduced into the electrothermal atomizer. The conversion factor calculated for typical flame conditions is approximately 10^{11} atoms cm^{-3}/ppm.

Table 1 collects the experimental detection limits obtained so far from flames and electrothermal atomizers such as open carbon cups. As one easily sees, even if work can still be done to improve flame detection limits, the flame should be abandoned in favor of electrothermal atomizers. This is even more substantiated by the data collected in Table 2 which are especially important when only microliter quantities of sample are available. Considering the actual atomizer volume probed by the laser, one can calculate[12] that the detection limit for lead corresponds to approximately 250 atoms/cm^3.

As repeatedly pointed out in the literature, Mie scattering is the major problem in laser excited fluorescence. Such scattering should not be confused with the (unavoidable) spurious reflections (from the optical components) of the laser beam into the fluorescence monochromator that can be minimized by proper and careful positioning of light baffles, traps and possibly polarizers, but is rather due to the presence of unvaporized particles created in the atomizer whenever the element sought is present in a large excess (1:10,000) of matrix. The most effective way of reducing the scattering effect is by the use of non resonance fluorescence transitions (see Figure 3). Indeed, the best detection limits reported in Table 1 and 2, especially with electrothermal atomization, have been obtained by measuring the fluorescence at a wavelength different from the excitation one.

Other ways have been proposed to correct for scattering[2,13] by taking advantage of the different frequency content of the saturated fluorescence and scattering signals. Time resolution is practically useless in strongly quenching atomizers because of the reduced lifetime of the excited fluorescent level, and polarizers cannot be very effective for Mie scatter as it would be in the case of Rayleigh scatter. In conclusion, if only resonance fluorescence transitions are available (Zn, Cd) the scattering will seriously detract from the attractiveness of the technique. These considerations indicate the importance of improving the analytical performances of the atomizer and work should proceed in this direction.

2.5. Other Analytical Considerations

Spectral interferences are known to play a minor role in atomic fluorescence. With laser excitation, the availability of many non-

Table 1. Detection Limited (ng/ml) obtained by Laser Excited Fluorescence Spectrometry[a)]

Element	Detection Limits	
	Flame[b)]	ETA[c)]
Ag	4	3×10^{-3}
Al	0.6	-
Ba	8	-
Bi	3	-
Ca	0.01	-
Cd	8	-
Co	19	2×10^{-3}
Cr	1	-
Cs	-	2×10^{-2} (d)
Cu	1	2×10^{-3}
Eu	20	10
Fe	0.06	10^{-3}
Ga	0.9	-
In	0.2	-
Ir	-	0.2
Li	0.5	-
Mg	0.002	-
Mn	0.4	6×10^{-3}
Mo	12	-
Na	0.1	0.02 (2)[e]
Ni	0.5	-
Pb	0.2	2.5×10^{-5}
Pt	-	4
Sn	3	-
Sr	0.1	-
Ti	2	-
Tl	4	-
V	30	-

a) Values are usually given in aqueous solutions and are calculated according to a limiting signal-to-rms noise ratio of 3.
b) Flames used are separated nitrous oxide-acetylene and separated air-acetylene burning on conventional slot or capillary burners at atmospheric pressure and with pneumatic and ultrasonic nebulization[32].
c) Electrothermal atomizers (graphite cuvettes or carbon rod atomizers)[33].
d) [See Reference 34].
e) Average number of atoms in the probe volume. The atomizer is a closed sodium cell (oven)[35].

Table 2. Absolute Detection Limits (fg) Obtained by Laser Excited Fluorescence and Electrothermal Atomization

Element	Detection Limit	
	a)	b)
Ag	100.	-
Bi	-	800.
Co	60.	200.
Cu	150.	800.
Eu	3×10^5	-
Fe	100.	1000.
In	-	100.
Ir	6×10^3	-
Mn	200.	-
Na	600.	-
Ni	-	1000.
Pb	1.5	5.
Pd	-	1000.
Pt	1.2×10^5	-
Tl	-	2.4

a) [See Reference 36].
b) [See Reference 37].

resonance transitions (see Figure 3) should still decrease the possibility of spectral interferences as it was clearly demonstrated in the case of gallium and manganese[9]. However, native flame species (OH, CH, CN, C_2) or molecular species formed in the combustion process can give rise to a fluorescence background[14]. Therefore, it is always advisable to scan the fluorescence spectrum in the vicinity of the analytical line.

Another point of concern for improving the analytical sensitivity is the spot size of the laser in the atomizer. The optimum spot size is of course dictated by the requirement that the collimator should be filled with light. However, one should be aware that much will be gained by enlarging the laser size into the flame, provided that the irradiance is still sufficient to saturate the transition.

Finally, the peak power of the laser should not be overrated in comparison with its spectral quality. Therefore, the use of etalons within the oscillator cavity will result in improved spectral irradiance over the absorption profile with the welcome advantage of better sensitivity and decreased scattering.

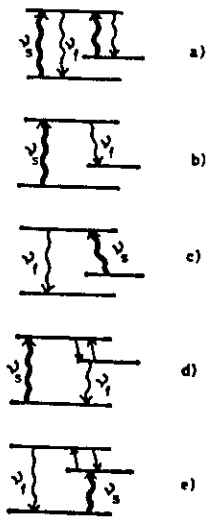

Fig. 3. Several types of fluorescence transitions observed with laser excitation[5]. ν_s = excitation frequency; ν_f = fluorescence frequency. a) resonance fluorescence; b) Stokes direct line fluorescence; c) Antistokes direct line fluorescence; d) Stepwise fluorescence; e) thermally assisted fluorescence.

3. DIAGNOSTIC APPLICATIONS

While the widespread acceptance of the use of lasers in analytical atomic fluorescence spectrometry in flames and plasmas can still be questioned because of the high cost of the overall apparatus and the lack of attaining (yet) the ultimate detection limits predicted by theoretical considerations, it is out of doubt that the technique of laser induced fluorescence (LIF) has gained a high popularity in combustion diagnostics with regard to the evaluation of the temperature and total number density of several species produced during the combustion process. This is well documented in a recent book edited by Crosley[15].

Like the Raman technique, LIF has the advantage of allowing local sampling of the parameter sought. This has the advantage over

the conventional absorption and emission methods that no special techniques such as the Abel inversion are required to convert line of sight information to radially resolved data. It is worth stressing, however, that spatial resolution can be obtained even with the absorption and the optogalvanic techniques in flames by crossing two laser beams, one acting as a weak probe and the other one as the perturbing beam[13]. One should also be aware that any inhomogeneity present in the probe volume would be averaged by the detecting system, thereby reducing the spatial resolution. Such inhomogeneities could be present both in the source (e.g. in the spatial profile of the laser beam) and in the system investigated (e.g. pronounced gradients in temperature and in the atomic or molecular densities in flames and plasmas).

The present discussion is applicable to combustion system at atmospheric pressure such as all analytically useful hydrogen- and acetylene-fuelled flames and to various types of plasmas such as the inductively coupled argon plasma or the microwave plasma. Among the parameters of interest to analytical chemists as well as to combustion engineers, we restrict our discussion to three of them, namely the temperature, the number density and the quantum efficiency. The reader is referred to some selected pertinent literature for the derivation of the relationships presented and for the details of the experimental set-up used.

The atomic system considered has 3 energy levels (see Figure 1b) indicated as 1, 2 and 3 in order of increasing energy (1 is the ground state).

Several assumptions are made in treating the interaction between the laser and the atoms (molecules). First, the vapor is assumed to be optically thin so that no self-absorption is present which would modify the equations given. Secondly, the laser irradiance is assumed to be homogenous over the entire volume probed by the detection system and the laser spectral bandwidth is considered to be much larger than the absorption profile. Finally, coherence effects are disregarded as well as laser enhanced chemistry and/or ionization, both of which have been demonstrated to occur in flames at atmospheric pressure[23,24].

3.1. Evaluation of Temperature

The underlying principle of most of the fluorescence methods is based upon the fact that level 2 is metastable and therefore not radiatively connected with the ground state, i.e. $A_{21} = 0$ in Figure 1b. Its thermal population is sensed by taking the ratio of two fluorescence transitions (resonance and antistokes) and assuming thermodynamic equilibrium in the system.

If the interaction between the laser and the atomic system is linear, we derive the following relationship

$$T_f = \frac{5040\ E_{12}}{\log \frac{E_{\lambda_{23}}}{E_{\lambda_{13}}} + 5 \log \frac{\lambda_{23}}{\lambda_{13}} + \log \frac{B^*_{F_{31}}}{B_{F_{32}}}} \qquad (6)$$

where E_{12} in the energy (eV) of the metastable level, $B^*_{F_{31}}$ is the antistokes fluorescence radiance excited at λ_{23}, and $B_{F_{32}}$ is the direct line fluorescence radiance excited at λ_{13}. Here, the electro-optical detection system needs to be calibrated and E_λ's measured; however, the knowledge of the transition probabilities is not necessary.

When optical saturation of the transitions is achieved and steady state values are measure, we obtain

$$\frac{B_{F_{32}}}{B^*_{F_{31}}} = \left(\frac{A_{32}\lambda_{13}}{A_{31}\lambda_{23}}\right) \left\{ \frac{1 + \frac{g_2}{g_3} + \frac{g_1}{g_3} e^{E/kT_f} + \frac{g_1}{g_2} e^{E/kT_f} \left(\frac{A_{31}+k_{31}}{k_{21}}\right)}{1 + \frac{g_1}{g_3} + \frac{g_2}{g_3} e^{-E/kT_f} + \left(\frac{A_{32}+k_{32}}{k_{21}}\right)} \right\} \qquad (7)$$

and one can see that the knowledge of k_{31}, k_{32} and k_{21} is needed to derive the temperature. Since the values of these constants are difficult to measure in flames at atmospheric pressure, this method is not attractive.

If the fluorescence waveform is temporally resolved and the measurements are taken at the peak, we have

$$\frac{B_{F_{31}}}{B^*_{F_{31}}} = \left(\frac{g_2+g_3}{g_1+g_3}\right) \frac{g_1}{g_2} e^{E/kT_f} \qquad (8)$$

where $B_{F_{31}}$ is the resonance fluorescence radiance, excited at λ_{13}. This method is certainly most attractive but has not yet been demonstrated experimentally.

The temperature can also be evaluated from termally assisted fluorescence measurements, i.e. measurements of the fluorescent emission radiated from levels whose energy is higher than that of

the level reached by the laser[18]. These higher levels must be populated by thermal collision processes and should reach their steady state values within the duration of the excitation pulse. If the ratio of two fluorescence transitions starting from levels i and j and terminating into the ground state is measured, we obtain

$$T_f = \frac{\Delta E_{ji}}{\ln \frac{A_{igi}}{A_{jgj}} + \ln \frac{\lambda_j}{\lambda_i} + \ln \frac{B_{Fj1}}{B_{Fi1}}} \qquad (9)$$

Usually, several fluorescence transitions are measured and the temperature is evaluated from the slope of the line obtained by plotting the normalized fluorescence signals versus E_{ij}. With this technique, only one laser is needed.

The above described laser induced fluorescence techniques have been used to obtain relative as well as absolute temperature profiles in flames with high spatial resolution (< 1 mm³).

3.2. Evaluation of Number Density[1,3,5,15,25-29]

When the optical transition is saturated, an absolute measurement of the fluorescence radiance ($Jsec^{-1}\ cm^{-2}\ sr^{-1}$) permits, for a two-level system, the direct evaluation of n_T. In this case, referring to the nomenclature of the 3-level system considered before, in absence of level 2, we obtain

$$B_{F_{31}} = \left(\frac{\ell}{4\pi}\right) A_{31}\ h\nu n_T \left(\frac{g_3}{g_1+g_3}\right) \qquad (10)$$

where ℓ is the homogenous depth of the fluorescence volume.

When level 2 is taken into consideration, the expression modifies and becomes complicated by the appearance of the (unknown) rate constants. If level 2 is radiatively coupled with level 1, we obtain

$$B_{F_{31}} = \left(\frac{\ell}{4\pi}\right) A_{31} h\nu n_T \left\{ \frac{1}{1 + \frac{g_1}{g_3} + \frac{k_{32}}{A_{21}+k_{21}+k_{23}}} \right\} \qquad (11)$$

If level 2 is radiatively coupled with level 3, we obtain

$$B_{F_{31}} = \left(\frac{\ell}{4\pi}\right) A_{31}\ h\nu n_T \left\{ \frac{1}{1 + \frac{g_1}{g_3} + \frac{g_2}{g_3} e^{-E/kT} + \frac{A_{32}+k_{32}}{k_{21}}} \right\} \qquad (12)$$

It is clear that in these cases the direct evaluation of n_T from a saturated fluorescence measurements is not possible.

The same considerations apply to the so-called "slope method", which consists in the plot of the reciprocal of the fluorescence signal versus the reciprocal of the laser power[3,5,7,25,28]. This plot results in a straight line, whose slope contains the quantum efficiency and the total number density. A peculiar outcome of the expression obtained for a 2-level system is that the intercept of the line allows to scale the ordinate values in absolute units[7]. Again, the expressions become more complicated for 3-level systems.

Several measurements in different flames for both atoms and radical species have been reported in the literature[15,25].

3.3. Evaluation of Quantum Efficiency

A direct evaluation of the quantum efficiency of a transition from saturated fluorescence measurements is again possible only for a 2-level atomic system, by deriving from an experimental saturation curve, the parameter E^s_ν, which is called the "stead state saturation spectral irradiance". Indeed, for a 2-level system, E^s_ν is given by the relationship

$$E^s_\nu = \left(\frac{g_1}{g_1+g_3} \right) \left(\frac{8\pi h\nu^3}{c^3} \right) \left(\frac{1}{Y} \right) \qquad (13)$$

where Y is the quantum efficiency, as defined previously.

The steady state saturation spectral irradiance for a 3-level system is still related to the quantum efficiency of the transitions by again the relations contain unknown rate constants. Y can also be evaluated, for a 2-level system, by the slope method described above.

Of course, the most direct evaluation of the overall quantum efficiency of a transition is given by the measurement of the lifetime of the excited level, provided that the radiative transition probabilities to lower levels are known so to allow the calculation of the radiative lifetime τ_{rad}, of the level. Then, if the lifetime τ, is measured, the quantum efficiency is simply given by the ratio (τ/τ_{rad}).

Such measurements have been made in flames[30] and recently in an inductively coupled argon plasma[31].

4. CONCLUSIONS

For analytical applications, the laser induced fluorescence technique has indeed the potential of achieving extremely low limits of detections as it was shown experimentally for electrothermal atomizers at atmospheric pressure and aqueous solutions. The ultimate impressive sensitivities predicted by theoretical considerations have only been achieved in closed vessels and other non-analytical atomizers. In flames and plasmas the sensitivity is yet far from being spectacular because of their inherent background noise and scattering. However, work is still needed in this area to fully characterize the technique. For electrothermal atomizers, the efforts should probably be only directed towards those elements for which the analytical community still demands more sensitivity of the technique.

In the field of combustion chemistry, the fluorescence method appears to be a remarkably attractive diagnostic tool, for both atomic and molecular species. However, because of the highly reactive medium, one should be aware of the many possible deactivation channels that are available to the laser excited atomic or molecular levels, ionization and chemical reactions being two examples of such channels. The interpretation of the experimental data will then require a more thorough investigation of these collateral effects.

REFERENCES

1. C. Th. J. Alkemade, T. Hollander, W. Snelleman, and P. J. T. Zeegers, "Metal Vapors in Flames", Pergamon Press, (1982).
2. C. Th. J. Alkemade, Appl.Spectroscopy, 35:1 (1981).
3. N. Omenetto, ed., "Analytical Laser Spectroscopy", Wiley, New York, (1979).
4. N. Omenetto and J. D. Winefordner, CRC Crit.Rev.Anal.Chem., 13:59 (1981).
5. N. Omenetto and J. D. Winefordner, Progress in Anal.Atom. Spectroscopy, 2:1 (1979).
6. G. M. Hieftje, J. C. Travis, and F. E. Lytle, eds., "Lasers in Chemical Analysis", The Humana Press, New York, (1981).
7. N. Omenetto, P. Benetti, L. P. Hart, J. D. Winefordner, and C. Th. J. Alkemade, Spectrochim.Acta, 28B:289 (1973).
8. C. A. Van Dijk, N. Omenetto, and J. D. Winefordner, Applied Spectroscopy, 35:389 (1981).
9. S. J. Weeks, H. Haraguchi, and J. D. Winefordner, Anal.Chem., 50:360 (1978).
10. N. Omenetto, G. D. Boutilier, S. J. Weeks, B. W. Smith, and J. D. Winefordner, Anal.Chem., 49:1076 (1977).
11. H. Falk, Progress Anal.Atom.Spectroscopy, 3:181 (1980).
12. M. A. Bolshov, A. V. Zybin, and V. G. Koloshinkov, Sov.Quantum Electronic, 7:1808 (1980).

II.81

13. R. P. Frueholz and J. A. Gelbwachs, Appl.Optics, 19:2735 (1980).
14. K. Fujiwara, N. Omenetto, J. D. Bradshaw, J. N. Bower, S. Nikdel and J. D. Winefordner, Spectrochim.Acta, 34B:317 (1979).
15. D. R. Crosley, "Laser Probes for Combustion Chemistry", ACS Symposium Series 134, Washington DC, (1980).
16. J. E. M. Goldsmith, Appl.Physics, B28, 2/3:304 (1982).
17. J. D. Bradshaw, N. Omenetto, J. N. Bower, G. Zizak and J. D. Winefordner, Appl.Optics, 19:2709 (1980).
18. G. Zizak, J. D. Bradshaw, and J. D. Winefordner, Appl. Spectroscopy, 35:59 (1981).
19. R. J. Cattolica, Appl.Optics, 20:1156 (1981).
20. R. G. Joklik and J. W. Daily, Appl.Optics, 21:4158 (1982).
21. R. P. Lucht, N. M. Laurendau, and D. W. Sweeney, Appl.Optics, 21:3729 (1982).
22. R. M. Measures, J.Appl.Physics, 39:5232 (1968).
23. C. H. Muller III, K. Schofield, and M. Steinberg, J.Chem.Phys., 72:6620 (1980).
24. J. C. Travis, G. C. Turk, and R. B. Green, Anal.Chem., 54:1006A (1982).
25. A. C. Eckbreth, P. A. Bonczyk, and J. A. Shirley, "Investigations of Saturated Laser Fluorescence and CARS Spectroscopic Techniques for Combustion Diagnostics", EPA Report 600/7-78-104 (1978).
26. J. W. Daily, Appl.Optics, 15:955 (1976).
27. J. W. Daily, Appl.Optics, 16:568 (1977).
28. A. P. Baronawski and J. R. McDonald, J.Chem.Phys., 66:3300 (1977).
29. C. D. Boutilier, M. B. Blackburn, J. M. Mermet, S. J. Weeks, H. Haraguchi, J. D. Winefordner, and N. Omenetto, Appl. Optics, 17:2291 (1978).
30. P. Hannaford, Procedings of the XXI CSI, Heyden & Son. Cambridge, England, p.250 (1979).
31. H. Uchida, M. A. Kosinski, N. Omenetto, and J. D. Winefordner, Spectrochim.Acta B, in press.
32. S. J. Weeks and J. D. Winefordner, (Chapter 8 in Reference 6), and J. J. Horvath, J. D. Bradshaw, J. N. Bower, N. S. Epstein and J. D. Winefordner, Anal.Chem., 53:6 (1981).
33. M. A. Bolshov, A. V. Zybin, and I. Smirenkina, Spectrochim.Acta, 36B:1143 (1981)
34. J. P. Hoimer and P. J. Hargis, Jr., Appl.Phys.Lett., 30:344 (1977).
35. W. M. Fairbank, Jr., T. W. Haensch, and A. L. Schwalow, J.Opt. Soc.Am., 65:199 (1975).
36. M. A. Bolshov, A. V. Zybin, and I. I. Smirenkina, Spectrochim. Acta, 36B:1143 (1981).
37. J. Tilch, H. J. Pätzold, H. Falk, and K. P. Schmidt, paper given at "Analytiktreffen 82", Neubrandenburg, DDR, November 82.

II.8

Pulsed Sources for Atomic Fluorescence

Nicolò Omenetto
Institute of Inorganic and General Chemistry
University of Pavia
Pavia, Italy

This article is aimed at assessing the characteristic features of pulsing the source of excitation in atomic fluorescence spectroscopy. Although there are other important parameters, both geometrical (solid angle of illumination and collection) and of more fundamental nature (quantum efficiency of the transition) which affect the fluorescence signal our discussion will be confined to the advantageous features and limitations of using pulsed excitation sources.

Pulsing Features and Signal-to-Noise Considerations

In the fluorescence literature on the excitation sources, no paper fails to conclude that their major requirement is a high radiance over the absorption line width of the analyte atoms. This holds true also in the case of pulsed sources. Narrow, broad line and continuum sources have been more or less successfully used and compared, both on an experimental and theoretical basis (*1*). Recently, several papers have appeared on the use of the pulsed, tunable dye lasers in atomic fluorescence studies (*1*).

The different sources of noise and their relative importance in atomic fluorescence work have been also discussed (*1, 2*). Although scanty information exists regarding temporal noise distribution in light sources and flames, it is generally assumed that the most important contribution to the total noise in a fluorescence setup is given by the flicker noise in the atomization system and by the total photodetector shot noise (assuming a photomultiplier is used). A possible exception which should not be overlooked is electronic noise in the amplifier readout chain, when high bandwidth systems are required. Usually, the further simplification is made that shot noise dominates over fluctuation noise and that background noise is the limiting noise in the system.

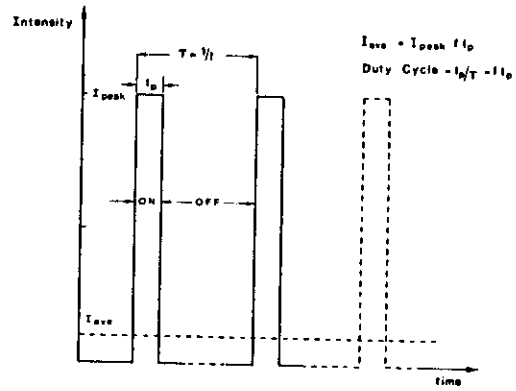

Figure 1. Simplified sketch of pulsed operation of source

In view of these considerations, the optimum fluorescence setup will rather obviously imply the combination of sources possessing a very high spectral radiance and stable, low background atomization devices. However, this condition should not be met at the expense of the spectral quality of the emitted radiation and the atomizing properties of the device used. In other words, self-absorption and self-reversal in the excitation source due to high current operation have to be avoided, and a low-temperature, low-background flame will be of limited analytical utility, being much more prone to chemical interferences than a high-temperature, high-background flame.

Both drawbacks can in principle be solved by a pulsed fluorescence system. In fact, one can achieve the goal of high source radiances without deterioration of the spectral characteristics of the emitted radiation by pulsing the source at very high peak radiances (high peak currents) for a given time duration and a given repetition rate. If this process is performed with a sufficient rest period between pulses (i.e., with a low duty cycle), then the average radiance (average current) of the source can be successfully maintained at a low, acceptable value. In Figure 1 is depicted a very simplified scheme showing the relationship between peak intensity and average intensity for an idealized square pulse and 100% modulation. The value of the duty cycle can be very different depending upon the type of source and pulsing circuitry: it may range from about 0.02 in the case of hollow cathode lamps to about 10^{-7} for dye lasers.

On the other hand, to take the greatest advantage of pulsing the

Reprinted from ANALYTICAL CHEMISTRY, Vol. 48, Page 75A, January 1976

source and using flames with good atomization efficiencies, it is also necessary to pulse or gate the detector, which will be "on" only during the source "on" time so that background noise (shot and fluctuation) will be greatly diminished. This can be accomplished in different ways, as will be seen later.

Assuming that the spectral distribution of the source is not modified by pulsing and that the fluorescence signal is linearly proportional to the source radiance, Omenetto et al. (3) have shown that the gain in signal-to-noise ratio due to pulsed operation (po) as compared to continuous operation (cw) is given by the following expression:

$$\Psi_{po/cw} = (B^0_{co}/B^0_{co})(1/(ft_p)^{1/2}) = (B^0_{peak}/B^0_{co})(ft_p)^{1/2} \quad (1)$$

$$\Psi_{po/cw} = (B^0_{co}/B^0_{co})^{1/2} \quad (1')$$

where B^0_{co} and B^0_{co} represent the average source radiances for the continuous and pulsed operation, respectively, B^0_{peak} is the peak radiance of the source, and ft_p is the duty cycle (see also Figure 1). Equation 1 holds for background shot noise limited systems, and Equation 1′ results when the system is source-carried shot noise limited (fluorescence or scatter). One can therefore see that pulsing may be very advantageous with gated detection, and the gain obtained is inversely proportional to the square root of the duty cycle. However, as indicated in Equation 1, peak power and duty cycle are inversely related to each other so that their maximum values are limited by the necessity of maintaining an acceptable power dissipation in the source.

It is worth stressing again that these considerations *only hold* if the fluorescence intensity does follow the source intensity, i.e., if the spectral distribution of the exciting source is not plagued by the onset, during the pulse, of phenomena such as self-absorption or self-reversal. If this happens, the predicted advantage of pulsing may be easily ruled out. It is therefore important to measure experimentally the line width in pulsed operation as compared to cw operation. Little is gained by the usual procedure of measuring wavelength integrated line intensities with a monochromator to see the increase in intensity vs. the discharge current. Finally, in resonance fluorescence work, pulsing the source and gating the detector will be useless if scattering problems with the atomization system are significant (Equation 1′).

Pulsed Sources

For the characterization of optical waveforms, electrical sparks between metal electrodes in pressurized gases have been widely used with pulse waveforms in the nanosecond range. Also, fast electrooptical shutters (Kerr cells, Pockel cells, etc.) can be used to obtain pulses with 10-nsec duration or less from steady light sources (*4*). A high-intensity, low-duty cycle spark discharge which might prove quite useful for exciting atomic fluorescence has been described (*5*). So far, analytical fluorescence studies have been performed with hollow cathode lamps, spectral continua, and tunable dye lasers. To the author's knowledge, no experiments have been reported on the use of electrodeless discharge lamps in the pulsed mode, even though these sources have been shown to be the most efficient conventional excitation sources in atomic fluorescence.

Pulsed Hollow Cathode Lamps. The usefulness of these sources, already known in emission spectroscopy (*6*), has been reported in atomic absorption by Dawson and Ellis (*7*) and subsequently by a number of authors (*8, 9*). Several commercial sealed-off lamps have been operated in the pulsed mode for atomic fluorescence studies. Typical values of peak current during the pulse range from 200 to 900 mA, pulse widths from 15 to several hundred microseconds, and repetition rates from 25 to several hundred hertz. The pulsed power supply, similar to that described by Dawson and Ellis (*7*), basically consists of a square wave pulse generator, pulse delay, and pulse width circuits to supply both driver pulses of variable frequency and width for the control of the power amplifier feeding the lamp and gating pulses of variable delay and width to the detector. Results have been reported also for demountable-type lamps, although with rather low values of peak pulse currents (less than 200 mA) superimposed to a constant DC level of several tens of milliamperes (*10*). A detailed study of the characteristic performances of commercial lamps operated in an intermittent mode was published by Cordos and Malmstadt (*11*). The sequential operation of the source allowed rapid multielement determination by atomic fluorescence (*12*), first described by Mitchell and Johannson (*13*). Computer-controlled, pulsed hollow cathode lamps have been recently used in a multielement approach, which operates by time division multiplexing (*14*).

As stated before, the quality of the lines emitted is important, and even if a gain of 50 to more than one hundredfold in the wavelength integrated intensity of the resonance lines has been observed, the width of the lines might be greatly different from that obtained in conventional cw operation. This is clearly borne out experimentally by the results of Human (*15*) who determined the signal-to-noise ratio for the fluorescence of copper and calcium. The fluorescence signal did not remain proportional to the source intensity, and instead of a ninefold increase from 20 to 900 mA, a value of only 16 was observed for copper. A more spectacular result has been obtained for copper and silver lamps operated in a somewhat similar mode by De Jong and Piepmeier (*16*). In their work on time resolved studies of atomic emission line profiles with a Fabry-Perot interferometer, the copper doublet was strongly self-reversed after the first 21 μsec of a 5-msec pulse, even though the wavelength integrated intensity increased linearly with the pulse current. The silver lamp showed extreme self-reversal even during the first 21 μsec. Understandably, there is a compromise to be reached between peak current and line width which depends on the particular combination of cathode material and filler gas. Even when using a multiple-element lamp, the resonance line intensities for different elements do not increase in the same way (*11*).

A new type of pulsed arc-glow hollow cathode lamp would seem to be worthy of further investigation because of the improved line shape and greater intensity as compared to a conventional lamp (*17*).

Pulsed Continuum Sources. The stringent demand for maximum pumping efficiency for the development of flash lamp pumped, tunable dye lasers has resulted in a considerable technological effort directed to improve the operating characteristics of these sources. Therefore, the innovations likely to appear in the design and output performances of flash lamps might be greatly beneficial for atomic fluorescence purposes.

A flash lamp is essentially an arc-chamber made of glass or quartz with each end having an electrode sealed to it. The basic flash tube circuit (Figure 2) consists of a high-voltage DC power supply, a charging resistance, an energy storage capacitor, and a high-voltage trigger pulse circuit. The capacitor is charged at the operating voltage, maintained below the self-flash lamp voltage so that the lamp operates only when triggered (*18*). The trigger circuit, consisting usually of a simple step-up transformer, pulsed from the discharge of a small capacitor by contacts or a thyratron switch, produces the high-voltage trigger pulse which ionizes the gas in the chamber. Several typical electrical parameters are collected in Table I, derived from Winefordner et al. (*18*). Of primary importance is the radiative efficiency of the lamp, which could be defined as the ratio of the optical energy emitted in the entire spectrum to the electrical energy delivered by the capacitor to the lamp. Values of approximately 50% can be achieved with xenon, and the radiative efficiency increases by increasing the peak current density. The spectral distribution of the radiation emitted depends upon the current density and time pulse duration: short pulses and high current densities shift the spectral output toward the ultraviolet region (*18, 19*). A great variety of lamp geometries (linear, miniature and capillary types, annular, helical, pi-shaped) are available, but the best arrangement for fluorescence would be given by short arcs or essentially point sources. Due to the high pressure in the arc discharge, an efficient lamp housing is mandatory. One serious drawback of flash lamps is their limited lifetime, typically 10^6 shots, extending up to 10^8 shots using properly designed circuits. A pulsed ultraviolet source developed to excite the fluorescence of SO_2 has been reported to have a lifetime in excess of 10,000 hr (*20*). Pulse durations normally range from several nanoseconds to hundreds of microseconds with peak powers up in the megawatt range. Repetition rates are usually below 100 Hz. Manufacturers of flash lamps worthy of investigation in atomic fluorescence include Xenon Corp. (Medford, Mass., especially with the Novatron series), EG&G (Boston, Mass.), and ILC Technology (Sunnyvale, Calif.).

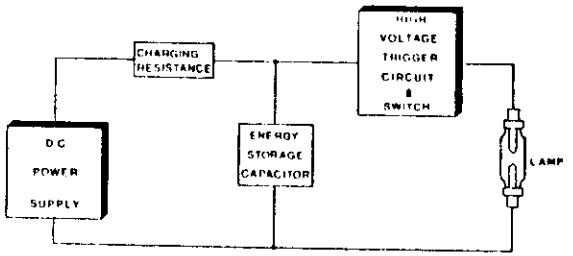

Figure 2. Oversimplified diagram of typical flash lamp circuit

A low-pressure, capillary-type xenon arc lamp has been recently investigated in atomic fluorescence work (*21*). The lamp was operated from a pulsed power supply at 7 kV with a 0.1-μF capacitor, giving a flash half width of approximately 6 μsec. Therefore (Table I), the flash input energy was 2.5 J with an average input power of 250 W (100 Hz repetition rate). No data on the radiative output energy, as well as on its spectral distribution, were reported. However, the detection limits obtained were poorer compared to an Eimac 150-W cw xenon source. This experimental evidence is rather disappointing, but no detailed investigations have been made to explain these unexpected results, although geometrical considerations on input fluxes on the flame seemed to play a significant role (*21*).

Table I. Electrical Characteristics of Flash Lamps[a]

Energy input per flash, J	$J = (1/2)CV^2$
Light flash duration, sec	$t_f = (1/2)R_fC$
Peak input power, W	$P_i = J/t_f$
Average input electrical power, W	$\bar{P}_i = Jf = P_i/t_f$
Average current drawn from DC power supply, mA	$\bar{I} = VCf$

[a] C = value of storage capacitor, μF; V = operating voltage, kV; R_f = effective arc resistance during the flash, Ω; and f = flash repetition rate, sec^{-1}. The value of the charging resistor should be chosen so that $R = 1/5\ fC$, and its power rating should be greater than $\bar{P}_i$. The value of f should never exceed about 0.1 $(t_f)^{-1}$ to prevent continuous ionization of the lamp.

Pulsed Tunable Dye Lasers. Extended tunability, high peak power, narrow bandwidth, and high beam collimation are important attributes of tunable dye lasers for atomic fluorescence work. Since the first papers appeared on laser excited atomic fluorescence, considerable progress has been made in this field (*1*). Pulsed dye lasers can be pumped by another laser or by a flash lamp. Interchanging of dye solution allows operation in the near UV–near IR range, extending with frequency doubling down to 250 nm. High peak power and low duty cycle would seem to permit full exploitation of the advantages of gated detection, as indicated in Equation 1.

Again, different types of noise might be predominant in laser excited fluorescence. Signal-carried scattering noise is the most important whenever it is impossible to take advantage of nonresonance fluorescence emission (*22*). Peak-to-peak fluctuations of the laser output should have no influence on the fluorescence signal, provided that its spectral irradiance is (much) higher than the saturation irradiance, which depends upon the lifetime of the atomic system (i.e., on the quantum efficiency of the transition). In fact, it is well known that a high radiation density is able to redistribute the population of the levels, causing the bleaching of the ground state. This would have remarkable consequences in improving the linearity of the analytical curves, provided that the bending observed at low light levels (i.e., with conventional excitation sources) can be attributed solely to self-absorption effects (*23*). Even more attractive is the possibility of fully exploiting the atomization characteristics of high-temperature, low-quantum efficiency mixtures, such as nitrous oxide–acetylene flames because of the less stringent dependence, for a two-level atomic system, on the quantum efficiency in near saturation conditions (*24*).

Bandwidths of the laser output, usually ranging from a few tenths of a nanometer to 10^{-2} nm with only the use of the dispersive element in the cavity, can be interferometrically narrowed down to 10^{-4} nm and even less, thereby allowing high-resolution spectroscopy studies. Also, the high collimation of the beam leads to very high irradiances even with moderate power, owing to the fact that the focal spot diameter of the laser can be approximated by the product of the beam divergence times the focal length of the lens used to focus it into the atomic vapor.

Some typical operating characteristic parameters of flash lamps and laser pumped dye lasers are summarized in Table II. This table is only intended to give an overall survey of some typical values which can be achieved with pulsed tunable lasers and does not represent ultimate performances.

Measuring System

Detection systems reported for pulsed fluorescence work have been

photomultipliers coupled with either a sampling oscilloscope or some form of boxcar integration schemes. The problems of measuring fast optical signals have been exhaustively discussed in two excellent papers by Lytle (25); therefore, we shall limit our discussion to a brief illustration of the widely used detection scheme involving a boxcar, which is analogous to a sampling oscilloscope with added flexibility of signal processing. Commercially available boxcars can be used either as a waveform retrieval system, also called "scan mode" of operation, or as a pulse measurement system, also called "single point" mode of operation (26). Basically, the boxcar is a sample and hold system, the sampling time of which is determined by a reference pulse related to the signal of interest. If one uses it in waveform retrieval applications, then the timing of the sampling window is slowly swept across the signal of interest, producing at the output a lengthened replica of the input waveform (Figure 3). For pulse measurement purposes, the instrument is arranged in such a way that the timing and width of the sampling window coincide with the signal pulse (Figure 4). In this last mode of operation, the boxcar bears a close resemblance to the phase sensitive amplifier (lock-in detector). However, the phase sensitive detector is always gated at half-cycle intervals, whereas the boxcar is gated so that it samples only the signal pulse (and noise) occurring during the sampling time.

A dual-channel boxcar integrator has been used to monitor separately any background emission between pulses (10). Similarly, a dual-channel synchronous integrator, which could be quickly patched together from standard functional cards and modules, was described (27). Here, the difference between the two integrated values of signal plus background and background alone gives the net fluorescence signal, assuming that the background emission during the OFF time of the source is equal to that measured during the ON time (i.e., in absence of any source-induced background signal). The corresponding digital synchronous photon counting system was used with a pulsed xenon lamp as excitation source. In this case, considerable RF interference was found from the high-voltage pulse to start the lamp; therefore, a delay in the gate opening (causing a loss of fluorescent signal) was necessary (27).

Analytical Results and Conclusions

Laser excited fluorescence studies have been carried out with both nitrogen laser pumped and flash lamp pumped dye lasers and have been almost exclusively limited to obtaining

Table II. Spectral Output Characteristics (Typical Values) of Tunable Dye Lasers

Pumping mode	Peak power, W	Pulse width, nsec	Repetition rate, Hz	Duty cycle	Bandwidth,[a] cm^{-1}
N_2-laser, 337.1 nm	10^4–10^5	3–10	10–500	$<10^{-3}$	10^{-2}–10^{-1}
Ruby–SH, 347.1 nm	10^6–10^8	10–30	~0.1	$<10^{-6}$	10^{-2}–10^{-1}
Flash lamp, ~50-nsec rise time	10^3–10^5	100–200	<0.1	$<10^{-6}$	10^{-2}–10^{-1}
Flash lamp, ~200-nsec rise-time	10^4–10^5	300–1000	5–20	$\sim10^{-5}$	10^{-2}–10^{-1}

[a] $\Delta\bar{\nu}$ (cm^{-1}) × λ^2 (cm^2) × 10^7 (nm cm^{-1}) = $\Delta\lambda$ (nm). $\Delta\bar{\nu}$ (cm^{-1}) × 3 × 10^{10} (cm sec^{-1}) = $\Delta\nu$ (Hz).

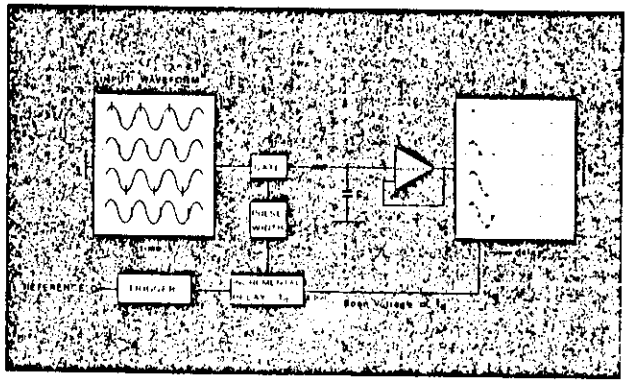

Figure 3. Scanning mode of operation of boxcar. In this way instrument might be thought of as single-channel signal averager

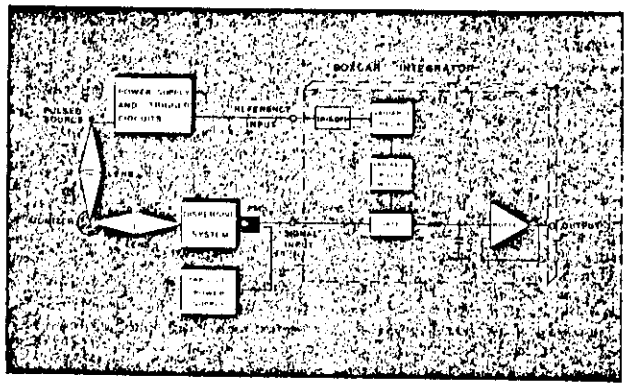

Figure 4. Simplified block diagram of fluorescence setup with pulsed source and boxcar detection. Operation is shown in single-point measurement mode

Table III. Comparison Between Pulsed Sources and Cw Sources Detection Limits in Atomic Fluorescence Flame Spectrometry

	Limits of detection, μg/m[a]				
	Pulsed sources			Cw sources	
Element	Laser	Line	Continuum	Line	Continuum, Eimac 150W
Ag	...	0.004	0.02	0.0001	0.006
Al	0.005	0.07	...	0.1	0.2
Au	...	...	...	0.003[b]	...
Be	...	...	0.2	0.01	0.07
Ca	0.005	0.0003	...	0.02	...
Cd	...	0.004	0.03	0.000001	0.01
Ce	0.5 (I)	...	...	...	...
Co	0.2	0.007	0.1	0.005	0.02
Cr	0.02	0.004	...	0.05	0.01
Cu	...	0.002	...	0.0005[b]	...
Dy	0.3 (I)	...	...	...	...
Er	0.5	...	...	...	...
Eu	0.02	...	...	...	...
Fe	0.3	0.008	...	0.008	...
Ga	0.02	...	...	0.01	...
Gd	0.8 (I)	...	...	...	...
Hf	100.	...	...	...	...
Ho	0.1	...	...	...	...
In	0.002	...	...	0.1	...
Lu	3.	...	...	...	...
Mg	0.0003[c]	0.001	0.004	0.001	0.0003
Mn	0.01	0.002	0.03	0.006	0.004
Mo	0.3	0.06	...	0.5	0.2
Nb	1.	...	...	...	...
Nd	2.	...	...	...	...
Ni	0.05	0.02	...	0.003	...
Os	150.	...	...	...	...
Pb	0.03[c]	0.07	...	0.01	...
Pr	1 (I)	...	...	...	...
Rh	0.1	...	...	3.	...
Ru	0.5	...	...	...	...
Sb	...	0.05	...	0.05	...
Sc	0.01	...	...	...	...
Se	...	1.	...	0.04	3.
Sm	0.1 (I)	...	...	...	...
Sn	...	0.2	...	0.05	...
Sr	0.01	0.01	...	0.03	...
Tb	0.5 (I)	...	...	...	...
Ti	0.1	...	...	4.	0.9
Tl	0.02	...	...	0.008	...
Tm	0.1	...	...	...	...
V	0.5	0.2	...	0.07	0.1
Yb	0.01	...	...	...	...
Zn	...	0.003	0.1	0.00001	0.006

[a] Values are for analyte in aqueous solutions. (I) means ionic fluorescence. Most of the detection limits reported are taken from refs. 1 and 31 and have been obtained in acetylene flames (air and nitrous oxide supported) and hydrogen flames (air and/or noble gas supported). The reader is referred to the original references for more complete information; see especially Browner's review (1). [b] Combined hollow cathode and high-frequency discharge, taken from Human (31). [c] Frequency doubled, flash lamp pumped dye laser, taken from Kuhl and Sperlein (32). An absolute flameless detection limit of 0.2 pg has been reported by Neumann and Kriese (33).

detection limits in aqueous solutions. On the contrary, a variety of applications of pulsed hollow cathode lamps have been reported (1, 3). Table III collects the detection limits obtained with the different types of pulsed sources and compares them with the corresponding cw source limits. Usually, such figures are defined on a basis of S/N (rms) = 2.

From the results presented in Table III, pulsed source detection limits do compete favorably with the corresponding cw source limits, obtained in most cases with intense electrodeless discharge lamps. The erratic quality of the laser results needs careful interpretation on the basis of parameters such as primary excitation wavelength, saturation of the fluorescence signal, and limiting noise in the system. Signal processing can be further developed and improved, as well as frequency doubling which will extend the tunability down to 200 nm without degrading the output power too significantly. Therefore, additional work is experimentally needed.

At the present state of the art of pulsed source atomic fluorescence spectrometry, one can generally say that the combined development of high radiance conventional pulsed sources (e.g., thermostated electrodeless discharge lamps) and novel signal processing techniques is likely to be expected and needed before pulsing can be considered definitely superior to cw excitation.

The very nature of the process of pulsing fits ideally in multielement determination systems on a rapid sequential basis, reducing instrumental complexity and cost (28). In view of the experimental data available up to now, this is probably the area in which pulsed fluorescence systems are worthy of investigation. Moreover, the time resolution capability of the fluorescence waveform allows one to foresee the attractive possibility of eliminating any nonspecific scattering signal in resonance fluorescence observations, by opening the gate *after* the source pulse has subsided.

Finally, it is now possible to produce extremely short excitation pulses of the order of a few nanoseconds with special continuum sources and even less than a nanosecond with nitrogen pumped dye lasers. Therefore, the possibility of lifetime determination via the direct fluorescence decay method might be feasible. This technique has been successfully used with a pulsed dye laser for the measurement of the lifetimes of some levels of nickel and iron atomic beams (29, 30). In addition, time resolved spectroscopy of the excited state will be of definite help in studying collisional relaxation processes.

References

(1) J. D. Winefordner and T. J. Vickers, *Anal. Chem.*, 36 (5), 192R (1974); R. F. Browner, *Analyst*, **99**, 617 (1974).
(2) T. C. O'Haver and J. D. Winefordner, *Fluoresc. News*, **6**, 1 (1972).
(3) N. Omenetto, L. M. Fraser, and J. D. Winefordner, in "Applied Spectroscopy Reviews", Vol 7, p 147, E. G. Brame, Ed., Marcel Dekker, New York, N.Y., 1973.
(4) S. Cova, M. Bertolaccini, and C. Bussolati, *Phys. Status Solidi A*, **18**, 11 (1973).
(5) J. Zyngor and S. R. Crouch, *Appl. Spectrosc.*, **26**, 631 (1972).
(6) M. Becart, G. Deprez, and J. Roig, Colloquium Spectroscopicum Internationale, p 312, Amsterdam, The Netherlands, 1956.
(7) J. B. Dawson and D. J. Ellis, *Spectrochim. Acta*, **23A**, 565 (1967).
(8) D. A. Katskov, G. G. Lebedev, and B. V. L'vov, *Zh. Prikl. Spektrosk.*, **10**, 245 (1969).
(9) D. E. Osten and E. H. Piepmeier, *Appl. Spectrosc.*, **27**, 165 (1973).
(10) J. O. Weide and M. L. Parsons, *Anal. Chem.*, **45**, 2117 (1973).
(11) E. Cordos and H. V. Malmstadt, *ibid.*, p 27.
(12) H. V. Malmstadt and E. Cordos, *Amer. Lab.*, **4**, 35 (1972).
(13) D. G. Mitchell and A. Johansson, *Spectrochim. Acta*, **25B**, 175 (1970); *ibid.*, **26B**, 677 (1971).
(14) E. F. Palermo, A. Montaser, and S. R. Crouch, *Anal. Chem.*, **46**, 2154 (1974).
(15) H.G.C. Human, *Spectrosc. Lett.*, **6**, 719 (1973).
(16) G. J. De Jong and E. H. Piepmeier, *Anal. Chem.*, **46**, 308 (1974); *Spectrochim. Acta*, **29B**, 159 (1974).
(17) G. J. De Jong and E. H. Piepmeier, *Spectrochim. Acta*, **29B**, 179 (1974).
(18) J. D. Winefordner, S. G. Schulman, and T. C. O'Haver, "Luminescence Spectrometry in Analytical Chemistry", Wiley, New York, N.Y., 1972.
(19) F. A. Charnava, L. N. Bekhovskaya, and I. M. Gurevich, *Zh. Prikl. Spektrosk.*, **11**, 790 (1969).
(20) W. J. Zolner, D. J. Mager, and D. A. Helm, *Anal. Instrum.*, **12**, 9 (1974).
(21) D. J. Johnson, F. W. Plankey, and J. D. Winefordner, *Anal. Chem.*, **46**, 1808 (1974).
(22) N. Omenetto, N. N. Hatch, L. M. Fraser, and J. D. Winefordner, *Spectrochim. Acta*, **28B**, 65 (1973); *Anal. Chem.*, **45**, 195 (1973).
(23) N. Omenetto, L. P. Hart, P. Benetti, and J. D. Winefordner, *Spectrochim. Acta*, **28B**, 301 (1973).
(24) N. Omenetto, P. Benetti, L. P. Hart, J. D. Winefordner, and C.Th.J. Alkemade, *ibid.*, p 289.
(25) F. E. Lytle, *Anal. Chem.*, **46**, 545A, 817A (1974).
(26) J.D.W. Abernethy, *Wireless World* (December 1970).
(27) E. Cordos and H. V. Malmstadt, *Anal. Chem.*, **44**, 2277 (1972).
(28) J. D. Winefordner, J. J. Fitzgerald, and N. Omenetto, *Appl. Spectrosc.*, **29**, 369 (1975).
(29) J. Heldt, H. Figger, K. Siomos, and H. Walther, *Astron. Astrophys.*, **39**, 371 (1975).
(30) H. Figger, K. Siomos, and H. Walther, *Z. Phys.*, **270**, 371 (1974).
(31) H.G.C. Human, *Spectrochim. Acta*, **27B**, 301 (1972).
(32) J. Kuhl and H. Spitschan, *Opt. Commun.*, **7**, 256 (1973).
(33) S. Neumann and M. Krinse, *Spectrochim. Acta*, **29B**, 127 (1974).

Work partially supported by the Consiglio Nazionale delle Ricerche.

Reprinted from **ANALYTICAL CHEMISTRY**, Vol. 49, Page 1076, June 1977

Pulsed vs. Continuous Wave Atomic Fluorescence Spectrometry

Sir: It is well known that the ideal experimental setup for atomic fluorescence spectroscopy has to combine the use of a high intensity source of excitation and a low background, highly efficient atomization reservoir. In recent years, several authors have attempted to assemble a fluorescence setup consisting of a pulsed excitation source and a gated detection system (*1, 2*). Understandably, the aim of this research was twofold: (i) high source radiances could be achieved within a narrow time interval while still maintaining the discharge conditions at a practical level of operation, and (ii) background noise due to the atomizer and detector could be greatly diminished because of the gated operation of the detector. Experimental results (*1–8*) were obtained using both continuum as well as line sources, such as xenon arcs and hollow cathode lamps. Moreover, tunable dye lasers, operated with a low duty cycle, have also been investigated because of their unique properties of high peak power, wavelength tunability and narrow spectral bandwidth.

Unfortunately results achieved with conventional sources operated in the pulsed mode are comparable to those obtained for similar sources operated in the continuous wave (cw) mode, and so *the predicted advantage of signal-to-noise ratio has never been fully realized*. Particularly disappointing are the results obtained for *pulsed* laser excitation where the experimental detection limits for flame atomizers are far less attractive than those predicted.

The aim of this note is to emphasize some of the drawbacks inherent in pulsed fluorescence work, which have been overlooked from the beginning both because of the lack of experimental information on the source characteristics when operated in a pulsed regime and, in the case of laser excitation, because of the fundamental relationship between the rate of photon absorption from the source (and photon fluorescence rate) and its spectral irradiance. The experimental and theoretical background upon which the foregoing considerations are based is largely available in the fluorescence literature. Nevertheless, by collecting all essential points together, we hope to help the reader and/or the potential user of the pulsed fluorescence technique to gain a more realistic

Table I. Summary of Reasons Why Atomic Fluorescence Signal-to-Noise Ratio in Pulsed Luminescence Spectrometry Does Not Necessarily Increase with Peak Source Power

Source type	Reason	Comment
Pulsed hollow cathode lamps	Self-reversal	Experimental results conclusive
Pulsed electrodeless discharge lamps	Probably self-reversal	No experimental results yet
Pulsed xenon lamp	Shift in spectral distribution; inefficient conversion of input power to light output	Experimental results conclusive
Tunable dye laser	Saturation[a] approached in luminescence (signal reaches plateau); scatter increases linearly with source power for resonance fluorescence; molecular fluorescence increases linearly with source power	Experimental results conclusive

[a] Molecular fluorescence with dye lasers is not as prone to saturation and thus the signal level should increase nearly linearly with source flux even with lasers.

appreciation of its benefits and shortcomings.

THEORETICAL EQUATIONS (1,3)

Assuming that the total noise in a fluorescence setup is due to atomizer source detector shot noise, the gain, G, in signal-to noise ratio due to source pulsing (po) and detector gating as compared to continuous wave operation (cw) of both source and detector can be expressed as follows:

$$G(\mathrm{po/cw}) = \{(E_\lambda{}^{\mathrm{p}})_{\mathrm{peak}}/(E_\lambda{}^{\mathrm{c}})_{\mathrm{av}}\}\{/t_{\mathrm{p}}\}^{1/2} \quad (1)$$

in the case of *background shot noise limited systems*, and

$$G(\mathrm{po/cw}) = \{(E_\lambda{}^{\mathrm{p}})_{\mathrm{peak}}/(E_\lambda{}^{\mathrm{c}})_{\mathrm{av}}\}^{1/2}\{/t_{\mathrm{p}}\}^{1/2} \quad (2)$$

in the case of *source-related or -induced shot noise limited systems*. Here, $(E_\lambda{}^{\mathrm{c}})_{\mathrm{av}}$ stands for the average spectral irradiance (erg s^{-1} cm^{-2} nm^{-1}) of an excitation source operated in the cw mode and $(E_\lambda{}^{\mathrm{p}})_{\mathrm{peak}}$ represents the peak spectral irradiance of the pulsed source, characterized by a pulse width t_{p} (s) and a repetition rate f (Hz). If source stability is poor causing flicker noise which is source related (scatter) or source induced (molecular fluorescence of flame gas species) signal, then there will be no gain with the pulsed source excitation. For narrow line sources, E_λ is replaced by E, the line irradiance, i.e., $E = \int_0 E_\lambda \mathrm{d}\lambda$.

For a non-degenerate two level atomic system, under steady-state conditions, the fluorescence radiance, B_{F}, (erg s^{-1} cm^{-2} sr^{-1}) is given by:

$$B_{\mathrm{F}} \quad (l/4\pi)Y\{\int k(\lambda)\mathrm{d}\lambda\{E_\lambda\{E_\lambda{}^{\mathrm{s}}/(E_\lambda + E_\lambda{}^{\mathrm{s}})\} \quad (3)$$

where l denotes the depth of the fluorescing region (cm), Y is the quantum efficiency of the transition, $k(\lambda)$ is the absorption coefficient (cm^{-1}), and $E_\lambda{}^{\mathrm{s}}$ is a parameter called "saturation spectral irradiance". For conventional excitation, $E_\lambda << E_\lambda{}^{\mathrm{s}}$, and therefore, the fluorescence radiance bears the usual linear dependence upon the quantum efficiency and the source spectral irradiance. However, if $E_\lambda > E_\lambda{}^{\mathrm{s}}$, the fluorescence radiance attains, at the limit of infinite E_λ, a maximum value, given by:

$$(B_{\mathrm{F}})_{\mathrm{max}} = (l/4\pi)h\nu A(n_{\mathrm{T}}/2) \quad (4)$$

where A (s^{-1}) is the Einstein spontaneous transition probability and n_{T} is the total atomic population density (cm^{-3}). The parameter $E_\lambda{}^{\mathrm{s}}$ can therefore be identified as the source spectral irradiance for which the fluorescence radiance reaches one half of the maximum value. This parameter is related to the atomic parameters of the transition as follows:

$$E_\lambda{}^{\mathrm{s}} = 7.6 \times 10^{23}\,(\lambda)^{-5}\,(Y)^{-1} \quad (5)$$

where λ has units of nm.

DISCUSSION

Case I: Conventional Excitation Sources. In the most favorable cases of narrow line width, good optical collection efficiency, and high inherent brightness of the discharge, the spectral irradiance reaching the atomic reservoir from sources such as hollow cathodes, electrodeless discharge lamps, and xenon arcs can attain a maximum value of $\sim 10^6$ erg s^{-1} cm^{-2} nm^{-1} (*9, 10*). Therefore in this case, $E_\lambda << E_\lambda{}^{\mathrm{s}}$ (see case II for numerical values of $E_\lambda{}^{\mathrm{s}}$), and no saturation of the fluorescence signal is expected.

When *pulsed hollow cathode lamps* are used for excitation, the value of the duty cycle (fraction of source "on-time") reported in the literature varies from 10^{-2} to 10^{-4}. Thus, according to Equation 1, the spectral peak irradiance of the lamp should exceed the average spectral irradiance of the cw source by *at least* 2–3 orders of magnitude if any appreciable gain in S/N ratio has to be achieved. While this increased intensity can be effectively measured by observing the *wavelength integrated* output of the lamp, it has been amply documented in the literature (*4–7*) that the line profile may be plagued by severe self-reversal effects, which therefore *do not justify* the use in Equation 1 of source (excitation) irradiances based upon input powers.

For *pulsed xenon arcs*, where self-reversal effects should be absent, two additional parameters have to be considered: (i) the spectral distribution of the light emitted changes due to pulsing and this can result in a significant increase of the background scatter as well as molecular fluorescence of flame species (*8*); and (ii) the optical efficiency of the lamp (i.e., the ratio between the spectral output and the electrical power input) may change with the peak electrical power dissipated during the pulse (*10*). Again, if Equation 1 is to be used, source spectral irradiances rather than input powers are required.

At this date, no experimental data are available with the use of electrodeless discharge lamps operated in a pulsed mode. However, the same problems reported for hollow cathode lamps should be seriously taken into consideration.

Case II: Pulsed Laser Excitation. *Saturation of the Fluorescence.* The duty cycle for a typical commercially available tunable dye laser ranges from 10^{-6} to 10^{-4} depending upon the kind of pump used (flashlamp or nitrogen laser). However, peak powers of several tens of kW are easily attainable, and therefore a remarkable improvement in S/N ratio should indeed be feasible if the assumptions made in the derivation of Equation 1 are met. Pulsed lasers may be, however, plagued with multimoding, which is similar to self-reversal. Again, *the use of Equation 1 for laser excitation is misleading*, unless proper attention is given to the saturation spectral irradiance limiting the maximum attainable fluorescence signal. According to the definition of saturation spectral irradiance, it is clear that having $E_\lambda >> E_\lambda{}^{\mathrm{s}}$ will result in at most doubling the fluorescence signal. Therefore, *it is $E_\lambda{}^{\mathrm{s}}$ and not E_λ that has to be substituted in Equation 1 to calculate the gain in the signal-to-noise ratio.* From Equation 5, one can calculate the values of $E_\lambda{}^{\mathrm{s}}$ for all resonance lines of the elements in the UV-visible region and for most atomizers characterized by widely different values of quantum efficiency. If Y varies from 10^{-1} to 1 and for λ's in the range 200–800 nm, Equation 5 shows that the two limiting values of $E_\lambda{}^{\mathrm{s}}$ (erg s^{-1} cm^{-2} nm^{-1}) range from approximately 10^9 to 10^{-5} erg s^{-1} cm^{-2} nm^{-1} (or 10^2–10^{-6} W cm^{-2} nm^{-1}). Clearly, the greatest gain for laser excitation will be realized when the atomic system requires a very high saturation irradiance. For example, if a laser of 50 kW peak power, operated at 10 Hz with 5-ns pulse width and 10^{-3}-nm effective spectral bandwidth is focused with a spot size of 10^{-2} cm^2 on a sample, this corresponds to a value of $(E_\lambda{}^{\mathrm{p}})_{\mathrm{peak}}$ of 5×10^{16} erg s^{-1} cm^{-2} nm^{-1}. If this value is inserted in Equation 1, one can see that the gain in S/N ratio, compared to a cw source of average spectral irradiance of 10^6 erg s^{-1} cm^{-2} nm^{-1}, is approximately 10^7 assuming background shot noise limitation, and if this value is inserted in Equation 2, one can see the gain in S/N value compared to the same cw source is approximately 50 assuming source related shot noise is dominant. This gain could indeed be realized if all the laser power is needed to saturate the transition. However, when saturation is achieved with the lowest value of $E_\lambda{}^{\mathrm{s}}$ (10^9) and this value is used in Equation 1, one can see that in this case *no gain will result, because essentially all laser power is wasted.* Therefore the full benefit of pulsed laser excitation will be achieved for atomizers with very low quantum efficiency and/or for resonance lines in the ultraviolet. For *molecular fluorescence* work, where saturation sets in at much higher irradiances compared to atoms, significantly better results are expected and indeed experimentally borne out (*11, 12*).

Scattering. It has been repeatedly pointed out that, while the fluorescence signal can be saturated, scattering due to unvaporized particles (Mie scattering) in the flame keeps increasing with the source intensity. For resonance fluorescence work, noise related to the scattered source radiation (shot and flicker) is expected to be the limiting noise in the system, and according to Equation 2, a deterioration in the ultimate S/N is easily predicted. When nonresonance fluorescence lines *cannot be used, scattering can still be minimized by time resolution*, i.e., by exciting with a pulse (much) shorter than the fluorescence emission pulse and delaying the aperture of the gated electronics. It is worth noting here that, *even in the absence of Mie scattering, with the high photon rates characteristic of laser excitation, Rayleigh scatter of radiation from atoms and molecules represents a fundamental limit for resonance fluorescence measurements in spectral regions where atomizer noise is negligible.* Finally, shot and flicker noise related to molecular fluorescence from flame species must be taken into account even when nonresonance fluorescence transitions are considered, the more so since such molecular fluorescence has been reported in flames for pulsed xenon continuum sources (*8*). For the case of laser excited nonresonance atomic fluorescence of elements with strong nonresonance transition probabilities, the detection limits should be superior to those obtained by excitation with conventional line sources. Experimental results have not shown this nor have satisfactory explanations been given to explain the discrepancies.

CONCLUSIONS

The simple considerations reported here show that pulsed fluorescence spectroscopy is experimentally plagued with certain drawbacks which have certainly limited its *analytical* usefulness. We stress here that our discussion did not take into account the detection system and the associated difficulty of processing very short pulses. However, these problems can be overcome with properly designed electronics. Finally, we are not claiming that pulsed fluorescence spectroscopy cannot be superior to conventional cw fluorescence spectroscopy, but we have rather indicated, on the basis of the experimental results reported in the literature, the parameters that must be properly investigated in order to achieve such a goal.

LITERATURE CITED

(1) N. Omenetto, L. M. Fraser, and J. D. Winefordner, in "Applied Spectroscopy Reviews", vol. 7, E. G. Brame, Ed., Marcel Dekker, N.Y., 1973 p 147.
(2) N. Omenetto, *Anal. Chem.*, **48**, 75A (1976).
(3) N. Omenetto, P. Benetti, L. P. Hart, J. D. Winefordner, and C. Th. J. Alkemade, *Spectrochim. Acta, Part B*, **28**, 289 (1973).
(4) H. G. C. Human, *Spectrosc. Lett.*, **6**, 719 (1973).
(5) G. J. DeJong and E. H. Piepmeier, *Anal. Chem.*, **46**, 318 (1974).
(6) G. J. DeJong and E. H. Piepmeier, *Spectrochim. Acta, Part B*, **29**, 159 (1974).
(7) E. H. Piepmeier and L. de Galan, *Spectrochim. Acta, Part B*, **30**, 263 (1975).
(8) W. K. Fowler, Ph.D. Thesis, University of Florida, Gainesville, Fla., 1976.
(9) J. M. Mansfield, M. P. Bratzel, H. O. Norgordon, D. O. Knapp, K. E. Zacha, and J. D. Winefordner, *Spectrochim. Acta, Part B*, **23**, 389 (1968).
(10) M. W. P. Cann, *Appl. Opt.*, **8**, 1645 (1969).
(11) R. N. Zare, paper given at the "Second Laser Spectroscopy Conference", Megeve, France, June 1975.
(12) J. H. Richardson, B. W. Wallin, D. C. Johnson, and L. W. Hrubesh, *Anal. Chim. Acta*, **86**, 263 (1976).

N. Omenetto[1]
G. D. Boutilier
S. J. Weeks
B. W. Smith
J. D. Winefordner*

Department of Chemistry
University of Florida
Gainesville, Florida 32611

[1] Present address, Institute of Inorganic & General Chemistry, University of Pavia, Pavia, Italy.

RECEIVED for review January 26, 1977. Accepted March 14, 1977. One of the authors (G.D.B.) wishes to acknowledge the support of a fellowship sponsored by the Procter & Gamble Company.

It is a usual practice to quote in the literature the detection limit as a figure of merit of a particular technique or method. There is nothing against this, provided that the procedure adopted is based on a statistical approach and the DL is clearly defined. DLs are commonly expressed in relative concentration units and refer to pure aqueous solutions of the elements. For the sake of illustration, let us take a typical example referring to the technique of emission spectrometry in which the time fluctuating signal x(t) is considered to be superimposed to a fluctuating background $x_b(t)$ (see Figure 1a). By definition, for the signal, we have

$$\text{Total Signal} = \bar{x}(t) + \bar{x}_b(t) \tag{1a}$$

$$\text{Net Signal} = \bar{x}(t) \tag{1b}$$

$$\text{Background} = \bar{x}_b(t) \tag{1c}$$

The bar above the symbols means that we are considering average values. Similarly, the noise accompanying the signal, defined as the random deviation of x(t) from the average, is given by

$$N(t) = x(t) - \bar{x}(t) \tag{2}$$

having thus, by definition, zero average value. The peak-to-peak noise and the root-mean-square noise are related to each other by the following relationship

$$N_{rms} \simeq \frac{1}{5} N_{ptp} \tag{3}$$

This relationship is justified since the individual excursions from the mean value are within 2.5 standard deviations, with 99% probability. Since random variations occur in both positive and negative directions, the peak-to-peak fluctuations will be comprised between 5 standard deviations.
The signal-to-noise ratio is therefore given by

$$\frac{\text{Net Signal}}{\text{Root-Mean-Square Noise}} = \frac{S}{N_{rms}} = \frac{\bar{x}(t)}{\sqrt{\langle x(t) - \bar{x}(t) \rangle^2}} \tag{4}$$

It is now easy to recognize that the denominator of this ratio, i.e. N_{rms}, is nothing else than the standard deviation of the measurements. Thus, the expression becomes

$$\frac{S}{N_{rms}} = \frac{\bar{x}(t)}{\sigma_x} = \frac{1}{RSD} \tag{5}$$

where σ_x is the standard deviation of the measurement and RSD the associated relative standard deviation.

If the limiting noise in the signal is caused by the fluctuations in the background, as it is the case at very low concentrations, then the standard deviation of the signal can be replaced by the standard deviation of the background. In such case the background has to be identified with the blank of the analysis. The signal-to-noise expression then becomes

$$\frac{S}{N_{rms}} = \frac{\bar{x}(t)}{\sigma_b} \tag{6}$$

Note that equation (6) should by no means be confused with the signal-to-background ratio (SBR), in which the magnitude of the background is compared with the signal. What matters in the detection limit is not the magnitude of the background, but rather its fluctuations. Now, in any analytical procedure, the measure, x, is related to a given concentration, c, of analyte by means of a calibration function x = f(c). If this function is linear, then the sensitivity, S', is defined as follows (see Figure 1b):

$$S' = \frac{\bar{x}(t) - \bar{x}'(t)}{c_o - c'} = \frac{\bar{x}(t)}{c_o} \tag{7}$$

If we now define the detection limit, c_L, as that concentration of the analyte in solution resulting in a signal-to-noise ratio of K, we can write

$$c_L = K\, c_o \frac{\sigma_b}{\bar{x}_o} \tag{8}$$

or, in a completely equivalent manner,

$$c_L = K \frac{\sigma_b}{S'} \tag{8a}$$

$$c_L = K\, c_o (RSD)_b \frac{1}{(SBR)} \tag{8b}$$

The detection limit can then experimentally be evaluated by measuring σ_b and $\bar{x}(t)$ at a given analyte concentration c_o and then extrapolating the result to a given value of K. The value of K is dictated by statistical considerations. It is usually taken as equal to 2 or 3.

The above considerations hold equally well for AAS and AFS.

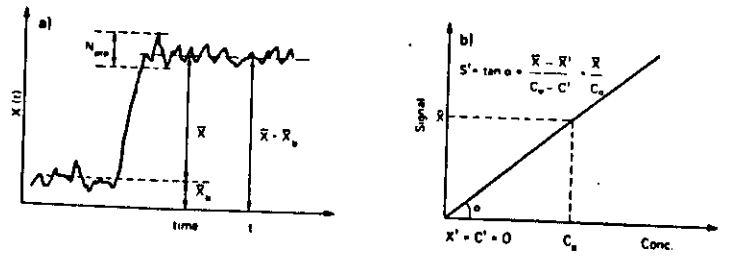

Figure 1: (a) Schematic representation of an emission (or fluorescence) signal superimposed to a fluctuating background;
(b) Calibration function and sensitivity

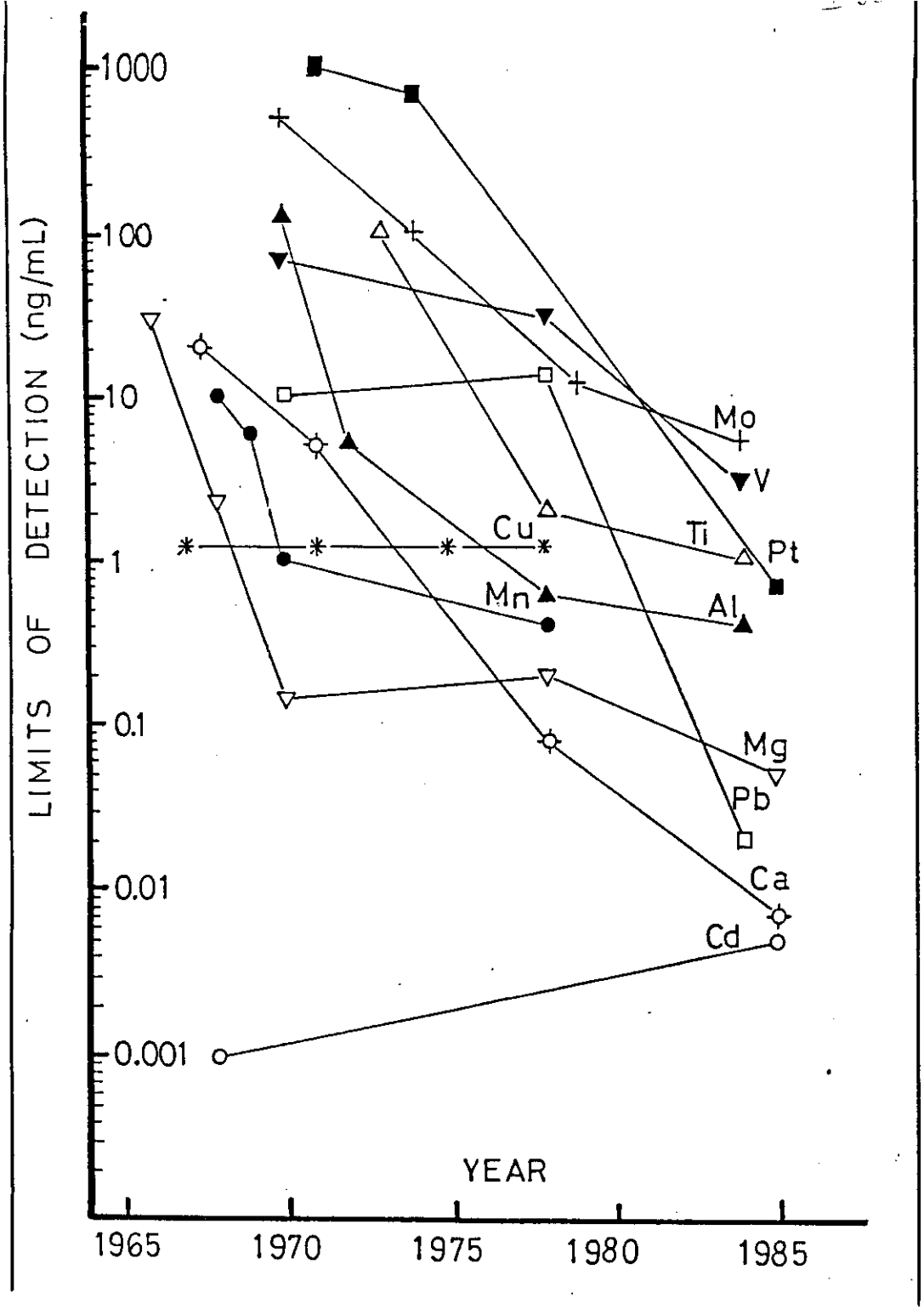
LIMITS OF DETECTION (ng/mL)
1000
100
10
1
0.1
0.01
0.001
YEAR
1965
1970
1975
1980
1985
Mo
V
Cu
Ti
Pt
Mn
Al
Mg
Pb
Ca
Cd